Hazelton

NEDC-21463-1
CLASS I
EPRI CONTRACT RP701-1
NOVEMBER 1976

EVALUATION OF NEAR-TERM BWR PIPING REMEDIES FIRST SEMIANNUAL PROGRESS REPORT APRIL — SEPTEMBER 1976

GENERAL ELECTRIC

NEDC-21463-1
Class I
EPRI Contract RP701-1
November 1976

EVALUATION OF NEAR-TERM BWR PIPING REMEDIES

First Semiannual Progress Report
April — September 1976

A. J. Giannuzzi

A. J. Giannuzzi
Project Engineer

Approved: J. C. Danko
J. C. Danko
Program Manager

Approved: J. S. Armijo
J. S. Armijo, Acting Manager
Plant Materials Engineering

BOILING WATER REACTOR SYSTEMS DEPARTMENT • GENERAL ELECTRIC COMPANY
SAN JOSE, CALIFORNIA 95125

GENERAL ELECTRIC

LEGAL NOTICE

This report was prepared by General Electric Company as an account of work sponsored by the Electric Power Institute, Inc. Neither the Electric Power Research Institute, members of Electric Power Research Institute, nor General Electric Company, nor any persons acting on behalf of either:

A. Makes any warranty or representation, express or implied, with respect to the accuracy, completeness, or usefulness of the information contained in this report, or that the use of any information, apparatus, method or process disclosed in this report may not infringe on privately owned rights; or

B. Assumes any liabilities with respect to the use of, or for damages resulting from the use of, any information, apparatus, method or process disclosed in this report.

TABLE OF CONTENTS

TABLE OF CONTENTS (Continued)

APPENDIX A

LIST OF ILLUSTRATIONS (Continued)

LIST OF ILLUSTRATIONS (Continued)

LIST OF ILLUSTRATIONS (Continued)

LIST OF TABLES

RP701-1 PROGRAM CONTRIBUTORS

TASK 1 — SCREENING MEASUREMENTS

D. C. Bertossa (Task Leader)

D. C. Bertossa
W. Vanderputten
P. P. Hallila
C. Schoenfeldt
A. J. Giannuzzi
T. Mehalko
T. L. Hayes
J. D. Heald
W. L. Walker
A. E. Pickett
V. M. Romero
W. L. Clarke
J. P. Higgins
D. A. Wettstein

TASK 2 — STATISTICAL PIPE TESTS

W. L. Walker (Task Leader)

W. L. Walker
A. J. Giannuzzi
S. A. Wilson
J. D. Heald
T. L. Gerber
I. R. Coussens
D. C. Bertossa
A. E. Pickett

TASK 3 — ELECTROCHEMICAL MEASUREMENTS

M. E. Indig (Task Leader)

A. R. McIlree
J. Weber

TASK 4 — FERRITE EFFECTS STUDIES

T. L. Devine (Task Leader)

R. E. Hanneman (Consultant)
M. G. Benz (Consultant)
J. Ross
C. Thompson
W. Moore
J. Hughes
T. Douglas
R. Horowitz

ACRONYMS AND ABBREVIATIONS

HAZ	Heat Affected Zone
TEM	Transmission Electron Microscopy
SEM	Scanning Electron Microscopy
CR&D	General Electric Corporate Research and Development Center
BWR	Boiling Water Reactor
SS	Stainless Steel
ASME	American Society of Mechanical Engineers
kg/mm^2	Kilograms per square millimeter
MPa	Mega Pascals
ksi	Kilopounds per square inch
IGSCC	Intergranular Stress Corrosion Cracking
SCC	Stress Corrosion Cracking
GE NED	General Electric Nuclear Energy Division
AISI	American Iron and Steel Institute
ASTM	American Society for Testing and Materials
EPRI	Electric Power Research Institute, Inc.
CERT	Constant Extension Rate Test
SHT	Solution Heat Treated
DOS	Degree of Sensitization
CRC	Corrosion Resistant Cladding
HSW	Heat Sink Welding
EPR	Electrochemical Potentiokinetic Reactivation
OCP	Oxygen Corrosion Potential
PRCT	Pressure Retaining Cast Transition
LEFT	Large Environmental Fatigue Test Facility
CL	Corrosion Loop

ABSTRACT

Full-size welded pipe and laboratory specimen screening tests have been performed to evaluate the intergranular stress corrosion cracking susceptibility of reference Type-304 stainless steel and candidate near-term remedies. The tests are designed to identify the candidate remedies to be included in the statistical pipe test program. The basis for the statistical pipe test program and the planned test matrix for the pipe tests are presented. Recent elastic-plastic modeling activity on elastic weld constraint is reported. In order to better understand the nature of the BWR environment, electrochemical potential measurements have been performed in an operating BWR during startup and full-power operating conditions. The results of these tests and laboratory welded specimen electrochemical tests are presented in this report. Fundamental studies designed to understand the role of ferrite on the intergranular stress corrosion cracking resistance of austenitic-based microduplex stainless steels have begun and preliminary results are presented.

1. SUMMARY

During this reporting period, significant technical results have been obtained for each of the program tasks and are reported in this document. The results include the following.

- Laboratory full-size-pipe and small-specimen screening tests of candidate pipe remedies
- Statistical basis for the definitive pipe tests of the pipe remedies
- Elastic weld constraint computer modeling
- In-reactor electrochemical potential measurements of Type-304 stainless steel
- Laboratory electrochemical potential measurements and polarization measurements of Type-304 stainless steel
- Studies of the factors which contribute to the intergranular stress corrosion cracking resistance of microduplex stainless steels.

The following summary highlights the work performed.

1.1 TASK 1 — SCREENING MEASUREMENTS

Stress corrosion tests of full-size welded pipe sections of 10.16-cm-diameter schedule 80 and small tensile specimens have been performed on Type-304 stainless steel and candidate remedies to evaluate their resistance to intergranular stress corrosion cracking in boiling water reactor environments. The remedies which have been considered to reduce or eliminate intergranular stress corrosion cracking susceptibility are the following.

A Solution heat treatment of welded pipes

B Application of corrosion resistant cladding to pipe inner surface prior to welding

C Application of heat sink welding techniques during pipe welding

D Application of pressure retaining cast transition to Type-304 stainless steel piping system

E Application of potential alternate piping materials, Types-316 and -316L stainless steel

A series of five full-size pipe tests have been performed to screen the remedies presently under consideration. These tests have included three cyclic axial loaded pipe tests in the Large Environmental Fatigue Test Facility and two 4-point bending pipe tests in the CL-4 test facility. Accelerated test conditions were used to reduce the required testing time to failure. These accelerants included high stress cyclic loading, high oxygen water environments, heavy grinding on the inner surface weld heat affected zones, and in some welds, high weld heat input. The accelerants varied from test to test and from condition to condition. They are described individually for each test. These pipe screening tests have provided the following results.

1 Type-304 stainless steel piping welds failed in laboratory 4-in. schedule 80 pipe tests routinely at stresses above the 289°C yield strength. Both high- and low-heat-input welds, ground and unground inner surfaces are susceptible to intergranular stress corrosion cracking in the weld heat affected zone. Post-weld grinding is a severe accelerant to intergranular stress corrosion cracking in this material.

2 All of the remedies examined show an improvement in resistance to intergranular stress corrosion cracking over welded Type-304 stainless steel piping. Solution heat treatment following butt welding appears to produce

immunity even when post-weld grinding is applied to the pipe inside surface. The use of corrosion resista cladding both as inlay and overlay in laboratory pipe tests appears to greatly improve the intergranular stre corrosion cracking resistance of welded Type-304 stainless steel. Heat sink welding appears to be a promisi product improvement if applied in the absence of post-weld grinding. Post-weld grinding appears to serious diminish the effectiveness of heat sink welding by eliminating the favorable residual stress state introduced b heat sink welding. The cast piping remedy has provided mixed results. Interdendritic stress corrosion crackin was observed in a cast pipe weld heat affected zone where <5% ferrite existed while another heat of cast pip was resistant to intergranular stress corrosion cracking in pipe tests. Further testing is planned.

3. The alternate piping materials Types-316 and -316L stainless steel tested and examined in these pipe tests t date have shown very promising results. However, a more substantial data base is required before performance improvement can clearly be established.

A limited number of laboratory specimen tests have been performed in support of the full-size-pipe screening tests. These tests indicate that heat sink welding does reduce the inner surface sensitization in the weld heat affected zone, thus reducing susceptibility to intergranular stress corrosion cracking. A cast pipe welded specimen containing 13 to 15% ferrite exhibited intergranular stress corrosion cracking susceptibility in a constant extension rate test. Further evaluation is in progress to understand the cause of the failure.

1.2 TASK 2 — STATISTICAL PIPE TESTS

A statistical formulation which provides the basis for the statistical pipe test program is presented. This statistical analysis differs from the earlier statistical approach in that the number of assumptions regarding the shape of the reference and alternate distribution curves are reduced by using time to first failure rather than mean time to failure as the fundamental parameter for comparison of factor improvement of the remedy to the reference material. This formulation is developed in detail in this report.

The elastic-plastic finite element analysis study designed to evaluate the effect of elastic constraint on the deformation behavior of large- and small-diameter Type-304 stainless steel pipe butt welds was performed during this report period. The addition of residual stress on the pipe inner surface in the model indicates that elastic constraint can occur in the presence of this stress contribution. Additional modeling and testing are planned to further elucidate the weld constraint theory.

1.3 TASK 3 — ELECTROCHEMICAL MEASUREMENTS

Electrochemical potentials have been measured both in-reactor (Vermont Yankee) and in the laboratory in order to establish the range of potentials present in both actual and simulated boiling water reactor environments for both as-welded Type-304 stainless steel piping material and the candidate remedies materials. The in-reactor measurements were performed during reactor startup and continued to full-power operation. Concurrently, water chemistry measurements were being performed by another organization (Nuclear Water and Waste Technology) under contract to EPRI in the Vermont Yankee boiling water reactor and these results have been made available to General Electric. The chemistry and electrochemical potential results have been analyzed and clear correlations appear to exist between particular chemical species in the water and the resultant electrochemical potentials developed. These results are being used to guide the laboratory test conditions so that meaningful intergranular stress corrosion experiments can be performed.

In addition, laboratory anodic polarization tests have begun in 288°C high purity water with 0.01 normal sodium sulfate addition (for electrical conductivity) to determine the polarization behavior for reference Type-304 stainless steel and the remedy materials. At present, the anodic polarization measurements have been performed for mill annealed Type-304 stainless steel in both forward and reverse potential scans. Based on the in-reactor and ex-reactor potential and potentiokinetic studies, the corrosion potential of Type-304 stainless steel in an operating reactor [−130 mV (standard hydrogen electrode)] lies within a passive potential region of −500 to +600 mV (standard hydrogen electrode).

TASK 4 — FERRITE EFFECT STUDY

Work was initiated at General Electric Corporate Research and Development Center to determine the factors which ibute to the resistance to intergranular stress corrosion cracking of austenitic-based microduplex stainless steels in the ng water reactor environment. The work in this task to date has been predominantly associated with purchasing or ting the alloys which will be used in the test program and evaluating screening tests designed to identify features that may e to the intergranular stress corrosion cracking resistance of Type-308 stainless steel alloys.

2. PROGRAM OBJECTIVE

This contract, RP701-1, covering an agreement between the Electric Power Research Institute and the General Electric Company, describes a 2-year program to verify the reliability of one or more near-term remedies to the boiling water reactor pipe cracking problem. The aim of the program is to provide a sound statistical basis with which to demonstrate that one or more of the recommended remedies will provide immunity to intergranular stress corrosion cracking of welded piping in boiling water reactor environments.

2.1 DESCRIPTION OF NEAR-TERM BWR PIPE REMEDIES

This program is investigating the intergranular stress corrosion cracking performance of reference Type-304 stainless steel and several candidate near-term piping remedies in both pipe test and specimen test in simulated boiling water reactor environments. The current list of candidate pipe remedies with a description of the procedure for application in welded piping and the rationale for consideration follows.

2.1.1 Solution Heat Treatment of Pipe Butt Welds

It has been demonstrated by the General Electric Company and by other organizations that weld sensitization of some heats of Type-304 stainless steel piping combined with high stress (or plastic strain) produces conditions for intergranular stress corrosion cracking in the boiling water reactor environment. Further, mill annealed and solution annealed Type-304 stainless steel piping is believed to be immune to intergranular stress corrosion cracking in the boiling water reactor environment. The basis for this immunity is the absence of carbides and hence no chromium depletion at the grain boundaries. A prime pipe-remedy candidate for welded Type-304 stainless steel piping systems is therefore to solution heat treat the pipe welds. Solution heat treatment of the pipe welds in addition to eliminating weld sensitization will also relieve the weld residual stresses. Wherever possible solution heat treatment of pipe welds will be performed in the pipe fabricator's shop according to procedures approved by the General Electric Company.

The procedure for applying solution heat treatment is presented in Figure 1. Here, the pipe is butt welded as in the case of reference Type-304 stainless steel. No unusual welding controls are employed during welding. Following the butt welding operation, the entire pipe segment is solution annealed at 1900 to 2000°F (1038 to 1093°C) for 15 minutes per inch of thickness but not less than 15 minutes nor more than 1 hour regardless of thickness, followed by quenching in circulating water to a temperature below 400°F (204°C). The metal temperature for the slowest cooling surface spends 2 minutes maximum in the temperature range of 1800 to 800°F (982 to 427°C).

2.1.2 Application of Corrosion Resistant Cladding to Pipe Inside Surface Prior to Field Butt Weld

The intergranular stress corrosion cracking observed in the bypass, and core spray lines of operating boiling water reactor plants has been exclusively associated with weld sensitized or furnace sensitized components. The carbide precipitation observed in the heat affected zone inside surface is also present in the weld metal. However, the nature of the duplex (austenitic-ferritic) structure of the weld metal provides immunity to intergranular stress corrosion cracking in the boiling water reactor although carbide precipitation is present. In fact, intergranular stress corrosion cracks propagating from the weld heat affected zone are blunted when they reach the weld metal. A minimum amount of ferrite must be present in the alloy to provide immunity to intergranular stress corrosion cracking in boiling water reactor water. Based on General Electric tests on duplex structures, the minimum ferrite level recommended for the corrosion resistant cladding is 8% after final processing, including field welding.

There are two variations of the proposed use of corrosion resistant cladding as shown in Figure 2.

1. Where a solution heat treatment can be performed in the shop prior to the final field weld, the cladding will consist of Type-308L stainless steel with high initial ferrite (to allow for reduction in ferrite during subsequent solution heat treatment as shown in region A of Figure 2). The solution heat treatment will then be performed to eliminate potentially unfavorable residual stresses introduced during the cladding operation and to eliminate the modest sensitization expected in the region of the inside surface of the Type-304 stainless steel im-

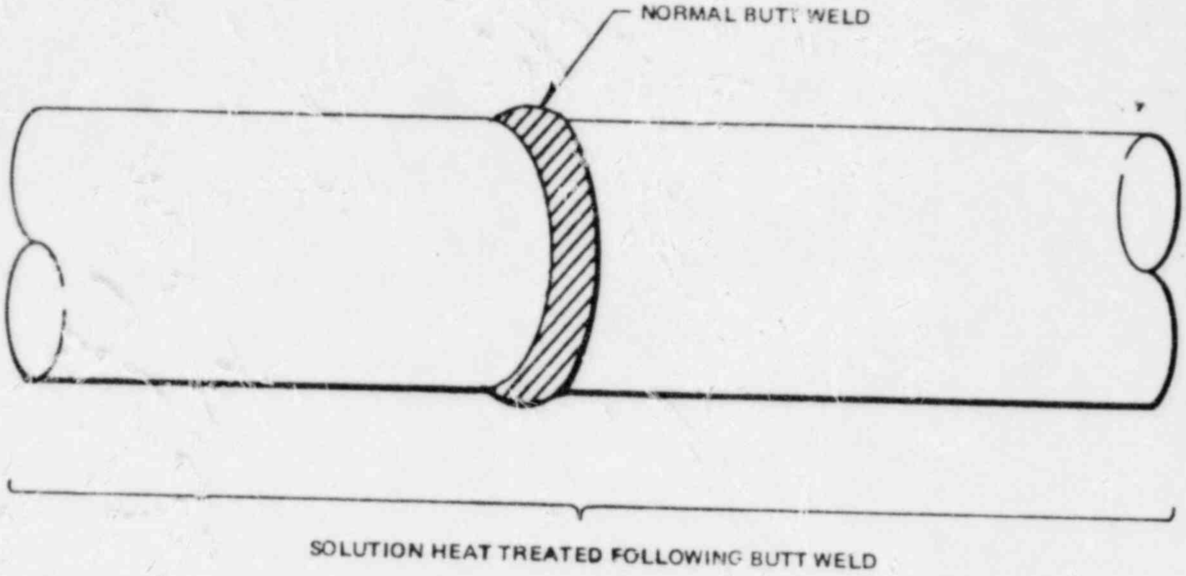

Figure 1. Application of Solution Heat Treatment of Type-304 Stainless Steel Pipe Welds

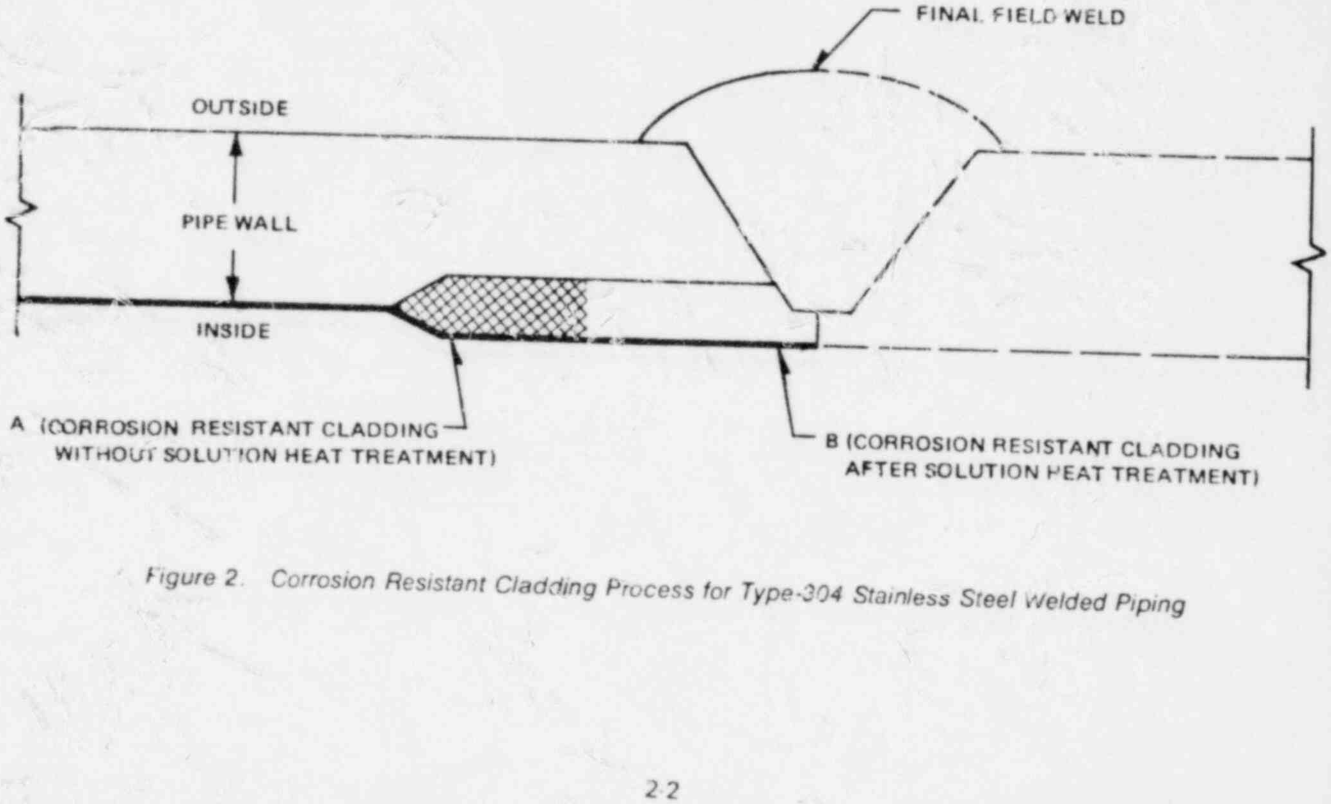

Figure 2. Corrosion Resistant Cladding Process for Type-304 Stainless Steel Welded Piping

mediately adjacent to the cladding. Following the solution heat treatment, region B will be deposited using Type-308L stainless steel and the field butt weld will be performed as in the reference Type-304 stainless steel butt welds.

2. Where a solution heat treatment cannot be performed (such as the final closure weld in a pipe repair of an operating reactor), the cladding material would then be Type-308L or -309 stainless steel with 0.035% carbon maximum and 8% ferrite minimum. In this case, both regions A and B in Figure 2 would be clad identically.

2.1.3 Application of Inside Surface Heat Sink Welding Control During Welding

Field and laboratory intergranular stress corrosion cracking data reveal that high residual welding stresses coupled with the applied stresses plus weld sensitization provide conditions for intergranular stress corrosion cracking of Type-304 stainless steel in the boiling water reactor environment. If a pipe can be welded without producing a sensitized structure and high residual tensile stresses in the weld heat affected zone the resultant component should be resistant to intergranular stress corrosion cracking in the boiling water reactor environment. The inside surface heat sink welding program is directed to the development and qualification of procedures that greatly reduce the sensitization produced on the inside surface of welded pipe and reduce or change the state of surface residual welding stresses from tension to compression. This approach will be used in shop or field applications where either the solution heat treatment or use of a corrosion resistant cladding are not possible.

Laboratory Type-304 stainless steel butt welds have been produced by General Electric licensees evaluating the inside surface heat sink welding techniques. It has been found that inside surface tensile surface residual stress is reduced substantially or changed from tension to compression as a result of this approach.

The inside surface heat sink welding program can be performed using still water, flowing or turbulent water, or water spray cooling of the inside surface by means of a sparger arrangement. In all cases the water cooling is applied following the initial root weld layer deposit. The weld is fabricated with normal field welding practice but with the addition of the inside surface water cooling following the root pass.

2.1.4 Application of Pressure Retaining Cast Transition to Type-304 Stainless Steel Piping Systems

Field and laboratory experience on intergranular stress corrosion cracking of austenitic stainless steels in the boiling water reactor environment reveal that the duplex (austenitic-ferritic) structure is highly resistant to intergranular stress corrosion cracking in the weld sensitized or furnace sensitized condition if a minimum amount of ferrite is present. Using this approach, cast transition pieces will be shop-welded to Type-304 stainless steel. The shop-welded pieces will be solution heat treated to remove the weld sensitization and relieve the weld residual stresses. The field welding would then consist of a butt weld of two cast pipes. This welding technique is presented in Figure 3. As in the corrosion resistant cladding remedy option, a minimum amount of ferrite must be present to provide resistance to intergranular stress corrosion cracking. The shop anneal following Type-304-duplex pipe weld may reduce the ferrite in the duplex pipe. Proper specifications will be employed to assure an 8% minimum ferrite level after the final field welds.

2.2 TASK OBJECTIVES

The work under this contract is divided into four major tasks. These tasks and a brief description of the task objectives are as follows.

2.2.1 Task 1 — Screening Measurements

The objective of this task is to perform full-size-pipe and laboratory specimen screening tests of several proposed pipe crack remedies to identify the most promising candidates for statistical verification in the pipe testing phase of the program. The screening tests will be performed in high purity, 550°F (288°C) oxygenated water at high stress using severe fabrication, process, and mechanical loading conditions to demonstrate a clear performance improvement of the remedy as compared to the reference Type-304 stainless steel piping specimens.

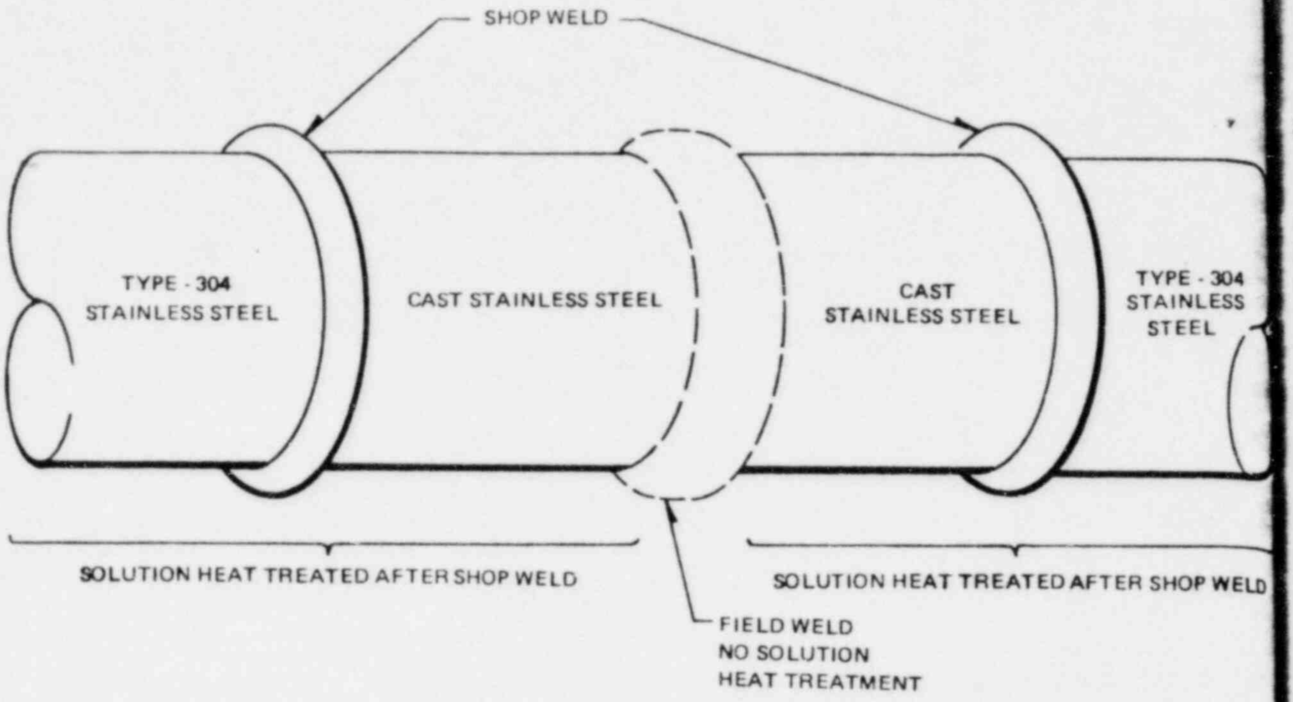

Figure 3. Application of Cast Transition Piece Candidate Remedy to Type-304 Stainless Steel Pipe Welds

2.2.2 Task 2 — Statistical Pipe Tests

The objective of this task is to verify the reliability of one or more of the candidate pipe remedies through full-size-pip testing of sufficient scope so as to provide a statistical demonstration of significant margin improvement of the remedy. Th testing is to be performed in 550°F (288°C) high purity oxygenated water at sufficient stress so as to cause the referenc Type-304 stainless steel welds to fail. Chemical, electrochemical, and metallurgical accelerants may be used whe considered appropriate to simulate worst case conditions and to increase the speed of data gathering.

2.2.3 Task 3 — Electrochemical Measurements

The objective of this task is to determine the corrosion potential of Type-304 stainless steel and remedy materials an system oxidation potentials in boiling water reactor environments, determine the range of potentials for stress corrosio cracking susceptibility, and immunity in simulated boiling water reactor environment and couple the laboratory and in-reacto measurements to assure the validity of the statistical pipe verification test program (Task 2). In-reactor test data on Type-30 stainless steel during startup, operation, and shutdown conditions will be used to set the minimum laboratory syste potentials for Type-304 stainless steel and the remedy materials. In addition, a rugged reference electrode will be develope for boiling water reactor application which can operate for extended periods of time over the range of temperatures that exis in the boiling water reactor environment.

2.2.4 Task 4 — Ferrite Studies

The objective of this task is to perform fundamental metallurgical studies to evaluate the role of ferrite on the resistance of duplex stainless steels to intergranular stress corrosion cracking in the boiling water reactor environment. The aim of this task is to identify the metallurgical conditions responsible for the increased resistance of duplex stainless steels to intergranular stress corrosion cracking in high purity oxygenated water.

3. TASK 1 — SCREENING MEASUREMENTS — RESULTS AND DISCUSSION

3.1 LABORATORY FULL-SIZE-PIPE TESTS

Full-size-pipe testing of 10.16-cm (4-in.) diameter schedule 80 butt welded pipe sections has been performed in the Large Environmental Fatigue Test Facility and in the CL-4 test loop to evaluate the intergranular stress corrosion cracking behavior of reference Type-304 stainless steel and screen the various candidate remedy materials. Three full-size-pipe tests have been completed in the Large Environmental Fatigue Test Facility (the second, third, and fourth Large Environmental Fatigue Test Facility tests) under axial loading conditions in 8 ppm oxygenated 288°C (550°F) high purity water and at stresses well above the yield strength of Type-304 stainless steel at test temperature. Two pipe tests have been completed in the CL-4 test facility (the second and third CL-4 tests) evaluating the reference and candidate remedy materials in four-point bending. As in the case of the Large Environmental Fatigue Test Facility tests, the CL-4 pipe tests are being performed in 8 ppm oxygenated water at 288°C (550°F) and at a maximum stress greater than the Type-304 stainless steel yield strength at test temperature.

The pipe remedies under consideration to reduce or eliminate parameters that promote intergranular stress corrosion cracking are the following.

a. Solution heat treatment of pipe butt welds.

b. Application of corrosion resistant cladding to pipe inside surface prior to field butt welding.

c. Application of heat sink welding techniques during pipe butt welding.

d. Application of pressure retaining cast transition to Type-304 stainless steel piping systems.

e. Application of potential alternate piping materials, Types-316 and -316L stainless steel.

Each of these remedies has been evaluated in the pipe tests performed in Large Environmental Fatigue Test Facility and in CL-4. Variations of corrosion resistant cladding have also been evaluated in the pipe tests. These variations include inlay, overlay, solution heat treatment following application of the corrosion resistant cladding, and application of the corrosion resistant cladding without solution heat treatment. The results of the pipe tests are presented individually and then summarized for each remedy.

3.1.1 Full-Size-Pipe Tests in Large Environmental Fatigue Test Facility

3.1.1.1 Introduction

One of the findings of the General Electric Pipe Task Force[*] was that intergranular stress corrosion cracking near welds in stainless steel piping systems seemed to correlate with the number of startup and shutdown cycles of the plant. This finding created considerable interest in evaluating the relative effect of cyclic load versus static load on the intergranular stress corrosion cracking behavior of Type-304 stainless steel.

As part of the Task Force study, an experimental pipe testing program was initiated. During the testing period in 1975, four full size (4- and 6-in. schedule 80) static and quasi-static pipe tests and one cyclic pipe test were conducted. The primary objective of these tests was to attempt to duplicate the recent intergranular stress corrosion cracking field cracks in the laboratory. The results of those tests were reported in the final Task Force report.[1]

---

[*] This Task Force was set up by General Electric to investigate the causes of intergranular stress corrosion cracking near welds in stainless steel piping materials.

The first cyclic pipe test was unsuccessful in generating intergranular stress corrosion cracking data. The crack that occurred was transgranular and due to pure fatigue. Analysis of the data revealed that the applied loading, i.e., applied stress level in combination with the relatively high test frequency (1 Hz), caused the mechanical fatigue cracking completely dominate the corrosion behavior. Therefore, as a result of this finding, together with the successful results fr the quasi-static test in which the field crack had been duplicated, it was decided to test a second cyclic specimen a substantially reduced test frequency. The applied stress level was also changed to duplicate the stress level used in the be tests of full-size-pipe sections in the CL-4 loop.

3.1.1.2 Test Objective

The cyclic tensile tests in the Large Environmental Fatigue Test Facility were designed to use axial cyclic loading full-size 4-in. (10.16-cm) schedule 80 welded pipe specimens of reference Type-304 stainless steel and potential reme methods to evaluate the relative intergranular stress corrosion cracking performance of the respective welds in full-s pipes. Accelerated test conditions were employed to reduce the required testing time. The accelerants used included hi stress, cyclic loading, high oxygen water environment, heavy grinding on the inside surface of the weld heat affected zon and in welds made with high weld heat input. The accelerants varied from test to test and from condition to condidition. Th are individually described in the test description of each of the cyclic pipe tests.

3.1.1.3 General Test Description and Procedures for the Large Environmental Fatigue Test Facility Cyclic Tension Tests

A. Specimen Description and Fabrication

Each of the test weldments was fabricated by butt welding eight 4-in. (10.16-cm) long segments of 4-in. (10.16-cm schedule 80 pipe together to form a 32-in. (81.26-cm) long test section. Machined end caps were butt welded to each end the test section to provide the closure necessary for pressurization. Both end caps were provided with threaded parts to allo the pressurized water environment to flow through the test sections. Loading adapters were welded to both end caps t provide a means to connect the specimens to the test machine.

The general test specimen configuration is presented in Figure 4. The test section includes eight butt welds (welds A through I). Each butt weld has two separate heat affected zones for a total of 18 possible crack initiation sites. However, welds A1, A2, I1, and I2 were fabricated from 4-in. (10.16-cm) schedule 160 pipe for the second Large Environmental Fatigue Test Facility test to avoid unwanted cracking in the end cap welds. Thus, 14 weld heat affected zones were tested at the high stress level in the second Large Environmental Fatigue Facility test. An additional transition piece was prepared for the third and fourth Large Environmental Fatigue Test Facility test so that 18 heat affected zones were tested at the high stress level in these Large Environmental Fatigue Test Facility tests.

B. Test Conditions

1. Loading

The cyclic axial load was applied to the ends of the specimen using the Large Environmental Fatigue Test Facility 500,000 pound (226,800 kg) universal test machine. The deflection feedback control mode was selected for the universal test machine based on safety considerations. As cracking occurs, in this mode, the specimen stiffness decreases and therefore the resulting load decreases.

During the first few cycles of testing, the applied deflection range was adjusted to maintain the desired stress range. These adjustments were made until a stable load-deflection relationship was established. This shakedown process to stable behavior is shown in Figure 5.

The axial stress was calculated based on the load divided by the cross sectional area at the typical weld preparation region (4.14 in.^{2}). The area at all of the weld preparations, except corrosion resistant cladding overlay welds, are the same as given above. The average area at corrosion resistant cladding weld preparations is 5.58 square inches and the resulting stress for these welds is 100% of the engineering yield stress.

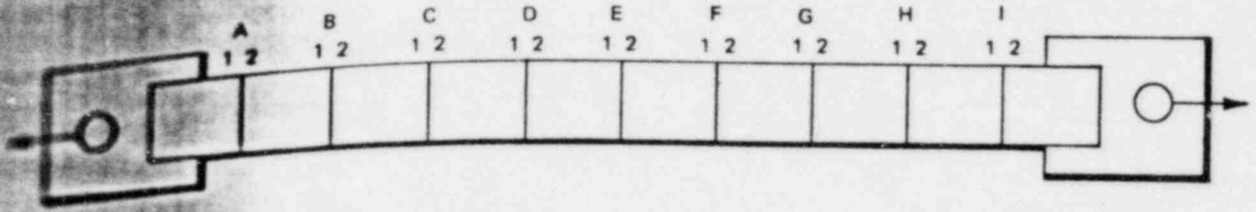

Figure 4. Weld Identification for Large Environmental Fatigue Pipe Tests

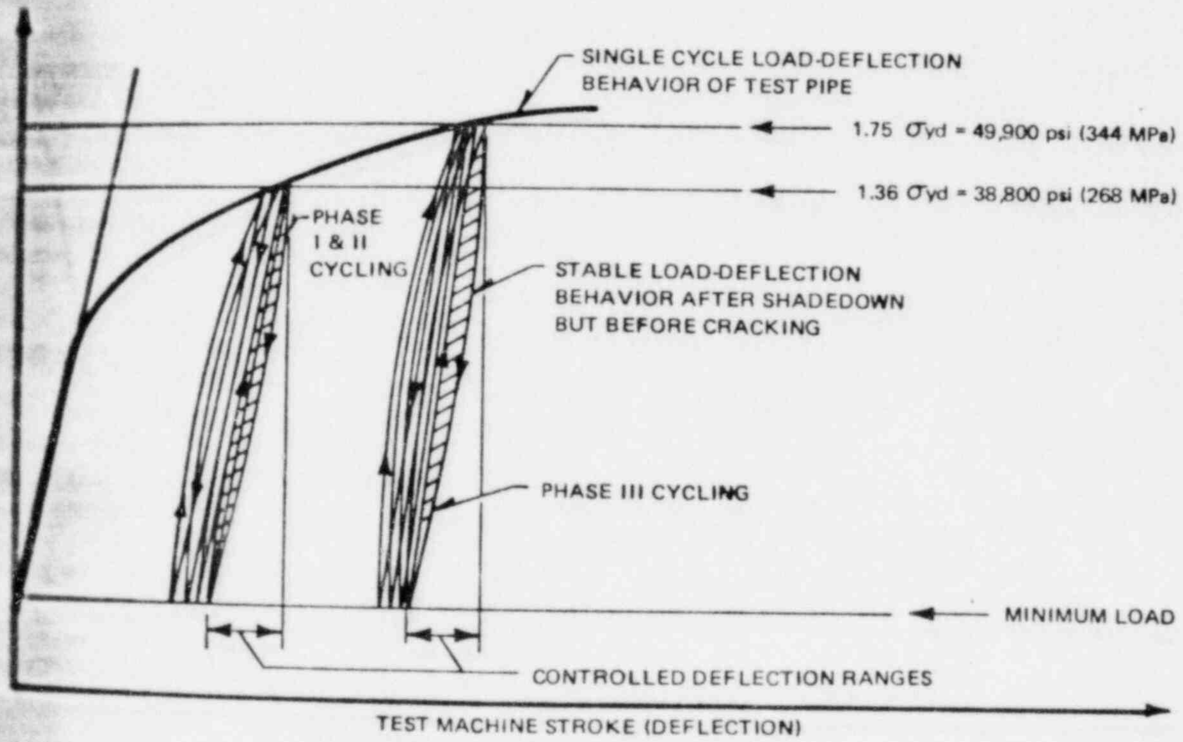

Figure 5. Demonstration of Shakedown Behavior

The maximum stress for each of the Large Environmental Fatigue Test Facility tests was selected to be equal to maximum bending stress used in the CL-4 bending tests. That stress level was 38,800 psi (268 MPa) which is 136% of 550°F (280°C) yield strength of the test material. The calculated stress level did not include pressure or residual stresse

During later phases of the second and fourth Large Environmental Fatigue Test Facility tests the maximum st level was increased to 175% of the 550°F (280°C) yield strength to further accelerate cracking.

2. Cyclic Wave Shape

The cyclic wave shape or control wave form used during all phases of each Large Environmental Fatigue Test Fac test was trapezoidal with a period of 1.5 hours (see Figure 6). During each cycle, the specimen was subjected to 5 minute minimum load [5000 lb (2268 kg)], 5 minutes during rising load, 75 minutes at full load and 5 minutes during decreasing lo The test frequecy was therefore 0.67 cycle per hour.

3. Test Environment

During all phases of the testing a high oxygen (8-12 ppm) demineralized water environment at 545°F (285°C) a 1120 psig (7.7 MPa) was circulated through the inside of the specimen. The flow rate was approximately 2-3 gpm (7.5-11 l/min). The electrical conductivity of the water was maintained below 1 μmho/cm (2.54 μmho/in.). Load was not applied u these conditions were established.

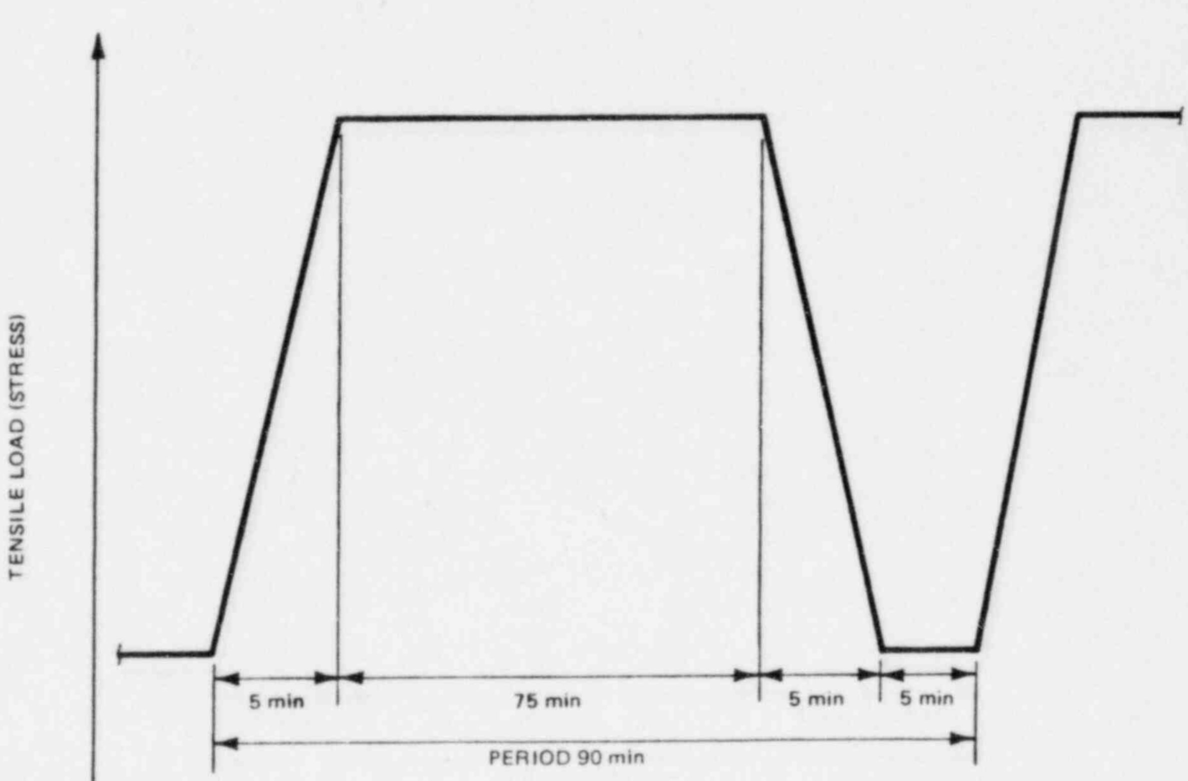

Figure 6. Cyclic Test Waveform

3.1.2 Discussion of Results

3.1.2.1 Second Full Size Cyclic Intergranular Stress Corrosion Cracking Pipe Test (Second Large Environmental Fatigue Test Facility Test)

a. Fabrication of the Test Pipe

The test weldment for the second Large Environmental Fatigue Test Facility cyclic tension test was composed of eight pipe segments and two end pieces, all joined by insert-type groove welds to produce a composite pipe of 32 inches (81.3 cm) in length, plus end pieces. Each segment was prepared with a unique material, weld practice, or weld treatment (e.g., inside surface temperature control, corrosion resistant cladding, solution heat treatment after butt welding). The weldment tested in Phase I of the test program is shown schematically in Figure 7 and the remade weldment tested in Phases II and III of the test program is presented in Figure 8. Also included in Figures 7 and 8 is a listing of the specific fabrication process used for each weldment. In Figures 9 and 10, the completed pipe weldment is shown in the Large Environmental Fatigue Test Facility. One of the remedies, the corrosion resistant cladding, was applied to the pipe inside surface both as an overlay and as an inlay for this test. When applied as an overlay, the clad pipe wall thickness was typically 0.380 inch (0.97 cm) whereas the inlayed clad pipe had a wall thickness which typically was 0.300 inch (0.76 cm). Consequently, the pipe test only stressed the overlayed weld heat affected zone to about 100% of the 288°C engineering yield strength. One of the overlayed welds (F2) and one inlayed weld (H1) were solution heat treated following the cladding whereas the overlayed weld (F1) was not solution heat treated after cladding. The solution heat treatment consisted of 1950°F (1066°C) for 1/2 hour plus water quench. In the screening test, Type-312 stainless steel weld metal was used as the pipe cladding material because of its high ferrite content in the as-deposited condition.

Both standard heat input welds practice and high heat input welds practice were used in the fabrication of the test weldment. Standard heat input practice is considered 40,000 joules/in. (15,750 joules/cm), maximum, with the first two weld layers formed by gas tungsten arc welding and the remaining two layers by shielded metal arc practice. For the high heat input welds, gas tungsten arc welding was employed for all the layers and the heat input was limited to a maximum of 76,000 joules/in. (30,000 joules/cm).

The pipes were welded in the 1 g position (pipe rotating, welding downhand) to produce welds as repeatable as practical using manual welding techniques. All welding start and stop locations were recorded and have been maintained in laboratory log books.

b. Description of Pipe Test in Large Environment Fatigue Test Facility

The pipe test was performed in the Large Environment Fatigue Test Facility at 288°C (550°F) in 8 ppm oxygenated water. The maximum stress applied to the pipe initially was 136% of the Type-304 stainless steel yield strength and the loading frequency was 0.67 cycle/hour. A detailed description of the test general procedure for all Large Environmental Fatigue Test Facility tests is presented in Subsection 3.1.1.3.

The testing was performed in three phases. The first phase of this test was defined as the period from the start of the test until a through-wall leak occurred near one of the unprotected test welds (Weld E2) after 233 hours (see Figure 7 for weld location). Subsequent ultrasonic examination near other unprotected welds revealed crack indications at welds B2, C1, D1, E2 and E1. A section of the specimen, including all of the ultrasonic test indications and the leaking crack, was then cut and removed for visual, dye penetrant, and metallographic verification of cracking and cracking mode.

To continue the test on the remaining uncracked welds, a new 4-in. (10.16-cm) long piece of centrifugally cast CF8 pipe was butt welded into the specimen between the points where the cuts were made. This re-welded specimen was then put back on test to begin Phase II.

The second phase of the test was stopped after 891 hours of additional testing for an ultrasonic test examination. No crack indications were identified in the pipe specimen and the pipe was returned to test.

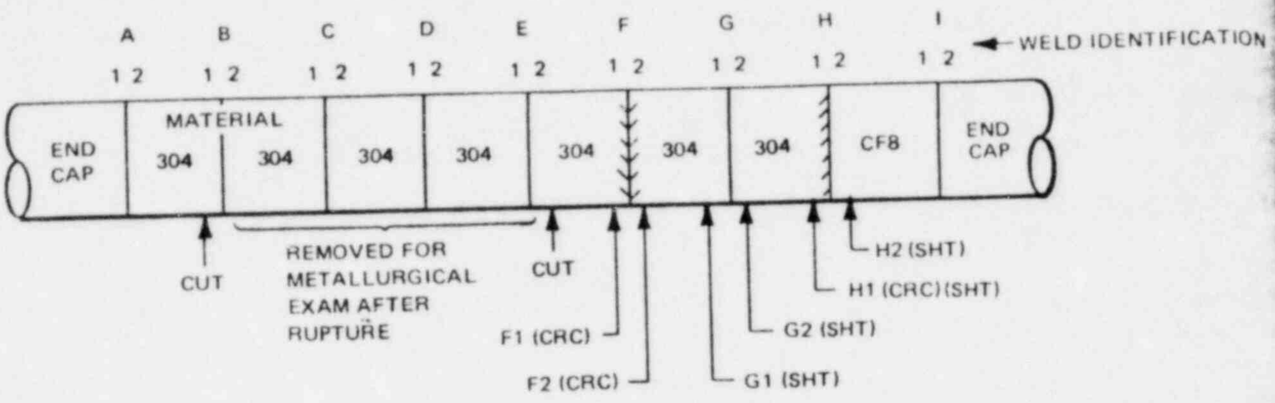

CRC – CORROSION RESISTANT CLADDING
SHT – SOLUTION HEAT TREATMENT

PIPE END PREPARATION INDENTIFICATION	INSIDE SURFACE	HEAT INPUT	HEAT TREATMENT	WELD DEPOSIT	MATERIAL TYPE	HEAT NO.
B1	GROUND	NORMAL[a]	NONE	NONE	316SS	2P6429
B2	GROUND	NORMAL[a]	NONE	NONE	304	M7616
C1	GROUND	HIGH[b]	NONE	NONE	304	M7616
C2	GROUND	HIGH[b]	NONE	NONE	304	M7772
D1	GROUND	NORMAL	NONE	NONE	304	M7772
D2	GROUND	NORMAL	NONE	NONE	304	454659
E1	GROUND	HIGH	NONE	NONE	304	454659
E2	GROUND	HIGH	NONE	NONE	304	M7616
F1	GROUND	NORMAL	NONE	OVERLAY	304	M7616
F2	GROUND[c]	NORMAL	SHT[d]	OVERLAY	304	M7616
G1	GROUND[c]	NORMAL	SHT[d]	NONE	304	M7616
G2	GROUND[c]	NORMAL	SHT[d]	NONE	304	M7616
H1	GROUND[c]	NORMAL	SHT[d]	INLAY	304	M7616
H2	GROUND[c]	NORMAL	SHT[d]	NONE	CF8	98695

a – 40,000J/in. (15, 750J/cm)

b – 76,000J/in. (30,000 J/cm)

c – PRIOR TO SOLUTION HEAT TREATMENT

d – SOLUTION HEAT TREATED OVERLAY PRIOR TO BUTT WELD

Figure 7. Phase I — Original Weldment Makeup for Second Cyclic Tension Test in Large Environmental Fatigue Test Facility

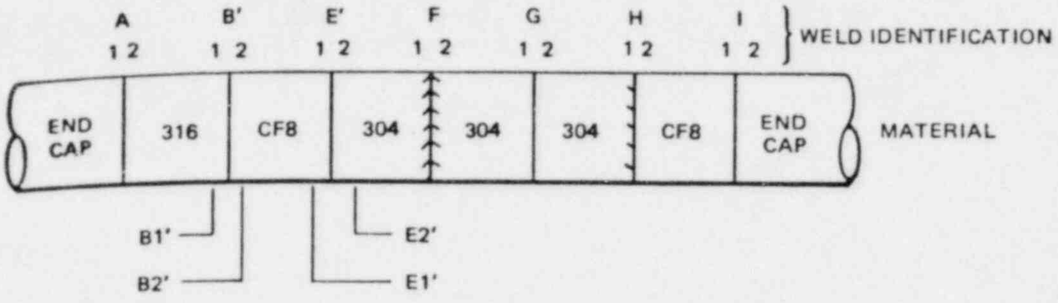

PIPE END PREPARATION IDENTIFICATION	INSIDE SURFACE CONDITION	HEAT INPUT	HEAT TREAT	WELD DEPOSIT	MATERIAL TYPE	HEAT NO.
B1'	MACHINED	NORMAL	NONE	NONE	316SS	2P6429
B2'	MACHINED	NORMAL	NONE	NONE	CF8	P521
E1'	MACHINED	NORMAL	NONE	NONE	CF8	P521
E2'	MACHINED	NORMAL	NONE	NONE	304	M7616
F1	GROUND	NORMAL	NONE	OVERLAY	304	M7616
F2	GROUND[a]	NORMAL	SHT[b]	OVERLAY	304	M7616
G1	GROUND[a]	NORMAL	SHT[b]	NONE	304	M7616
G2	GROUND[a]	NORMAL	SHT[b]	NONE	304	M7616
H1	GROUND[a]	NORMAL	SHT[b]	INLA	304	M7616
H2	GROUND[a]	NORMAL	SHT[b]	NONE	CF8	98695

[a] – PRIOR TO SOLUTION HEAT TREATMENT

[b] – SOLUTION HEAT TREATED

Figure 9. Phases II and III — Re-made Weldment

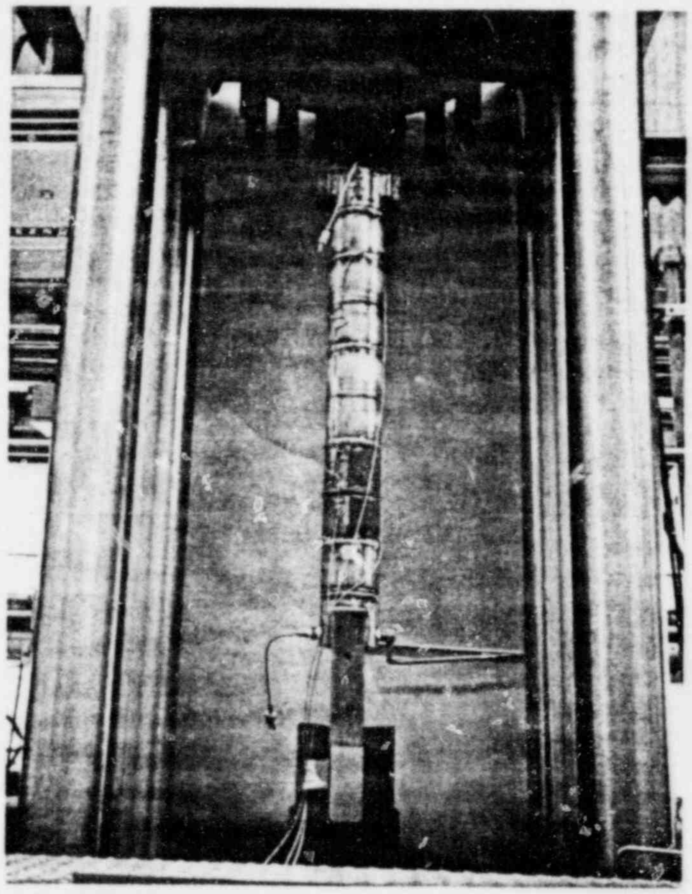

Figure 9. Pipe Weldment for Second Cyclic Tension Test in Large Environmental Fatigue Test Facility

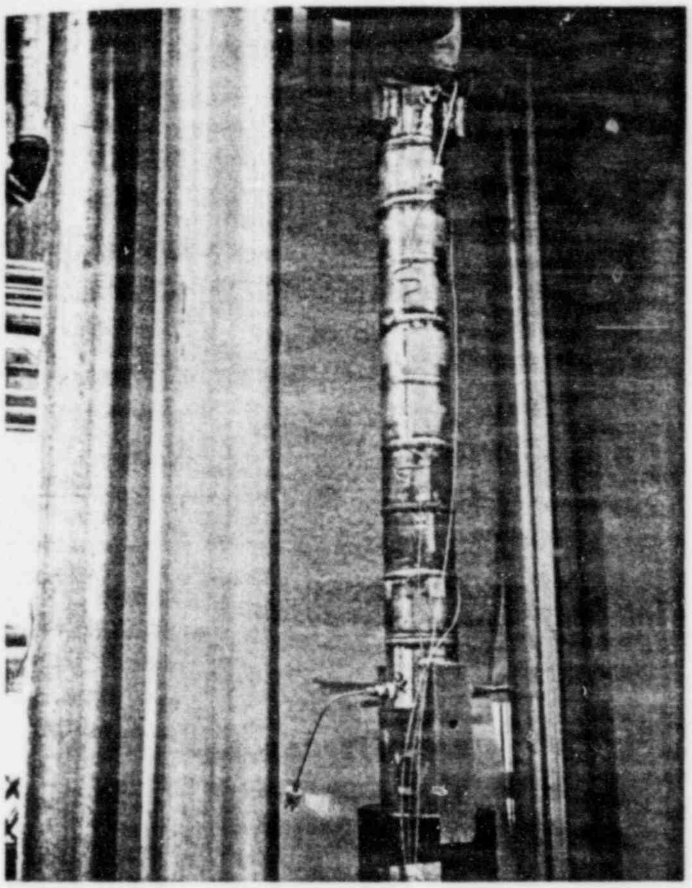

Figure 10. Another View of Pipe Weldment Shown in Figure 9

The load was then increased to 175% of the Type-304 stainless steel yield strength at temperature to furth accelerate cracking. This third phase of the test ran for 260 additional hours. Ultrasonic testing performed after this ti identified cracking in the heat affected zone of weld E2′ (see Figure 8 for location of Weld E2′). The pipe was cut apart and complete dye penetrant inspection was performed. Cracking was identified in the heat affected zones of additional welds. complete weld-by-weld summary including test time and cracking data is presented in Table 1 for the reference welds and Table 2 for the remedy welds. Metallurgical investigation of the cracked welds followed the dye penetrant tests.

3. Post-Test Metallurgical Examination of Second Large Environmental Fatigue Test Facility Pipe

The primary method used for periodically inspecting the test welds for crack initiation was during testing by ultrason measurement. Baseline ultrasonic test measurements were made and recorded at the beginning of each phase of testing These measurements were then compared to the data obtained at the end of each phase. Changes relative to the baseline were assumed to be indications of cracking. When significant ultrasonic test indications were identified, visual and dye penetrant inspections were performed on the pipe. In each case post-test metallurgical evaluation was performed t determine the extent of cracking and crack morphology. This metallurgical evaluation included macro examination of the pipe inside surface and macro and micro examination by destructive metallography.

The macro and micro examination of each of the welds where dye penetrant indications were observed confirmed the cracking as intergranular stress corrosion cracking in the weld heat affected zone. This result was particularly surprising for the cast CF8 pipe where no cracking was expected (Weld E1′). Subsequent ferrite measurements of this weld indicated that the residual ferrite was less than 5%. A comparison welded cast pipe section with 11% to 14% ferrite (Weld H2) did not crack during the test. A photograph of typical cracking observed in the cast pipe with less than 5% ferrite is shown in Figure 11 where an interdendritic stress corrosion crack is seen with a depth of 136 mils (0.35 cm). Additional stress corrosion cracks were observed in this pipe weld heat affected zone with crack depth of from 13 to 144 mils (0.033 to 0.360 cm).

The crack depths for these cracks were surprising considering that the cracks on the pipe inside surface were no more than 80 mils (0.2 cm) in length. The extremely short crack fronts in this material were probably a result of the long columnar grains extending in the direction of crack growth providing an easy path crack propagation. An additional factor contributing to the rapid crack growth was the very high level of applied stress during this phase of the test [175 percent of 288°C (550°F) yield stress].

A typical crack in the reference unprotected Type-304 stainless steel weld heat affected zone (Weld E2′) is presented in Figures 12 and 13. As seen in Figure 12, multiple cracking at a distance of 0.2 to 0.3 inch from the weld fusion line occurred. A micro section shown in Figure 13 shows a typical intergranular crack to a depth of 51 mils (0.13 cm). The cracking in this pipe occurred at 175% of the 288°C (550°F) yield strength. No grinding was performed on this weld.

One conclusion resulting from this pipe test is that grinding, particularly post-weld grinding, is a clear accelerant to intergranular stress corrosion cracking in as-welded Type-304 stainless steel piping. In Figure 14 a photomacrograph shows the cracking on the C1 side on the heat affected zone of Weld C in the pre-weld and in the post-weld regions of the pipe. Of particular interest is the intergranular stress corrosion cracking observed exclusively in three localized ground spots where the grinding wheel accidentally contacted the pipe inside surface after butt welding. Cracks are observed to initiate only in these three localized grind spots as shown in Figure 14. This evidence and the large extent of cracking in general in the ground regions on the pipe inside surface, provide evidence that grinding is a strong accelerant to intergranular stress corrosion cracking in welded Type-304 stainless steel piping.

4. Conclusions

The following findings or observations can be made on the results of the second Large Environmental Fatigue Test Facility cyclic tension test.

(1) The laboratory pipe tests duplicate the intergranular stress corrosion cracking found in Type-304 stainless steel piping used in boiling water reactor systems.

Table 1

TEST SUMMARY, UNPROTECTED TYPES-304 AND -316 STAINLESS STEEL TEST WELDS, SECOND LARGE ENVIRONMENTAL FATIGUE TEST FACILITY CYCLIC PIPE TEST

Pipe Material	Heat No.	Weld Heat[a]	Grinding Pre (0-90°) Post (180-270°)	Weld Identification	Test Phases I $\sigma = 1.36\ \sigma yd$	Test Phases II $\sigma = 1.36\ \sigma yd$	Test Phases III $\sigma = 1.75\ \sigma yd$
316	2P6429	Std	Both	B1		No cracks by DP	
304	M7616	Std	Both	B2		4 cracks by DP	
304	M7616	High	Both	C1		4 cracks by DP	
304	M7772	High	Both	C2		No cracks by DP	
304	M7772	Std	Both	D1		No cracks by DP	
304	454659	Std	Both	D2		1 crack by DP	
304	454659	High	Both	E1		No cracks by DP	
304	M7616	High	Both	E2		1 leak + 1 crack by DP	
316	2P6429	Std	None	B1'		No cracks by UT	No cracks by PT
304	M7616	Std	None	E2'		No cracks by UT	6 cracks by PT
					124	718	891 Test cycles
					233	1124	1384 Test hours

---

[a] Std = 40,000 J/in (15,750 J/cm), Maximum
High = 76,200 J/in (30,000 J/cm), Maximum
DP = Dye Penetrant
UT = Ultrasonic Test
PTM = Post Test Metallurgical

Table 2
TEST SUMMARY; PROTECTED (FIXES) TEST WELDS, SECOND LARGE ENVIRONMENTAL FATIGUE TEST FACILITY CYCLIC PIPE TEST

				Protection Method[b]				Test Phases		
Pipe Material	Heat No.	Weld Heat[a]	Grinding	CRC	SHT	New Material	Weld Identification	I $\sigma_{max} = 1.36\ \sigma yd$	II $\sigma_{max} = 1.36\ \sigma yd$	III $\sigma_{max} = 1.75\ \sigma yd$
304	M7616	Std	180-270°	312 overlay	None	No	F1	NC[c]	NC	NC
304	M7616	Std	180-270°	312 overlay	Yes BBW[d]	No	F2	NC	NC	NC
304	M7616	Std	0-90°	None	Yes ABW[d]	No	G1	NC	NC	NC
304	M7616	Std	0-90°	None	Yes ABW[d]	No	G2	NC	NC	NC
304	M7616	Std	180-270°	312 overlay	Yes BBW[d]	No	H1	NC	NC	NC
CF8	ESCO	Std	180-270°	None	Yes BBW[d]	CF8	H2	NC	NC	NC
CF8	WISC.	Std	None	None	None	CF8	B2′		NC	3 small crack indications by PT
CF8	WISC.	Std	None	None	None	CF8	E1′		NC	3 small cracks found by PT
								124	718	891 Test Cycles
								235	1124	1384 Test Hours

---

[a] Std Heat = 40,000 J/in. (15,750 J/cm)
[b] CRC = Corrosion Resistant Cladding
SHT = Solution Heat Treatment — Solution Anneal
[c] NC = No Cracks Detected by Ultrasonic Test
UT = Ultrasonic Test
PT = Post-Test Metallurgical
[d] BBW — Before Butt Weld
ABW — After Butt Weld

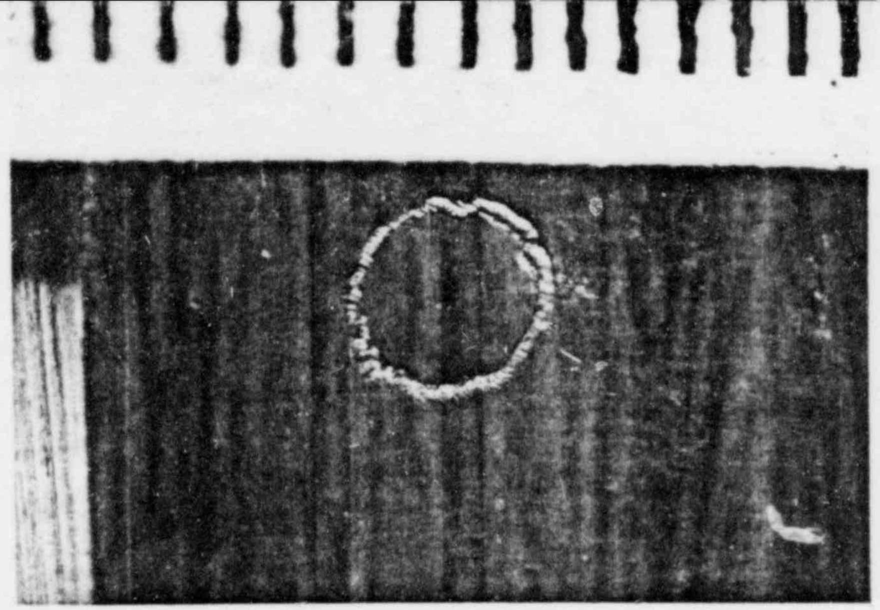

7X

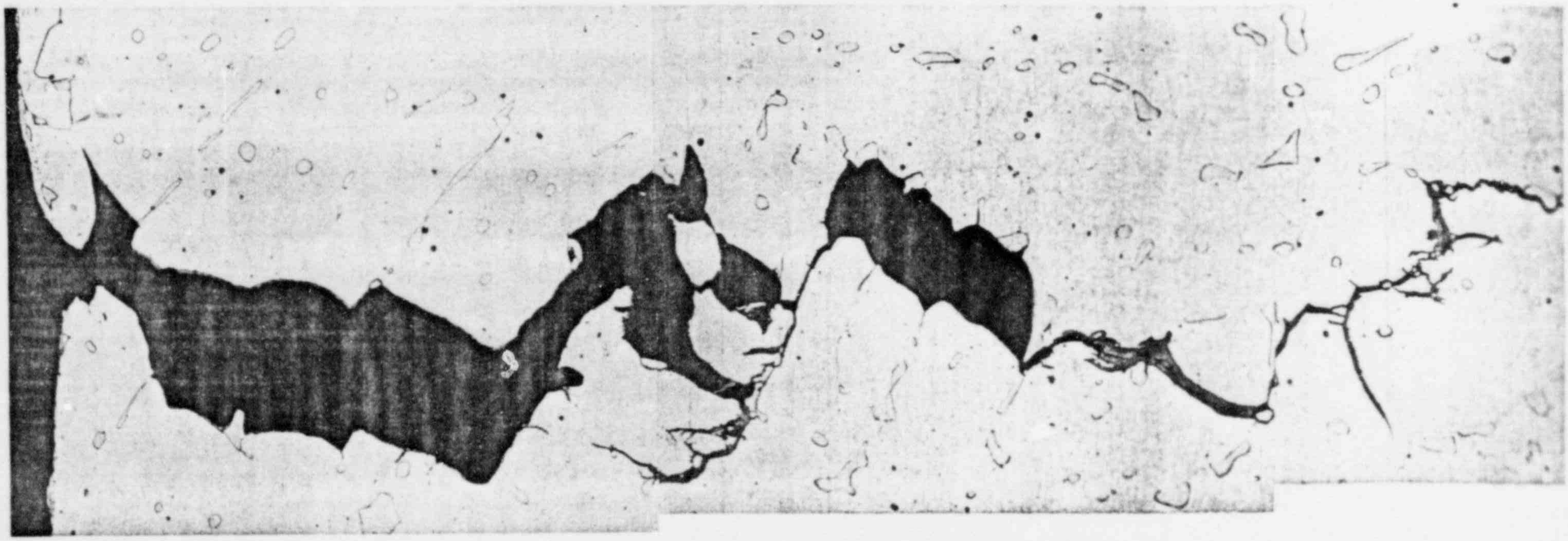

750X

Figure 11 Ma

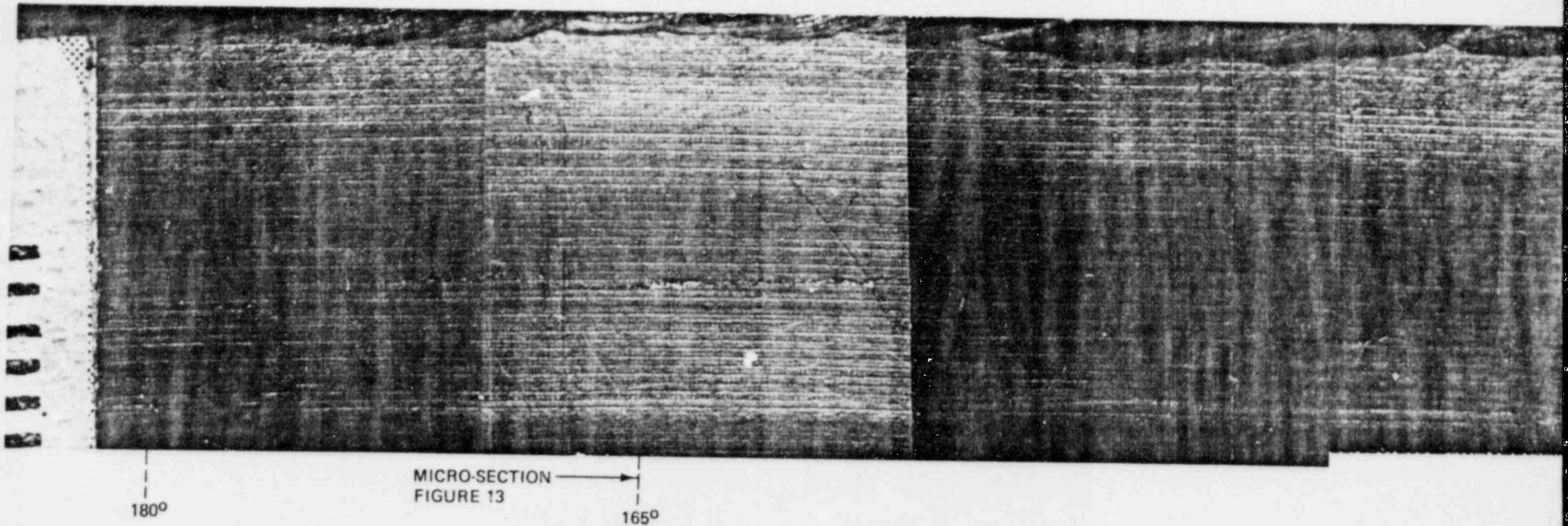
180°
MICRO-SECTION FIGURE 13
165°

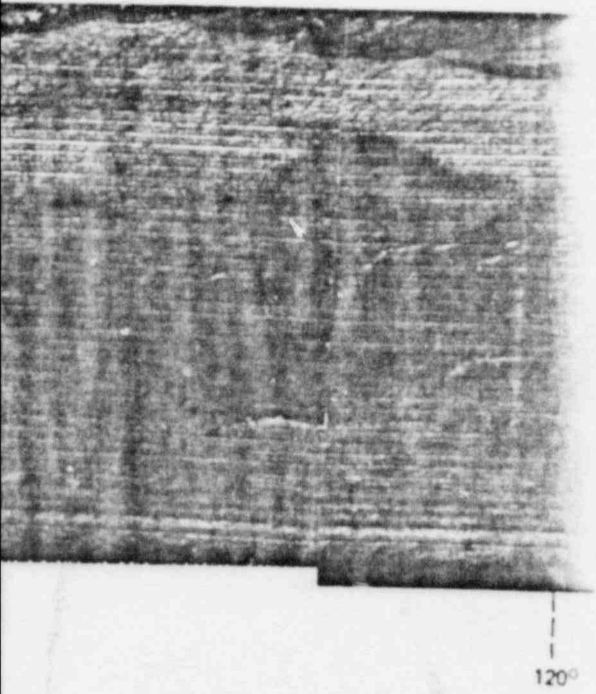

Figure 12. Macro Phot
Crack in Ty
Weld Heat A
120 to 180 D

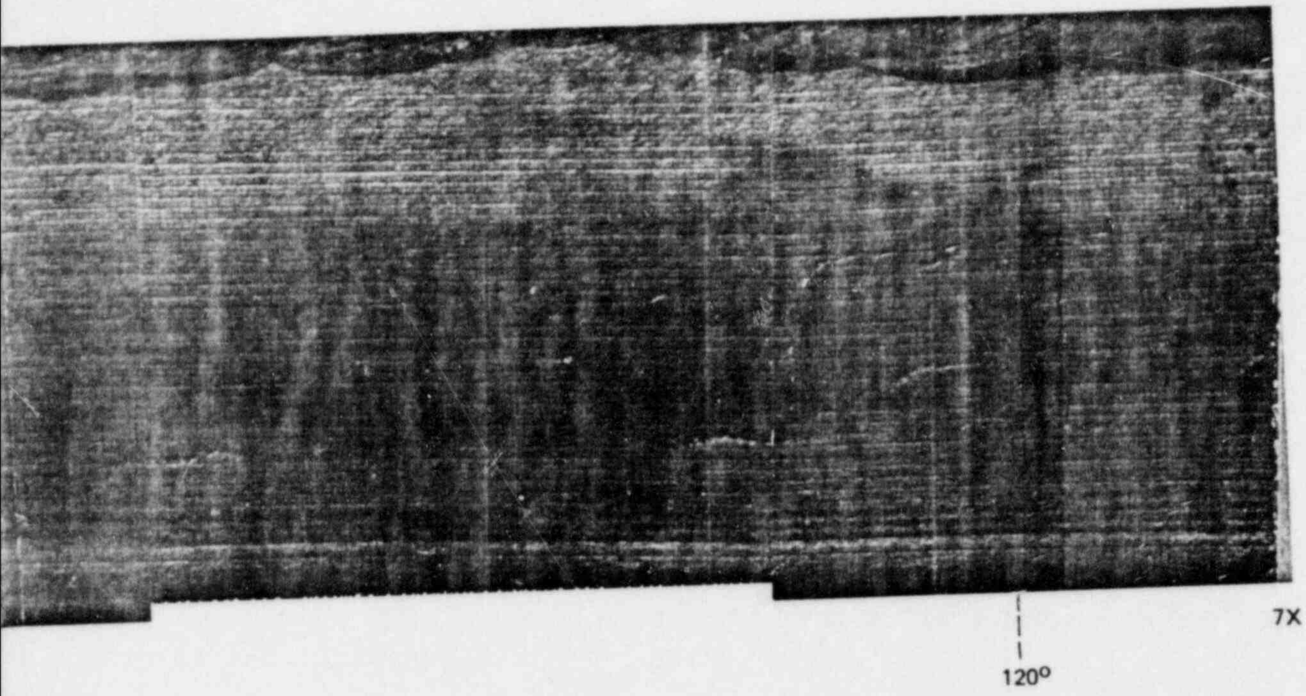

Figure 12. *Macro Photograph of Intergranular Crack in Type-304 Stainless Steel Weld Heat Affected Zone, Side E2', 120 to 180 Degrees*

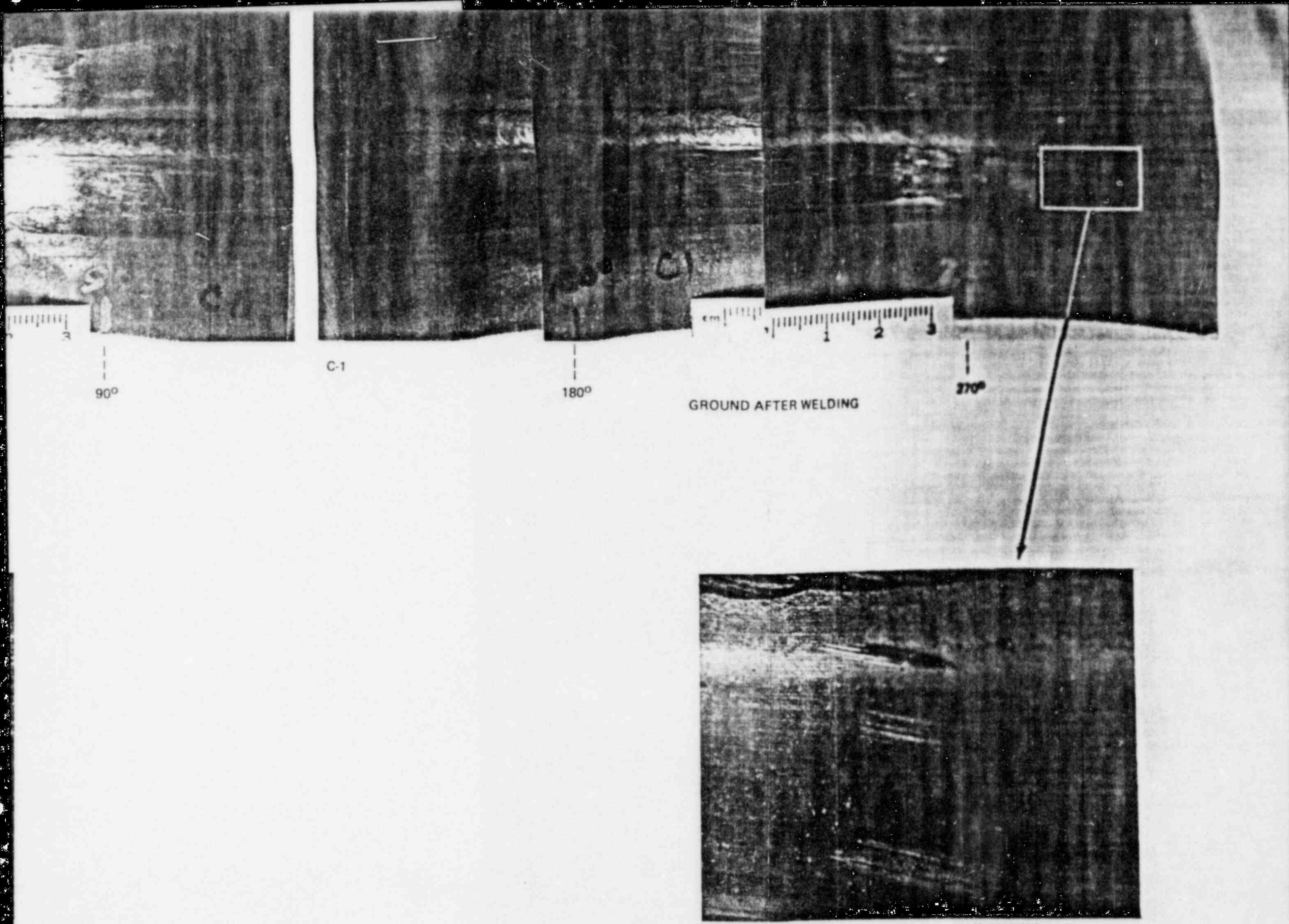

Figure 14. Weld C Inside Pipe Showing Cracks on C1 Side in Machined Regions, in Large Ground Areas, and in Localized Ground Spots

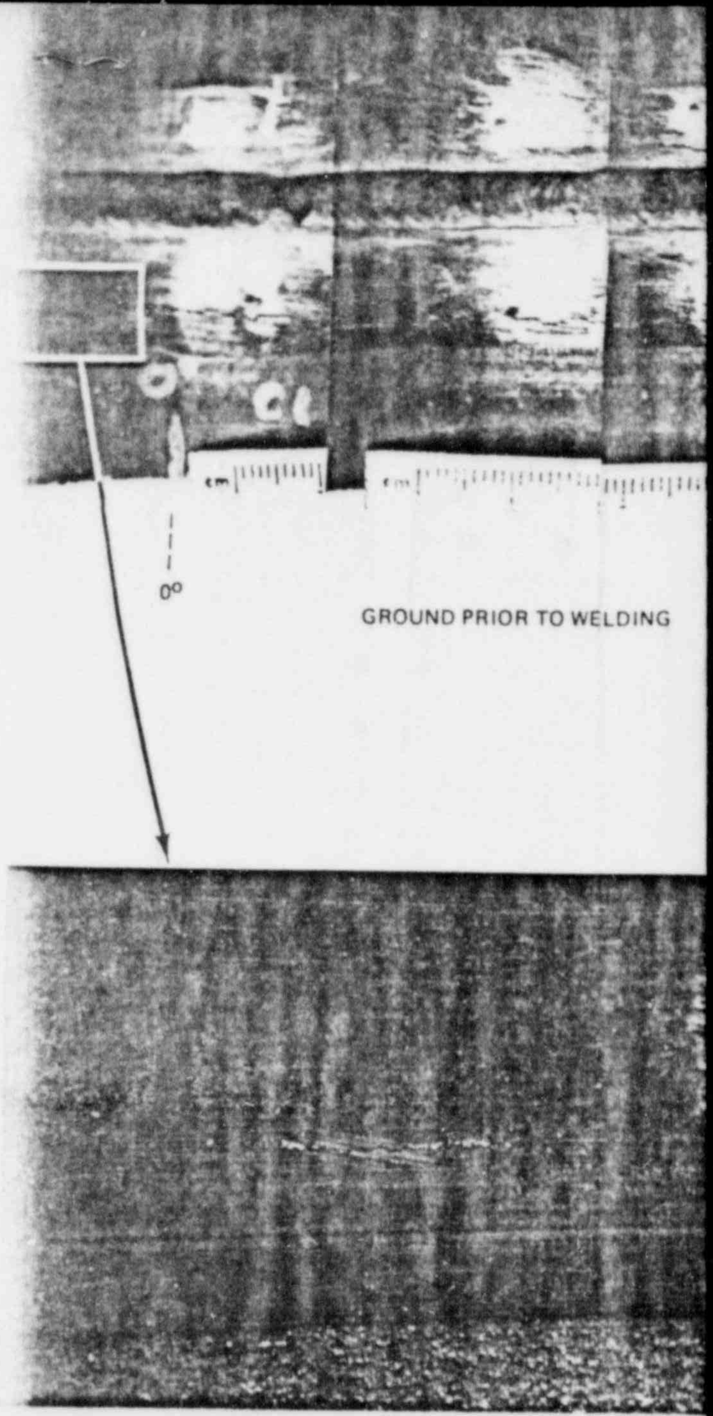
cm
cm
0°
GROUND PRIOR TO WELDING

(2) Under the test conditions described the pipe remedy methods were effective in preventing intergranular stress corrosion cracking with the possible exception of one heat of CF8 pipe where the ferrite level was below the minimum 8% level recommended for boiling water reactor use. The others remedies survived all three phases of this test (1384 hours) without cracking.

(3) The combination of low frequency — high stress loading, high oxygen environment, high heat input welds, and surface grinding appears to accelerate intergranular stress corrosion cracking in Type-304 stainless steel as seen by comparing failure times with those of field failures.

(4) Unprotected welds in Type-304 stainless steel will crack even with controlled welding heat input and no grinding, but the cracking takes longer.

(5) Mistreatment of unprotected Type-304 stainless steel welds has an additional accelerating effect. The order of decreasing severity appears to be:

   a. High heat input plus inside surface grinding.
   b. Controlled heat input [~40,000 J/in. (15,750 J/cm)] plus post-weld grinding.
   c. High heat input without grinding.
   d. Controlled heat input without grinding.

(6) Laboratory ultrasonic inspection can effectively locate inside surface cracks from intergranular stress corrosion cracking in Type-304 stainless steel pipe weldments before deep penetration and leaking occur when a prior, well-documented, sensitive baseline inspection has been performed.

(7) Minute grinding marks are sufficient to trigger integranular stress corrosion cracking in Type-304 stainless steel heat affected zones.

3.1.2.2 Third Full Size Cyclic Intergranular Stress Corrosion Cracking Pipe Test (Third Large Environmental Fatigue Test Facility Test)

1. The third full-size cyclic intergranular stress corrosion cracking pipe test was designed to test exclusively the heat sink welding pipe remedy. The welded pipe was fabricated by joining eight 4-in. (10.16-cm) long 4-in. schedule 80 pipe segments of Type-304 stainless steel as shown in Figure 15. However, unlike the second Large Environmental Fatigue Test Facility test, additional transition piece was included as part of the welded pipe so that two additional welds could be tested, welds A and I. This transition piece consisted of 4-in.-diameter schedule 160 Type-316 stainless steel, one end of which was machined to schedule 80 in order to match the Type-304 stainless steel pipe.

This full-size-pipe test was performed to explore potential benefits to be derived from heat sink welding of Type-304 stainless steel pipe. Prior laboratory work at General Electric on inside surface water cooled Type-304 stainless steel pipe welds indicated that inside surface water cooling reduced the time that weld heat affected zones spent in the sensitizing temperature range. This third Large Environmental Fatigue Test Facility test was designed to explore the benefits indicated in the laboratory tests.

The test welds were fabricated from Heat M7616 Type-304 stainless steel piping, which had failed readily in the second Large Environmental Fatigue Test Facility cyclic tension test as welded pipe in both the ground and unground conditions as both high- and low-heat-input welds (for both the heat sink and the reference welds). Pre- and post-weld grinding was applied to quadrants of each weld. The weld fabrication description and summary of fabrication treatments are presented in Figure 16.

The inside surface cooling procedure for the heat sink welds originates from prior General Electric laboratory tests. A description of this technique follows.

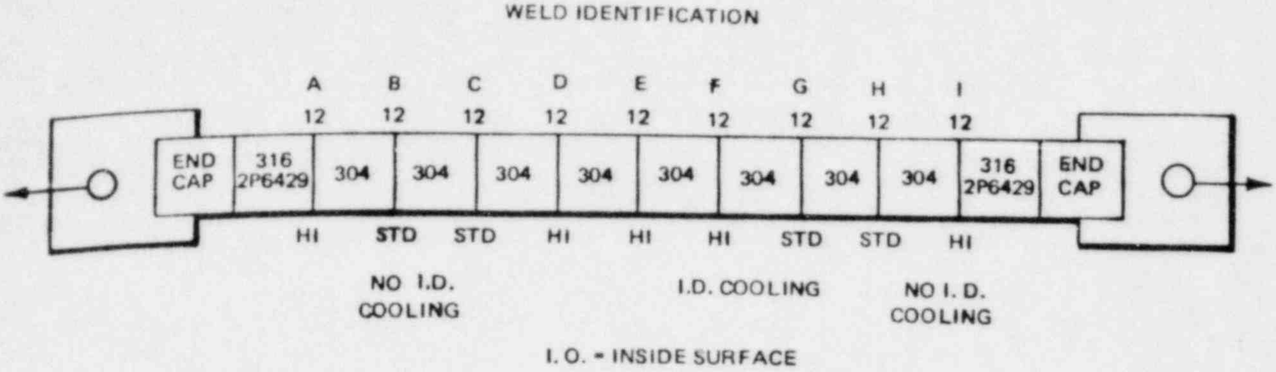

NOTES: 1. WELD HEAT INPUT
HI ≃70,000J/in. (27,560J/cm)
STD ≃40,000J/in. (15,750J/cm)

2. GRINDING DETAILS ALL TEST WELDS A THROUGH 1
0 - 90° GRIND PRIOR TO WELDING
90 - 180° NO GRINDING
180 - 270° GRIND AFTER WELDING
270 - 360° NO GRINDING

3. ALL TYPE-304 STAINLESS STEEL FROM HEAT M7616 (THE MOST SUSCEPTIBLE HEAT)

Figure 15. Test Configuration, Third Cyclic Tension Test in Large Environmental Fatigue Test Facility

The heat sink welding practice used to prepare this welded pipe did not include any cooling of the root layer, other than the normal gas back purging. Subsequent weld passes were water spray cooled on the inside surface using the following procedure:

- A 1-in. (2.54-cm) outer diameter spray nozzle was fabricated from galvanized pipe.
- At the pipe end 16 holes, each 1/16 inch (0.16 cm) in diameter were drilled in an equally spaced pattern.
- A water flow rate of 2 gpm (0.15 l/sec) was employed for spray cooling. This was obtained by use of a regulator providing 9 psi (0.0063 kg/mm²) water pressure.
- The spray nozzle was inserted in the pipe a correct distance to completely cover the weld area with water spray.
- The pipe was rotated during welding while the welder added filler metal at the 12 o'clock position (1 g).

It was possible to visually observe the pipe inside surface during this operation and a momentary bright red color was visible in the area under the weld arc. However, the outside surface temperature of the weld immediately after welding was approximately 70°F (21°C). Standard-heat-input welds were limited to 40,000 J/in. (15,750 J/cm). The welding procedures for the reference Type-304 stainless steel welds are as described in the Second Large Environmental Fatigue Test Facility cyclic tension test.

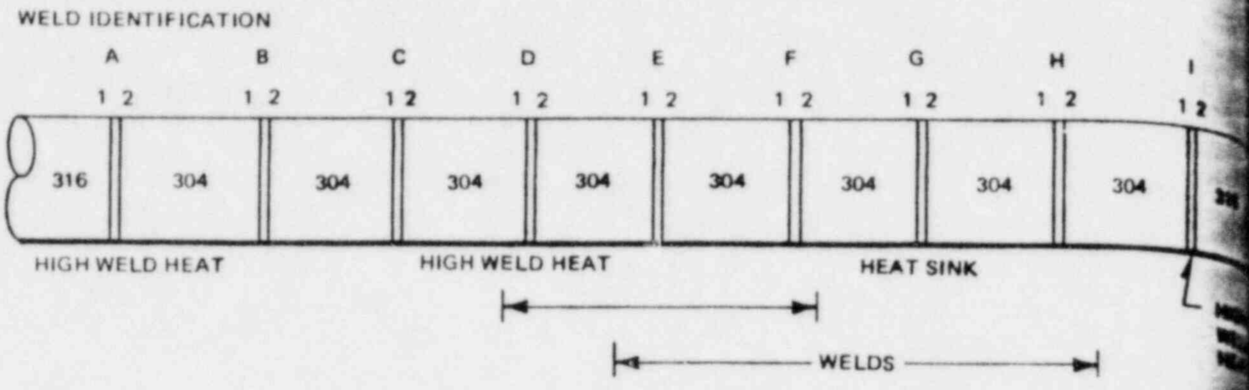

NOTES:

1. THE HIGH HEAT INPUT ON WELDS A, D, E, F, AND I WAS PRIMARILY APPLIED IN PASS 2.
2. THE WATER COOLED WELDS (E, F, G, & H) WERE WATER SPRAYED ON THE INSIDE SURFACE DURING PASSES 2, 3, AND THE CROWN.
3. SUMMATION OF FABRICATION TREATMENTS:

WELD IDENTIFICATION	HEAT AFFECTED ZONE	HEAT INPUT	GRINDING ON INSIDE SURFACE	WATER COOLED
A	A1	HIGH	QUADRANT[a]	NO
	A2	HIGH	QUADRANT[a]	NO
B	B1	NORMAL	QUADRANT[a]	NO
	B2	NORMAL	QUADRANT[a]	NO
C	C1	NORMAL	QUADRANT[a]	NO
	C2	NORMAL	QUADRANT[a]	NO
D	D1	HIGH	QUADRANT[a]	NO
	D2	HIGH	QUADRANT[a]	NO
E	E1	HIGH	QUADRANT[a]	YES
	E2	HIGH	QUADRANT[a]	YES
F	F1	HIGH	QUADRANT[a]	YES
	F2	HIGH	QUADRANT[a]	YES
G	G1	NORMAL	QUADRANT[a]	YES
	G2	NORMAL	QUADRANT[a]	YES
H	H1	NORMAL	QUADRANT[a]	YES
	H2	NORMAL	QUADRANT[a]	YES
I	I1	HIGH	QUADRANT[a]	NO
	I2	HIGH	QUADRANT[a]	NO

[a]GRINDING QUADRANT	CONDITION OF COUNTERBORE
0 - 90°	GROUND PRIOR TO WELDING
90 - 180°	NO INSIDE SURFACE GRINDING OR REPAIR
180 - 270°	
270 - 360°	GROUND AFTER WELDING

Figure 16. Fabrication Description for Third Cyclic Tension Test

3 Description of Third Cyclic Tension Test in the Large Environmental Fatigue Test Facility

The third cyclic intergranular stress corrosion cracking pipe test was performed in the Large Environmental Fatigue Test Facility using the same cyclic loading conditions, water chemistry, and test temperature as described in the generalized test procedure for the Large Environmental Fatigue Test Facility tests (see Subsection 3.1.1.3). The maximum load applied to this pipe was 136% of the Type-304 stainless steel yield strength at test temperature. The test consisted of one phase which lasted 122 test cycles (183 hours) when a through-wall leak developed in the heat affected zone of one of the reference welds. Subsequent ultrasonic testing and liquid penetrant examination revealed cracks in 14 of the 16 Type-304 stainless steel weld heat affected zones (8 of 8 reference and 6 of 8 inside-surface-cooled-weld heat affected zones). No cracking was observed in the two Type-316 stainless steel weld heat affected zones. A post-test examination including macro and micro photography was instituted to identify the extent of cracking and the fracture morphology of the test welds.

3 Post-Test Nondestructive Testing and Metallurgical Examination

The nondestructive examination of the test weldment used in the third test included acoustic emission monitoring of cracking noise during this test and ultrasonic examination of the test welds before and after the test. The acoustic emission monitoring program was performed in hope that one could discern a recognizable pattern which would provide useful information regarding the onset of crack initiation and crack propagation rates as well as predicting specimen failure.

The ultrasonic test post-test inspection indentified crack indications in 15 of the 16 welds. The indications ranged from multiple cracks extending 360 degrees around the pipe (as shown in unprotected weld heat affected zones A2, D1, and I1), to small indications of 1/2 inch (1.27 cm) in length (as presented in heat sink weld heat affected zone F2). A schematic display of the ultrasonic test results is presented in Figure 17 along with the welding and grinding specimen details.

Following the ultrasonic examination, the pipe was cut axially into two halves and liquid red dye penetrant measurements were performed on the inside surface of the pipe to confirm the findings of the post-test ultrasonic examination of the pipe. The penetrant indications on the pipe confirmed the ultrasonic test indications and revealed cracks in 14 of the 16 heat affected zones in the welded pipe. These heat affected zones included all eight of the reference heat affected zones and six of eight of the heat-sink-welded heat affected zones. No cracking was found in the two Type-316 stainless steel heat affected zones. A schematic summary of the liquid penetrant indications is also presented in Figure 17. The results are nearly identical to those presented in the ultrasonic test summary, as shown in Figure 17. The only discrepancies occurred in the heat sink welds E2 and F2 where small-amplitude ultrasonic test indications were observed which were not confirmed by liquid penetrant.

It is noteworthy that the cracking in the six heat affected zones of the heat sink welds is almost exclusively associated with post weld grinding. Only in weld heat affected zone E1 does the cracking appear to extend appreciably beyond the post weld ground region and the weld E is a high-heat-input weld. Another observation is that the cracking is much more extensive in the reference Type-304 stainless steel welds with eight out of eight heat affected zones cracked and the cracking generally extends into the unground and ground welding regions as well as being on the post-weld ground pipe surface. Table 3 summarizes the dramatic difference in degree of cracking between the reference and heat sink welds when measured on a quadrant-by-quadrant basis. It appears clear that almost all (if not all) of the cracking in the heat sink weldments was associated with post-weld grinding. Post-weld grinding typically introduces high tensile residual stresses on Type-304 stainless steel piping surfaces (see results of Electric Power Research Institute/General Electric Program RP 449-2 for details, NEDO-20985-1 through -5). This post-weld grinding procedure probably overwhelmed the more favorable stress state which existed following heat sink welding, thus providing a condition of initiation of intergranular stress corrosion cracking. These results show the dominant effect of state of surface stress on the intergranular stress corrosion cracking susceptibility of Type-304 stainless steel in this environment. The differences in the extent of intergranular stress corrosion cracking between the heat sink welds and the reference welds are shown in Figures 18 and 19. In Figure 18, the heat sink welds G and H are shown at 3X magnification on the pipe inside surface. The linear crack indications in the ground regions in the heat affected zone of each weld can be observed (with the aid of liquid penetrant). The cracks are exclusively associated with the grinding and are very tight. One was unable to see the cracks visually without the aid of liquid penetrant. A section through one of the cracks in the heat affected zone of weld H identified the crack as an intergranular stress corrosion crack with a depth of approximately 1 millimeter (40 mils).

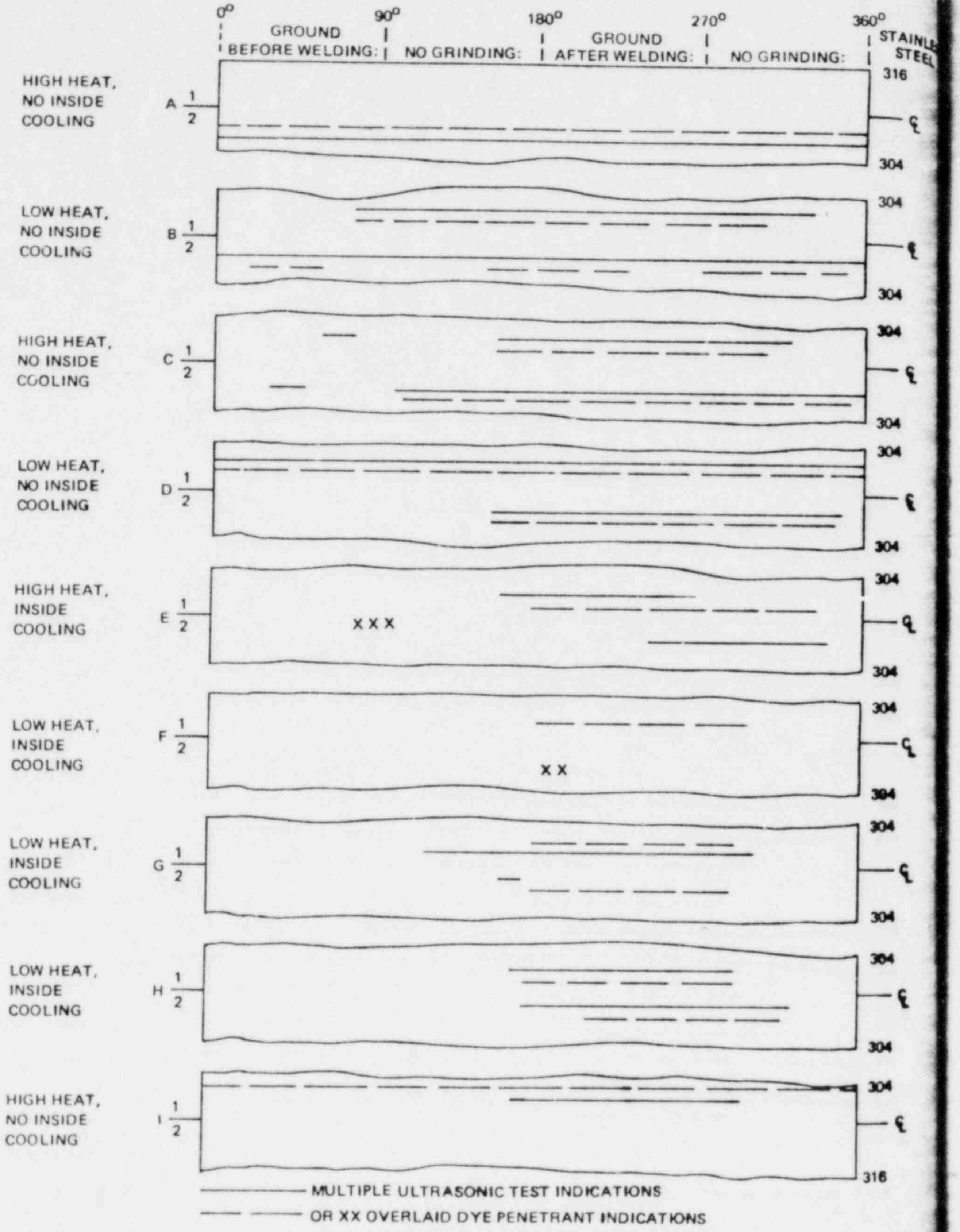

Figure 17. Ultrasonic Inspection and Liquid Penetrant Results for Third Cyclic Tension Test in Large Environme Fatigue Test Facility

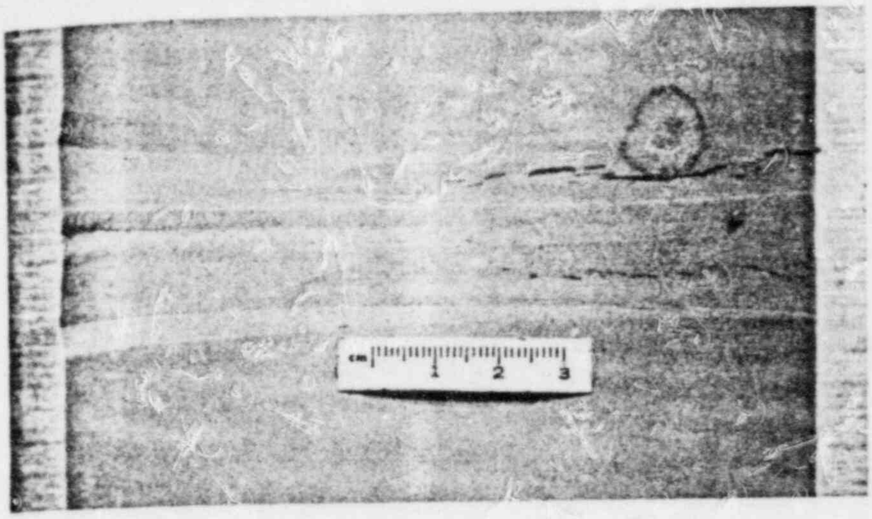

WELD G

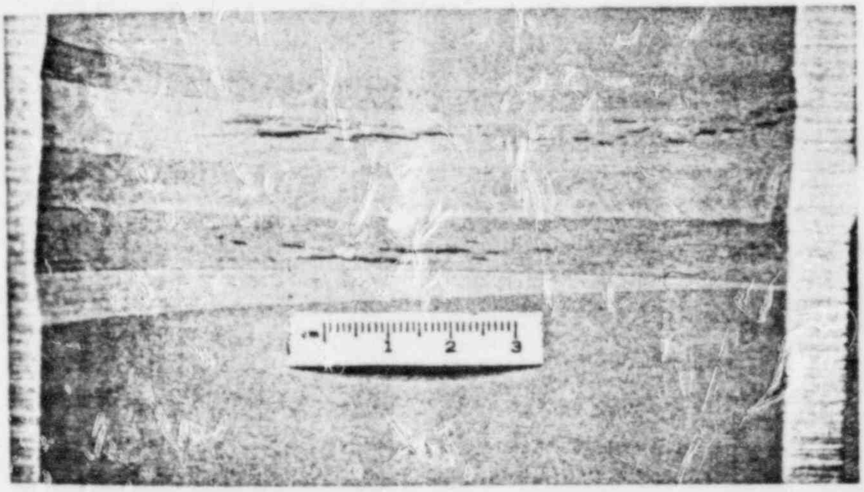

WELD H

Figure 18. Heat Sink Welds Showing Cracking on Inside Surface

Table 3
HEAT AFFECTED ZONE CRACKING COMPARISON BETWEEN REFERENCE AND HEAT SINK WELDS OF TYPE-304 STAINLESS STEEL (LIQUID PENETRANT RESULTS)

Surface Condition	HAZ Quadrants Cracked/Total HAZ Quadrants Reference Welds	 Heat Sink Welds
Ground Before Butt Welding	4/8	0/8
Ground After Butt Welding	8/8	6/8
Unground	13/16	1/16

HAZ — Heat Affected Zone

Figure 19 shows the extent of cracking in welds B, C, and D which are reference unprotected Type-304 stainless welds. Here, cracking is seen to occur in both ground and unground sections in the weld heat affected zone. As evidenced the amount of red dye observed in the figure, the cracks are rather open and deep. No metallography was performed for of the reference pipe cracks as one crack penetrated the outside surface and leaked. Further, the results of the second L Environmental Fatigue Test Facility test clearly identified this cracking mode as intergranular stress corrosion crack

4. Conclusions

The results of the third Large Environmental Fatigue Test Facility cyclic tension test resulted in the follo conclusions:

(1) Acoustic emission is not yet well enough understood to be used as an on-line nondestructive test discrimin of intergranular stress corrosion cracking in stainless steel piping systems.

(2) Heat sink welding appears to improve the resistance of Type-304 stainless steel to intergranular str corrosion cracking in pipe tests in the absence of post-weld grinding.

(3) Post-weld grinding of Type-304 stainless steel weld heat affected zones is a strong accelerant to intergran stress corrosion cracking. Pre-weld grinding has little effect.

3.1.2.3 Fourth Full-Size Cyclic Intergranular Stress Corrosion Cracking Pipe Test (Fourth Large Environmental Fatigue Test Facility Test)

1. Fabrication of Pipe

The fourth Large Environmental Fatigue Test Facility cyclic tension test was designed to provide information on intergranular stress corrosion cracking susceptibility of the potential alternate piping materials Types-316 and -3 stainless steel in the boiling water reactor environment. As in the second and third Large Environmental Fatigue Test Fac test, eight 4-in. (10.16-cm) long 4-inch schedule 80 pipe segments were butt welded together to provide a welded pipe shown in Figure 20. As in the third Large Environmental Fatigue Test Facility test a transition piece of 4-in. schedule Type-316 stainless steel was welded to test sections A and I so that a total of 18 heat affected zones were available testing. Also included on test were two reference welds of Type-304 stainless steel from a resistant pipe heat (heat M77 provide a standard with which to compare the intergranular stress corrosion cracking behavior of the Types-316 and -3 stainless steel pipe sections. A total of two heats of Type-316 stainless steel, one heat of Type-316L stainless steel, and heat of Type-304 stainless steel were included in the test.

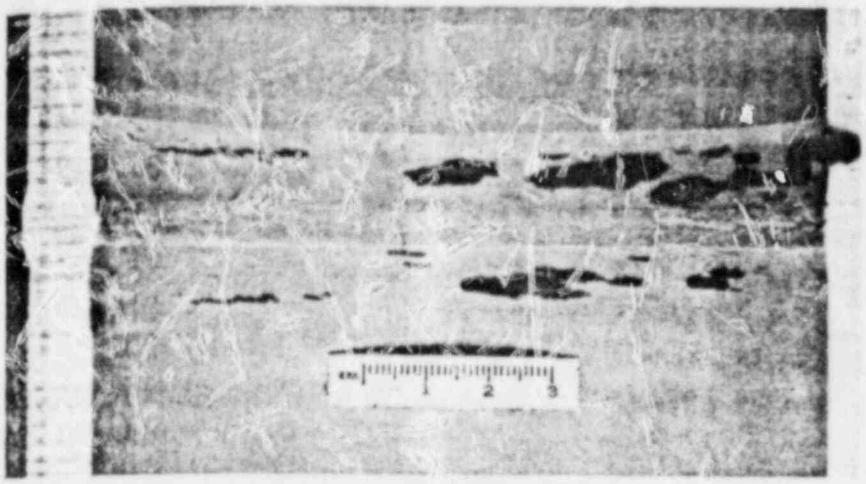

WELD B

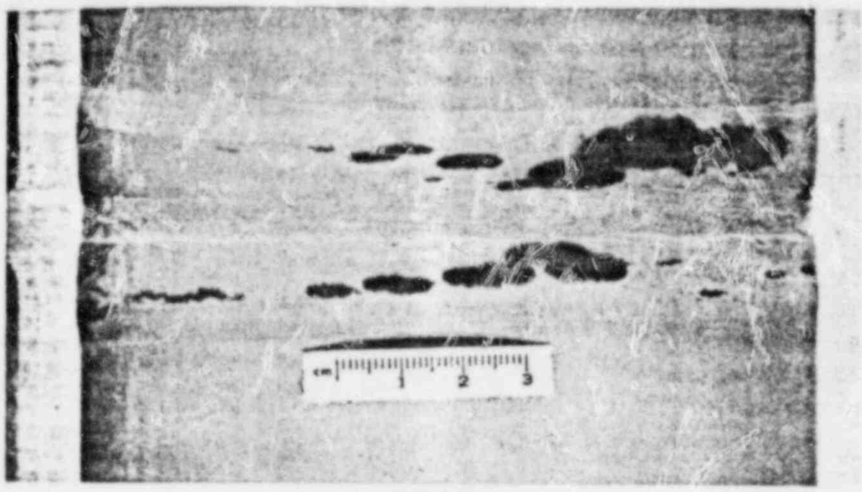

WELD C

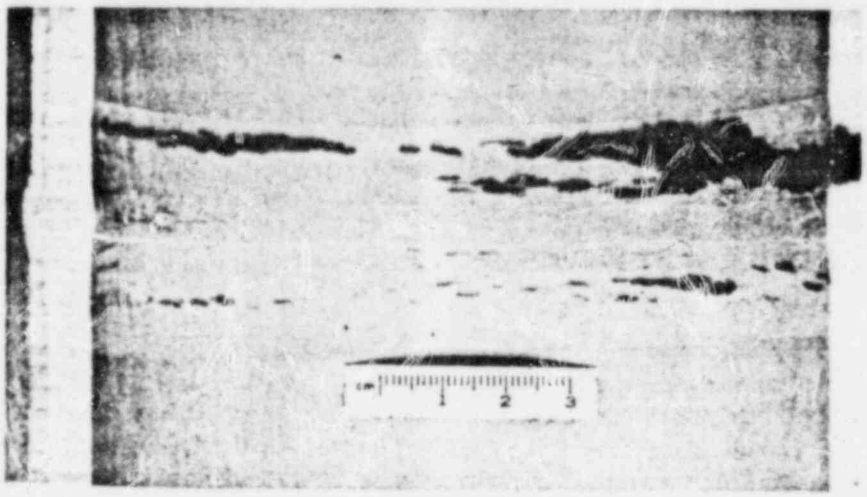

WELD D

Figure 19. Reference Unprotected Welds Showing Evidence of Cracking

All welds were fabricated using high-heat-input techniques. The first two layers were welded using a gas tungs technique and the third and fourth layers were welded using shielded metal arc technique. All layers were one pass Following the butt welding of welds F, G, H, and I (as shown in Figure 20) this test section (bounded by weld prepara and the transition piece) was heat treated at 915°F ± 15°F (490°C ± 8°C) for 24 hours (to further accelerate the intergra stress corrosion cracking tendency). Pre- and post-weld grinding similar to that performed in the third Large Environm Fatigue Test Facility test was performed on each weld heat affected zone in quadrants, the 0-to-90 degree quadran pre-weld ground and with the exception of weld E which was inaccessible for post-weld grinding, the 180-to-270 quadrant was post-weld ground. The complete weldment was ultrasonic test inspected prior to test.

2. Description of Pipe Test in the Large Environmental Fatigue Test Facility

The testing conditions used for Phase I of the fourth Large Environmental Fatigue Test Facility cyclic tensile test as described in the general test procedure (see Subsection 3.1.1.3 for details). The pipe was load cycled at a frequen 0.67 cycle/hour to a maximum stress of 136% of the Type-304 stainless steel 550°F (288°C) yield strength a temperature in oxygenated high purity water.

The first phase of the fourth Large Environmental Fatigue Test Facility test ran for 578 cycles (867 hours) after the weldment was removed from test for ultrasonic test inspection. Indications were observed in weld heat affected zone and G1 (the reference Type-304 stainless steel which received the post-weld low temperature sensitization). No indications were observed in the weldment. The pipe section including welds F and G was removed and replaced by welding a 4-in. (10.16-cm) long piece of Type-316L stainless steel 4-in. (10.16-cm) schedule 80 pipe (without post-weld temperature sensitization) forming the new test welds F′ and G′. The pipe configuration for Phase I and for Phase II is sh in Figure 21.

Phase II of the test program lasted an additional 139 cycles (209 hours) after which ultrasonic test inspection performed. No crack indications were found on the weldment. In an attempt to further accelerate cracking, the load increased to 175% of the Type-304 stainless steel 550°F (283°C) yield strength at temperature (Phase III). This third and phase of the test was stopped after 159 cycles of additional testing (239 hours) due to a test loop shutdown. During shutdown the specimen was examined by ultrasonic testing. Indications were observed in some of the weldments. The was terminated at this point to allow a complete ultrasonic, liquid penetrant, and metallographic examinations of the we

3. Post-Test Nondestructive Testing and Metallurgical Examination of Fourth Large Environmental Fatigue Test Facility Cyclic Test Weldment

The post-test ultrasonic, liquid penetrant, and metallographic examinations of the weldment used in the fourth L Environmental Fatigue Test Facility cyclic tension test has begun. The examination is in its early stages and will be repo in future reports. At present, not enough information is available to draw conclusions as to the mode of or extent of crack the test weldment.

3.1.3 Full Size Pipe Tests in CL-4 Test Facility

3.1.3.1 Test Objective

In an effort to obtain additional pipe test data and to evaluate loading conditions representative of expected conditions (i.e., pipe bending), a series of bend tests have been performed in the CL-4 test loop to evaluate the intergran stress corrosion cracking susceptibility of reference Type-304 stainless steel and the potential remedies. The initial tes the series (the first three-point bend test and the first four-point bend test) investigated the behavior of unprotected Type stainless steel piping weldments in 8 ppm oxygen high purity water at 288°C (550°F) and at high applied stress (max outer fiber stress was 136% of yield strength at temperature). The test results, reported in the General Electric Pipe T Force Report,[1] revealed that this test condition could produce intergranular stress corrosion cracking in Type-304 stai steel.

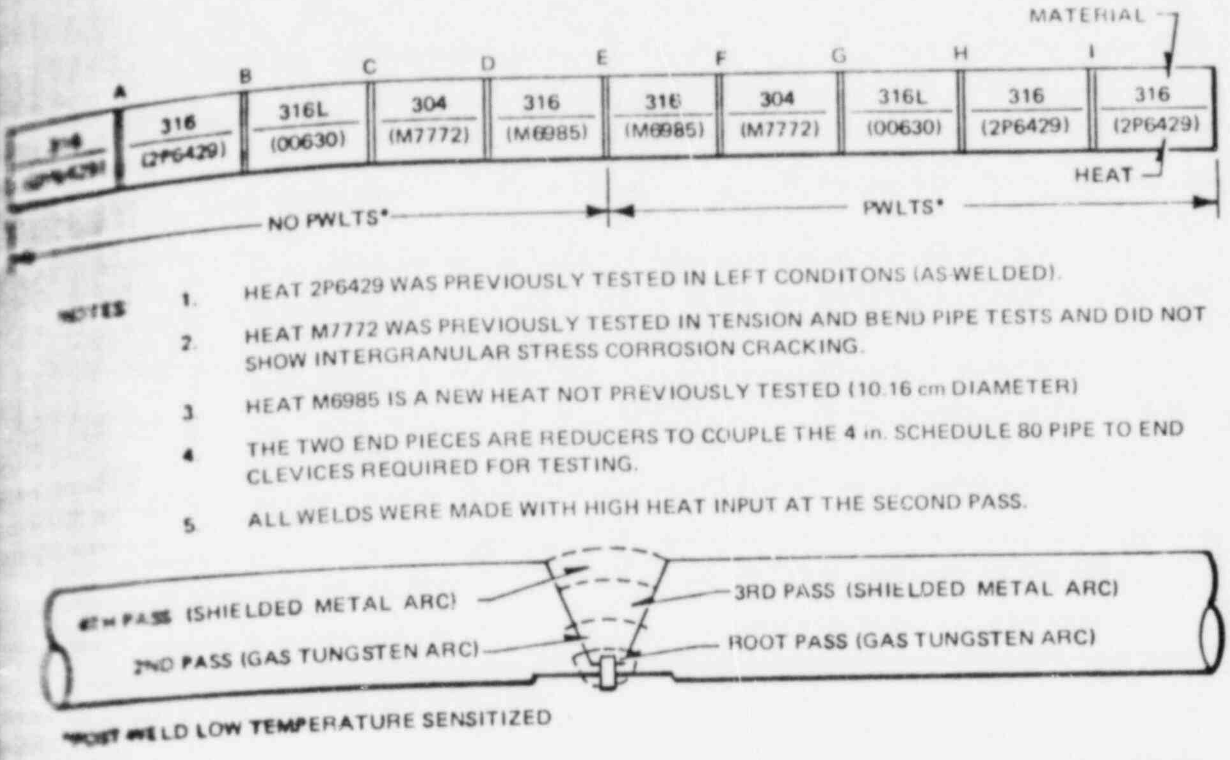

NOTES

1. HEAT 2P6429 WAS PREVIOUSLY TESTED IN LEFT CONDITONS (AS WELDED).
2. HEAT M7772 WAS PREVIOUSLY TESTED IN TENSION AND BEND PIPE TESTS AND DID NOT SHOW INTERGRANULAR STRESS CORROSION CRACKING.
3. HEAT M6985 IS A NEW HEAT NOT PREVIOUSLY TESTED (10.16 cm DIAMETER)
4. THE TWO END PIECES ARE REDUCERS TO COUPLE THE 4 in. SCHEDULE 80 PIPE TO END CLEVICES REQUIRED FOR TESTING.
5. ALL WELDS WERE MADE WITH HIGH HEAT INPUT AT THE SECOND PASS.

Figure 20 *Test Weldment for Fourth Cyclic Tension Test in Large Environmental Fatigue Test Facility*

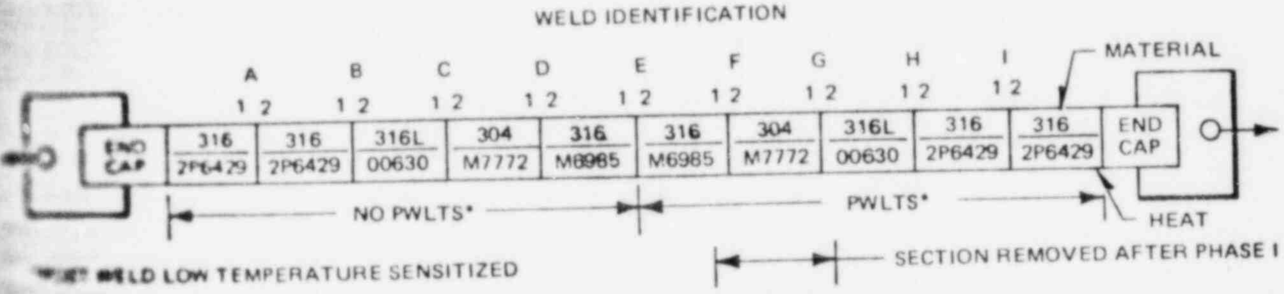

(a) PHASE I TEST CONFIGURATION

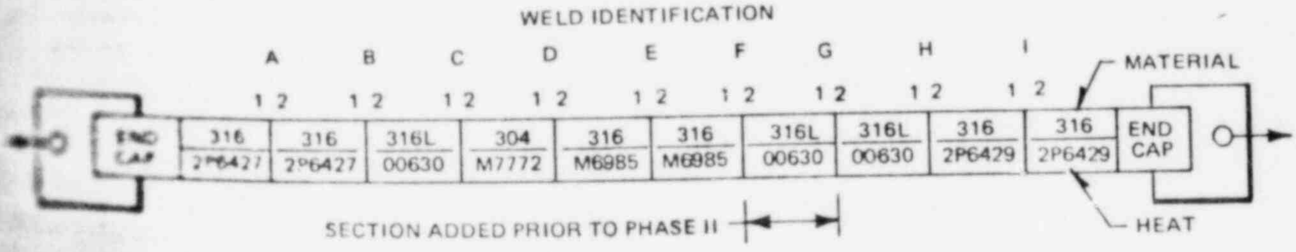

(b) PHASES II AND III TEST CONFIGURATION

Figure 21 *Test Configuration, Fourth Cyclic Tension Test in Large Environmental Fatigue Test Facility*

Two additional pipe tests have been performed in the CL-4 test facility under four-point bending conditions, the sec four-point bend test and the third four-point bend test; these tests screened the potential remedies and/or protec methods. The remainder of this section describes the weld fabrication details, test procedures, and test results for th four-point bend pipe tests.

3.1.4 Technical Summary of Full-Size Pipe Bend Tests in CL-4 Test Facility

3.1.4.1 Second Four-Point Bend Intergranular Stress Corrosion Cracking Pipe Test

A. Fabrication of Pipe Weldments

The four-point bend test fixture, shown in Figure 22, tests two companion pipes by loading the pipes against e other using hydraulic jacks and fixed position ends. The pipes are loaded in bending and the region between the hydra jacks is at the same load throughout the length of pipe. In this manner, a large number of test welds can be exposed to t same loading conditions.

In the second 4-in. (10.16-cm) schedule 80 four-point bend test pipe set, the potential pipe remedies which w tested included solution heat treatment after welding, corrosion resistant weld cladding with and without solution h treatment after cladding (applied as an inlay only), using either Type-312 stainless steel or 309L-Mo stainless steel as t weld material, cast CF8 pipe, rolled and seam welded unprotected Type-304 stainless steel, and reference seaml Type-304 stainless steel pipe. A schematic of the welded pipe pair and the fabrication details are presented in Figure 23 a the accompanying table. Note that all specimens were ground on the inside surface at the counterbore and weld root arou the entire pipe circumference. Welding was performed in the 1 g position (pipe rotating, welding performed downhand) wi maximum heat input of 76,000 J/in. (30,000 J/cm). Gas tungsten arc and shielded metal arc processes were employed the pipe butt welding.

For the inlay weld deposits, the shielded metal arc process was employed at normal heat input values. The weld parameters used for both butt and cladding deposits are presented in Figure 24.

B. Description of Pipe Test in CL-4 Test Loop

The second four-point bend pipe test pair was loaded in bending (as shown in Figure 22) at 288°C (550°F) in 8 pp oxygenated water with a maximum outer fiber tensile stress of 136% of the Type-304 stainless steel yield strength temperature applied to the weld. In this loading configuration, approximately 14% of the circumference of the pipe is loaded at least 90% of the maximum load, and approximately 25% of the circumference of the pipe was loaded above the yi strength of Type-304 stainless steel at temperature. The pipes were load cycled periodically (typically daily) to simula reactor startup and shutdown conditions. The second CL-4 pipe test ran for a total of 3812 hours and 328 load-unload cycl during which time the test loop was shutdown on three other occasions for ultrasonic test inspection of the test pipe pair. N indications significantly above background were observed during any of the interim inspections. Following the 3812-hour te an additional ultrasonic testing inspection has been performed. Small indications have been identified in some welds. Th welded pipe pair has been removed from test and liquid penetrant and metallographic examinations are under way.

3.1.4.2 Third Four-Point Bend Intergranular Stress Corrosion Cracking Pipe Test

A. Fabrication of Pipe Weldments

The four-point bend test fixture used for the third four-point bend pipe test was a fixture similar to that show in Figure for the second four-point pipe bend test. In this bend test pipe set, the corrosion resistant cladding pipe remedy was th principal remedy evaluated, as an overlay using both Type-308L stainless steel and Type-312 stainless steel for claddi material. A drawing of the procedure used for applying the overlay is shown in Figure 25. In Figure 25, clad region A wa solution heat treated following the cladding operation (as shown in the marked region of the figure) and region B was th

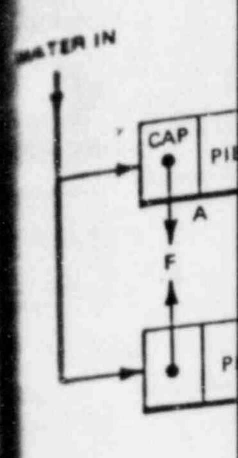

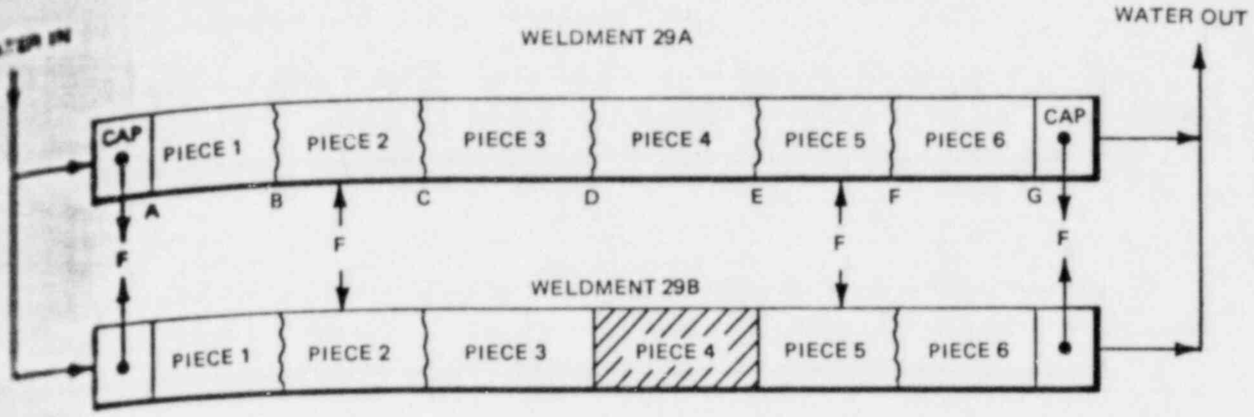

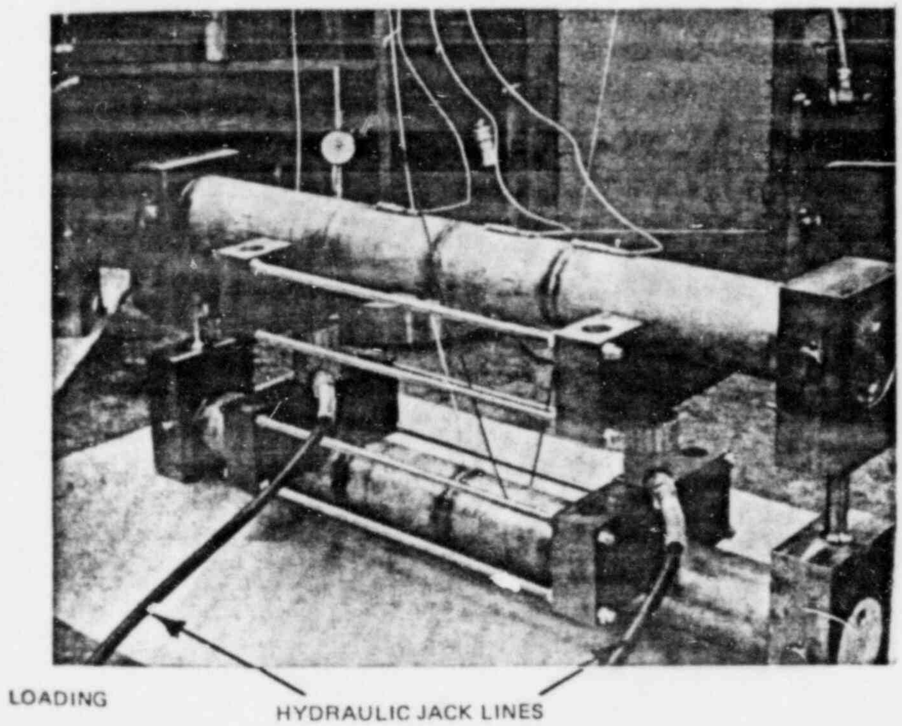

Figure 22. Four-Point Static Bend Test Pipe Weldments Set in Position

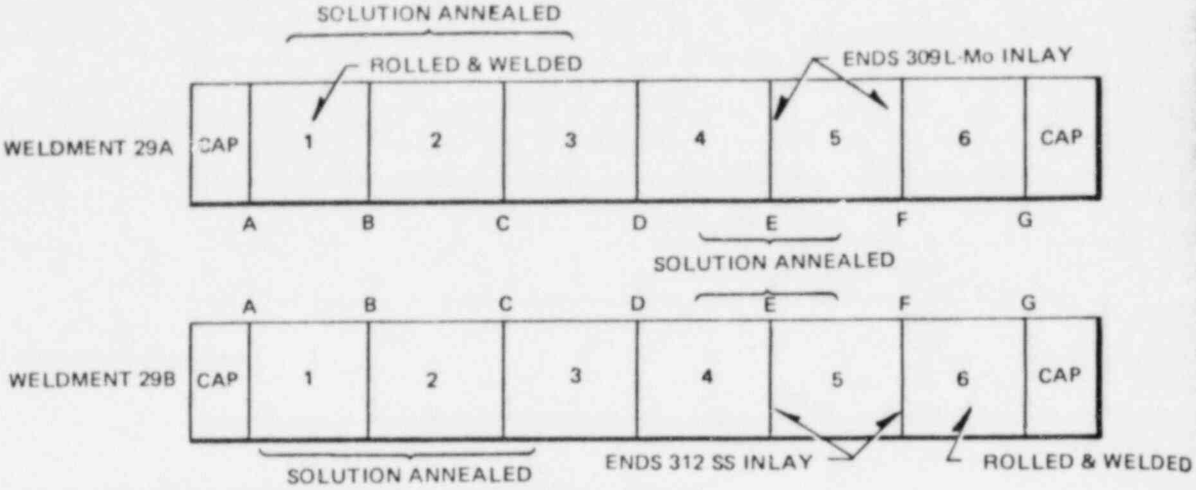

NOTE: PIECE 5 WAS FLARED AT EACH END AND WELD INLAYED.
INLAY FOR 29A IS E309 Mo-L-16.
INLAY FOR 29B IS E312-16.

PIPE END PREPARATION IDENTIFICATION	HEAT INPUT	HEAT TREATMENT	INSIDE SURFACE CONDITION	WELD DEPOSIT	MATERIAL	
					TYPE	HEAT NO
29A-A1 29A-A2	END PIECE (GTA WELD)					
29A-B1	5G	SHT	GROUND[a]	NONE	304	F50343
29A-B2	5G	SHT	GROUND[a]	NONE	304	M7616
29A-C1	5G	SHT	GROUND[a]	NONE	304	M7616
29A-C2	5G	SHT	GROUND[a]	NONE	CF8	P520
29A-D1	5G	NONE[c]	GROUND[a]	NONE	CF8	P520
29A-D2	5G	NONE	GROUND[a]	NONE	CF8	98695
29A-E1	5G	SHT	GROUND[a]	NONE	CF8	98695
29A-E2	5G	SHT	GROUND[a]	309-L-Mo INLAY	304	7616
29A-F1	5G	NONE[c]	GROUND[a]	309 Mo-L INLAY	304	7616
29A-F2	5G	NONE[c]	GROUND[a]	NONE	304	2P6396
29A-G1 29A-G2	END PIECE WELD					
29B-A1 29B-A2	END PIECE					
29B-B1	5G	SHT	GROUND[a]	NONE	304	2P6396
29B-B2	5G	SHT	GROUND[a]	NONE	304	454659
29B-C1	5G	SHT	GROUND[a]	NONE	304	454659
29B-C2	5G	SHT	GROUND[a]	NONE	CF8	P521
29B-D1	5G	NONE[c]	GROUND[a]	NONE	CF8	P521
29B-D2	5G	NONE[c]	GROUND[a]	NONE	CF3	CENTR.
29B-E1	5G	SHT	GROUND[a]	NONE	CF3	CENTR.
29B-E2	5G	SHT	GROUND[a]	312 INLAY	304	F50343
29B-F1	5G	NONE[c]	GROUND[a]	312 INLAY	304	F50343
29B-F2	5G	NONE	GROUND[a]	NONE	304[b]	F50343
29B-G1 29B-G2	END PIECE WELD					

a – ALL SPECIMENS GROUND ON INSIDE SURFACE AT COUNTERBONE AND WELD ROOT AROUND ENTIRE CIRCUMFERENCE

b – ROLLED & WELDED PIPE

c – SOLUTION ANNEALED PRIOR TO BUTT WELD

SHT – SOLUTION HEAT TREATMENT

Figure 23. Makeup of Static Four-Point Bend Test Weldments

1. Pipe Butt Welds

A. Root Insert Weld (Gas tungsten arc)

Amps	100	Approximately 38,000 J/in. (15,000 J/cm)
Volts	14 to 16	
Travel	2.2 in./min	

B. Second Weld Layer (Gas tungsten arc) — 1 Weave Pass

Amps	110	Approximately 76,000 J/in. (30,000 J/cm)
Volts	15	
Travel	1.2 to 1.5 in./min	

C. Third to Finish Weld Layers (Shielded metal arc) — 4 X Rod Diameter Weave

Amps	100 to 105	Approximately 36,000 J/in. (14,200 J/cm)
Volts	23 to 25	
Travel	3.5 to 4.0 in./min	

2. Cladding Weld Deposits

— With Type E312-16 Filler Metal

A. First Layer (3/32-in.-diameter Electrodes)

Amps	70
Volts	22
Travel	4 to 6 in./min

B. Second Layer (1/8-in.-diameter Electrodes)

Amps	95
Volts	23
Travel	5 to 8 in./min

— With E309L-Mo-16 Filler Metal

Both Layers (1/8-in.-diameter Electrodes)

Amps	95
Volts	23
Travel	5 to 8 in./min

Figure 24. Welding Procedures for Second CL-4 Pipe Bend Test

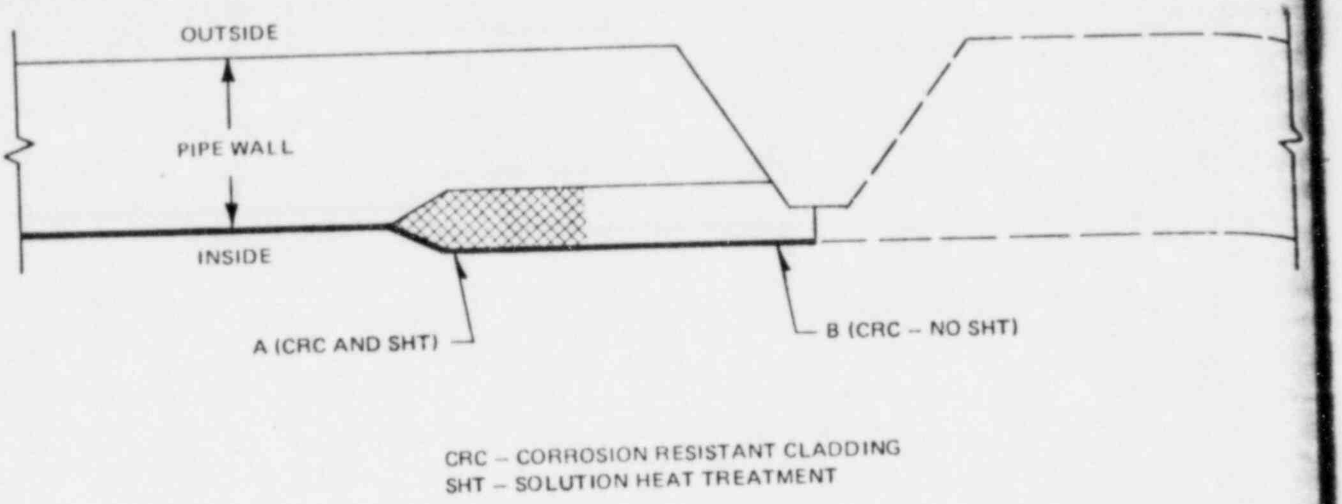

Figure 25. Cladding Process for Third CL-4 Pipe Bend Test

clad. Type-308L stainless steel was used as cladding material for region B exclusively. However, for region A, Type-312 stainless steel or Type-308L stainless steel was used as cladding material where solution heat treatment followed the cladding. The purpose of using Type-312 stainless steel was that the residual ferrite following solution heat treatment remained above the minimum 8% ferrite specified for providing immunity to intergranular stress corrosion cracking. In addition to the corrosion resistant clad pipe welds, reference unprotected Type-304 stainless steel and unprotected Type-316L stainless steel were also tested.

The pipe pair tested in the third pipe bend test is shown in Figure 26. The two pipe weldments, 36A and 36B, were weld overlayed at weld joints C and D. For weldment 36A, welds C and D were overlayed exclusively with Type-308L stainless steel. For weldment 36B, weld D was clad exclusively with Type-308L stainless steel while weld C was clad with Types-312 and -308L stainless steel as described above. The welding procedures and details for both pipe weldments are presented in Table 4. The welding heat input parameters for butt welding and cladding are as presented in the second CL-4 pipe test.

B. Description of Pipe Test in CL-4 Test Loop

The third four-point bend pipe test pair (pipe weldments 36A and 36B) were loaded in bending at 288°C (550°F) in 8 ppm oxygenated water with a maximum outer fiber stress of 136% of the Type-304 stainless steel yield strength at test temperature applied to the weld. The pipes were load cycled periodically to simulate reactor startup and shutdown condition. The pipe test consisted of two phases. Phase I consisted of 1380 hours on test and 100 load-unload cycles after which ultrasonic test examination was performed. The ultrasonic testing indicated cracking in an unprotected weld heat affected zone of both pipes (heat affected zone E1). Weld E was removed from both pipe specimens and the pipes were rewelded and returned to test.

During the second phase of the test, test weldment 36B developed a through-wall leak 2.5 inches (6.3 cm) long on the outer surface and 5.5 inches (13.8 cm) long on the inner surface. Weld B was removed from the pipe, the pipe was rewelded and returned to test to complete the scheduled Phase II program. Phase II continued for an additional 722 hours (and 122 load-unload cycles) when a leak developed in weld heat affected zone B2 of weldment 36A. At this point, following a total test time of 2683 hours and 292 load-unload cycles, the pipes were removed from test and a complete ultrasonic test inspection

Table 4
THIRD FOUR-POINT BEND TEST FABRICATION DATA
4-in. SCHEDULE 80 PIPE

Identification			Heat	Grinding				Protection Method		
Weld	HAZ	Pipe Material	Input	0-90	90-180	180-270	270-360	CRC	Thermal Treatment	New Material
[illegible]	B1	ASTM A312 Type-316L	Std	None	None	None	None	None	None	316L Pipe
B	B2	ASTM A312 Type-304		None	None	None	None	None	None	No
[illegible]	C1	ASTM A312 Type-304	Std	Buffed	Buffed	Buffed	Buffed	308L Clad	SHT Portion Prior to Butt Weld	308L Clad
C	C2	ASTM A312 Type-304		Buffed	Buffed	Buffed	Buffed	308L Clad	SHT Portion Prior to Butt Weld	308L Clad
[illegible]	D1	ASTM A312 Type-304	Std	Buffed	Buffed	Buffed	Buffed	308L Clad	SHT Portion Prior to Butt Weld	308L Clad
D	D2	ASTM A312 Type-304		Buffed	Buffed	Buffed	Buffed	308L Clad	SHT Portion Prior to Butt Weld	308L Clad
[illegible]	E1	ASTM A312 Type-304	High	ABW	ABW	ABW	ABW	None	None	No
E	E2	ASTM A312 Type-318L		ABW	ABW	ABW	ABW	None	None	316L
[illegible]	B1	ASTM A312 Type-316L	Std	None	None	None	None	None	None	316L Pipe
B	B2	ASTM A312 Type-304		None	None	None	None	None	None	No
[illegible]	C1	ASTM A312 Type-304	High	ABW	ABW	ABW	ABW	Weld Clad 312/308L	SHT 312 Portion Prior to Butt Weld	E312 and E308L Clad
C	C2	ASTM A312 Type-304		ABW	ABW	ABW	ABW	Weld Clad 312/308L	SHT 312 Portion Prior to Butt Weld	E312 and E308L Clad
[illegible]	D1	ASTM A312 Type-304	High	ABW	ABW	ABW	ABW	Clad E308L	SHT Initial 3/4-in. BBW	E308L Clad
D	D2	ASTM A312 Type-304		ABW	ABW	ABW	ABW	Clad E308L	SHT Initial 3/4-in. BBW	E308L Clad
	E1	ASTM A312 Type-304	High	ABW	ABW	ABW	ABW	None	None	No
E	E2	ASTM A312 Type-316L		ABW	ABW	ABW	ABW	None	None	316L Pipe

---

ABW – After Butt Welding
BBW – Before Butt Welding
SHT – Solution Heat Treatment
HAZ – Heat Affected Zone
CRC – Corrosion Resistant Cladding

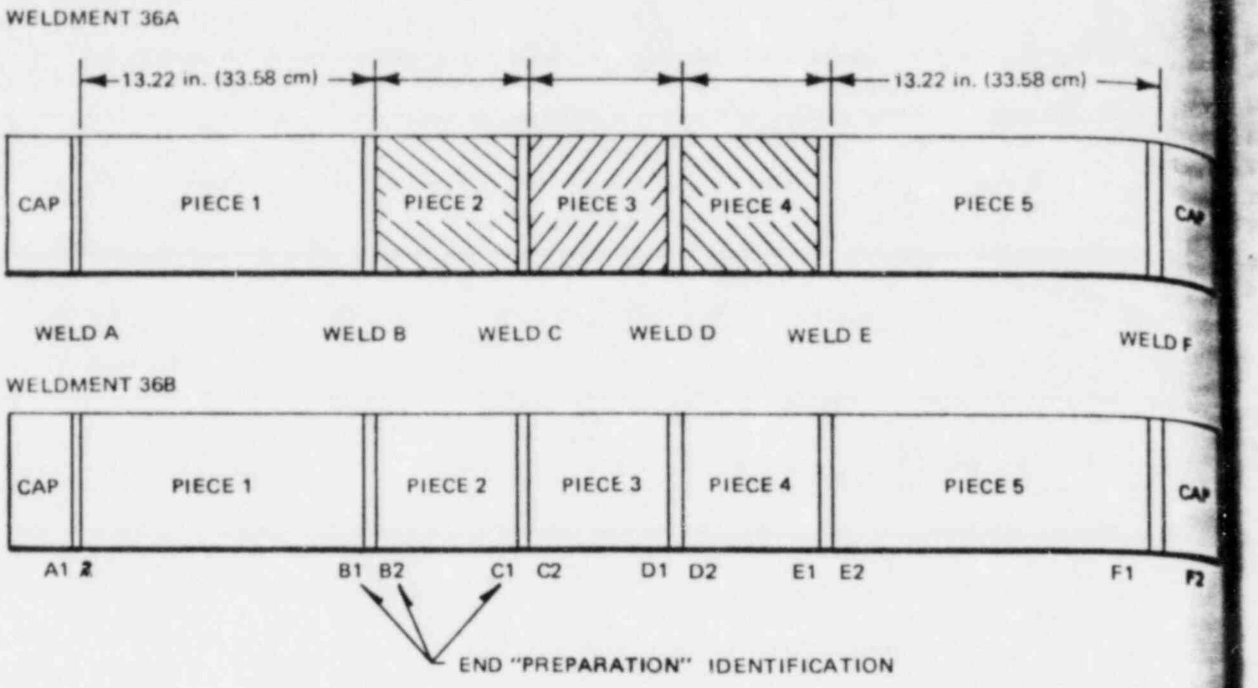

Figure 26. Test Weldments for Third Full-Size Pipe Bend Test in CL-4 Test Facility

was instituted. Weldment 36A revealed ultrasonic test indications at weld heat affected zone E1' (the replacement following Phase I of the test), weldment 36B revealed ultrasonic test indications at weld heat affected zone E1' and also indications in the corrosion resistant cladding weld heat affected zones D1 and D2. Metallurgical examination of ultrasonic test indications is presently in progress. A summary of all results obtained to date for this pipe pair is presente Table 5. No indications were found in the Type-316L stainless steel weld heat affected zones or in the corrosion resis cladding weld heat affected zones of pipe 36A. All reference Type-304 stainless steel weld heat affected zones have crac or have indicated cracking (by ultrasonic testing). The corrosion resistant cladding welds have not cracked but ultrasonic indications have been observed in the weld 36B-D where Type-308L stainless steel cladding was used. These indicat have not been confirmed as cracks at this time. It should be noted, however, that this weld, 36B-D, was inside surface grou following the cladding and butt welding. The post-test metallographic results will be reported in future progress repo

3.1.5 Summary of Pipe Test Results

The laboratory pipe tests in the Large Environmental Fatigue Test Facility and CL-4 pipe test facility investigated intergranular stress corrosion cracking behavior of Type-304 stainless steel and remedy methods at 288°C (550°F) in 8 p oxygen high purity water. High stress, high oxygen, high weld heat input, grinding, and cyclic loading conditions were uti to accelerate cracking in the reference and remedy pipes. These pipe screening tests have provided the following resu

(1) Type-304 stainless steel welded piping material can be failed in laboratory 4-in. (10.16-cm) schedule 80 p tests routinely at stresses above the 289°C (550°F) yield strength. Both high- and low-heat-input welds, gro and unground inside surfaces are susceptible to intergranular stress corrosion cracking in the weld affected zone. Post-weld grinding is a severe accelerant to intergranular stress corrosion cracking in material.

Table 5
SUMMARY OF PHASE II RESULTS

Weld	Heat Affected Zone	Number of Cycles to 136% YS 550°F	Exposure Time (hours)	Ultrasonic Test	Liquid Penetrant	Metallographic
36A B	B1	292	2,683	No Indications	No Data	No Data
	B2	292	2,683	Leaking Crack	Crack	IGSCC
36A C	C1	292	2,683	No Indications	No Data	No Data
	C2	292	2,683	No Indications	No Data	No Data
36A D	D1	292	2,683	No Indications	No Data	No Data
	D2	292	2,683	No Indications	No Data	No Data
36A E	E1	100	1,380	Crack at 90°	Crack	IGSCC
	E2	100	1,380	No Indications	No Indications	No Data
36A E	E1′	192	703	Indications	No Data	No Data
	E2′	192	703	No Indications	No Data	No Data
36B B	B1	170	1,961	No Indications	No Indications	No Data
	B2	170	1,961	Leaking Crack	Crack	IGSCC
36B B	B1′	122	722	No Indications	No Data	No Data
	B2′	122	722	No Indications	No Data	No Data
36B C	C1	292	2,683	No Indications	No Data	No Data
	C2	292	2,683	No Indications	No Data	No Data
36B D	D1	292	2,683	Indications	No Data	No Data
	D2	292	2,683	Indications	No Data	No Data
36B E	E1	100	1,380	Crack 0 to 90°	Crack	No Data
	E2	100	1,380	No Indications	No Indications	No Data
36B E	E1′	192	703	Cracklike Indication	No Data	No Data
	E2′	192	703	No Indications	No Data	No Data

IGSCC — intergranular stress corrosion cracking
YS — yield strength

(2) All of the remedies examined show an improvement in resistance to intergranular stress corrosion crac relative to that of Type-304 stainless steel piping. Solution heat treatment following butt welding appear provide an immune remedy even when post-weld grinding is applied to the pipe inside surface. The us corrosion resistant cladding both as overlay and as inlay in laboratory pipe tests appears to greatly improve intergranular stress corrosion cracking resistance of Type-304 stainless steel. Further testing will be perfor to quantify the improvement. Heat sink welding appears to be a promising product improvement if applied in absence of post-weld grinding. Post-weld grinding appears to seriously diminish the effectiveness of heat welding by eliminating the favorable residual stress state introduced by heat sink welding. The cast p remedy has provided mixed results. Interdendritic stress corrosion cracking was observed in a cast pipe w heat affected zone where <5% ferrite existed. Further testing is required to identify the margin improvem using this potential near-term remedy.

(3) The alternate materials Types-316 and -316L stainless steel examined in these pipe tests to date have sho very promising results. However, a more substantial data base is required before a performance improvem can be clearly established.

A summary of the pipe test results is provided in Tables 6 and 7 for the reference and remedy methods, comparing materials test by test. The results of the fourth Large Environmental Fatigue Test Facility test are not included since the d are presently being analyzed.

Two additional axial loaded pipe screening tests are planned to complete the series of screening tests prior to inauguration of the statistical pipe test program. The pipe tests will include all the remedies and protection methods describ in this section and will provide the basis for the selection of the remedies to be included in the statistical test progra

3.2 Laboratory Specimen Tests

3.2.1 Test Objective

Laboratory test specimens have been prepared from the inside surface of butt welded 4-in. (10.16-cm) schedule reference Type-304 stainless steel pipes and the potential remedy methods for degree of sensitization measurements a intergranular stress corrosion tests. The degree of sensitization evaluation was performed by electrochemical potentiokine backscan measurements, and intergranular stress corrosion cracking evaluation using constant load and constant extensi rate testing of the reference Type-304 stainless steel and the candidate remedies. These tests are designed to complem the pipe test screening effort by increasing the intergranular stress corrosion data base by small specimen testing a providing information regarding the degree of sensitization of candidate remedies. However, the main thrust of the screeni program has been full-size-pipe testing in order to generate the intergranular stress corrosion cracking information requi to select the piping candidate remedies for the statistical pipe test program.

The intergranular stress corrosion cracking laboratory specimen tests and the degree of sensitization tests perform to date are presented below.

3.2.2 Technical Summary of Laboratory Specimen Tests

3.2.2.1 Laboratory Specimen Intergranular Stress Corrosion Cracking Tests

Samples, removed from the inside surface of 4-in. (10.16-cm) schedule 80 pipe weldments of the reference Type-30 stainless steel and candidate remedies are undergoing intergranular stress corrosion cracking evaluation in constant loa and constant extension rate tests. Four pipe weldments are presently under investigation. These include reference Type-30 stainless steel butt welded to itself, heat sink welded Type-304 stainless steel welded to itself using inside surface wa cooling, cast CF8 butt welded to itself following a solution heat treatment of the CF8 spool pieces, and Type-304 stainl steel butt welded to cast CF8 and then solution heat treated. Samples removed from the inside surface of these welds a undergoing test by both constant load and constant extension rate methods in 288°C (550°F) high purity water with 8 pp

Table 6
CYCLIC TENSION TEST SUMMARY IN LARGE ENVIRONMENTAL FATIGUE TEST FACILITY

Material/or Protection Method	No. of Heats Evaluated	No. of Heats with Failures	No. of Heat Affected Zones Failed/Tested	Remarks
A. Second Large Environmental Fatigue Test Facility Test Tension Test				
Unprotected Type-304 Stainless Steel	3	2	5/8	Most cracks in ground region, two failures in machined region
Type-304 Stainless Steel + Corrosion Resistant Cladding	1	0	0/3	Pipe heat failed in unprotected condition
CF8	2	1	2/3	Intergranular stress corrosion cracking in heat of CF8 with <5% ferrite Failure at 175% of yield strength at test temperature
Type-304 Stainless Steel Solution Heat Treatment	1	0	0/2	Pipe heat failed in unprotected condition
Type-316 Stainless Steel	1	0	0/2	No cracking even at 175% of yield strength at test temperature
B. Third Large Environmental Fatigue Test Facility Test				
Unprotected Type-304 Stainless Steel	1	1	8/8	Post-weld grinding*
Heat Sink Welded Type-304 Stainless Steel	1	1	6/8	Post-weld grinding*
Unprotected Type-304 Stainless Steel	1	1	7/8	Machined surface
Heat Sink Welded Type-304 Stainless Steel	1	1	1/8	Machined surface
Unprotected Type-304 Stainless Steel	1	1	4/8	Pre-weld grinding
Heat Sink Welded Type-304 Stainless Steel	1	0	0/8	Pre-weld grinding

---

*Post-weld grinding is known to introduce large tensile residual stresses thus neutralizing the beneficial residual stress effects of heat sink welding.

Table 7
CYCLIC BEND TEST SUMMARY IN CL-4 TEST FACILITY

Material/or Protection Method	No. of Heats Evaluated	No. of Heats with Failures	No. of Heat Affected Zones Failed/Tested	Remarks
A. First Three-Point Bend Test				
Unprotected Type-304 Stainless Steel	2	1	4/8	Both ground and unground w failed
B. First Four-Point Bend Test				
Unprotected Type-304 Stainless Steel	3	2	5/12	Only ground heat affected zones showed cracking
C. Second Four-Point Bend Test				
Unprotected Type-304 Stainless Steel	2	0	0/2	No post-test examination performed to date; 3800 hours on test
Type-304 + Solution Heat Treatment	4	0	0/6	No post-test examination performed to date; 3800 hours on test
CF8	3	0	0/6	No post-test examination performed to date; 3800 hours on test
Corrosion Resistant Cladding	2	0	0/4	No post-test examination performed to date; 3800 hours on test
CF3	1	0	0/2	No post-test examination performed to date; 3800 hours on test
D. Third Four-Point Bend Test				
Unprotected Type-304 Stainless Steel	2	2	4/4	Both ground and unground wel failed
Corrosion Resistant Cladding	1	0	0/4	After 2600 hours on test
Corrosion Resistant Cladding	2	*	*/4	*Small ultrasonic test indications in one heat. Dye penetrant and metallography not yet performe
Type-316L Stainless Steel	1	0	0/4	After 2600 hours on test

---

* Post-weld grinding is known to introduce large tensile residual stresses thus neutralizing the beneficial residual stress effects of heat sink weldi

dissolved oxygen. The results of the constant load and constant extension rate tests are presented in Table 8. The 304/304 control samples have not failed after constant load testing for >6200 hours, nor did the constant extension rate sample reveal any intergranular stress corrosion cracking susceptibility. It is not surprising, therefore, that the inside surface cooled samples from the same heat of Type-304 stainless steel are exhibiting identical behavior. This pipe heat, containing approximately 1% residual ferrite, has been particularly resistant to intergranular stress corrosion cracking in tests (see NEDO-20985-5 for details).

Problems have been experienced with the CF8 material (heat 98695) used in this investigation. One of two samples tested by constant load in the annealed and welded condition failed by transgranular stress corrosion cracking, while the constant extension rate sample failed by intergranular stress corrosion cracking.

Two of the samples which were annealed after welding failed in the constant load tests (one ductilely and one by intergranular stress corrosion cracking); both samples failed in the CF8 side of the 304/CF8 weld joint. The constant extension rate sample also failed in the CF8 portion, and the fracture was by ductile rupture.

The CF8 used in these tests contained 11 to 15% ferrite, and, based on previous experience with high ferrite castings, should not be susceptible to stress corrosion cracking. However, metallographic examination indicates that the ferrite particles are completely decorated with precipitates (presently unidentified) which provide continuous paths for crack propagation, assuming the precipitates are carbides and/or sigma phase. Further study of the intergranular stress corrosion cracking is under way.

3.2.2.2 Laboratory Degree of Sensitization Tests

A program has been implemented to evaluate the degree of sensitization in large-diameter pipe weldments produced for the laboratory specimen heat sink welding study. Initially, the 10-in. (25.4-cm) schedule 80 Type-304 stainless steel pipe weldments have been received for evaluation. The weldments are identified as follows: (1) TW-4, reference manual weld, high heat input; (2) TW-13, reference automatic weld, high heat input; and (3) TW-15, manual weld, water spray inside surface cooled, high heat input.

Samples have been prepared and submitted for mechanical property determination of the weldments at both room temperature and 288°C. Samples have also been prepared for stress corrosion testing; the constant load tests have begun. The constant extension rate tests will be performed soon.

Electrochemical degree of sensitization measurements are in progress; the results to date are given in Table 9. The as-received pipe used in weld TW-4 is slightly sensitized [Pa $\overline{>}$ 0.010 C/cm² (0.025 C/in.²) considered sensitized], but certainly not to the extent indicating grossly improper heat treatment. The maximum* degree of sensitization occurs about 50 mils (1.27 mm) from the weld fusion line, and is greatest for TW-13, followed by TW-4, and then the spray cooled TW-15.

Additional laboratory specimen tests evaluating the intergranular stress corrosion cracking behavior of reference Type-304 stainless steel and potential remedies under chemical and electrochemical potential control are presented in Task 3 of this report. These tests will identify regions of possible susceptibility of the remedies to integranular stress corrosion cracking in near boiling water reactor environments if such regions in fact exist.

---

*The [illegible] C/cm² (5.49 C/in.²) value shown in Table 9 for TW-13 at the fusion line is an artifact, as this sample contained portions of the weld deposit; the ferrite in the weld deposit always produces unusually high active peaks during the electrochemical potentiokinetic reactivation backscan test.

Table 8
STATUS OF INTERGRANULAR STRESS CORROSION CRACKING TESTING OF PIPE REMEDY SPECIMENS

A. Constant Load Tests

Weldment	Specimen Test Condition	Stress, ksi (MPa)	Failure Time (h)	Ductile	IGSCC	TGSCC
Type-304 Stainless Steel to itself	As Welded	40 (276)	6198 (NF)			
Type-314 Stainless Steel to itself	As Welded	40 (276)	1328 (NF)			
Type-304 Stainless Steel to itself	Heat Sink Welded	40 (276)	6217 (NF)			
Type-304 Stainless Steel to itself	Heat Sink Welded	40 (276)	5980 (NF)			
CF8 Stainless Steel to itself	Annealed and Welded	35 (241)	6098 (NF)			
CF8 Stainless Steel to itself	Annealed and Welded	35 (241)	469			X
Type-304 Stainless Steel to CF8 Stainless Steel	Welded then Annealed	40 (276)	372	X		
Type-304 Stainless Steel to CF8 Stainless Steel	Welded then Annealed	40 (276)	1263 (NF)			
Type-304 Stainless Steel to CF8 Stainless Steel	Welded then Annealed	40 (276)	299			X

B. Constant Extension Rate Tests

Weldment	Specimen Test Condition	Fracture Stress ksi (MPa)	Failure Time (h)	Reduction of Area (%)	Fracture Mode
Type-304 Stainless Steel to itself	As Welded	66.7 (460)	124	33.3	Ductile
Type-304 Stainless Steel to itself	Heat Sink Welded	65 (448)	107	25.0	Ductile
CF8 Stainless Steel to itself	Annealed and Welded	47 (324)	71	26.4	IGSCC
Type-304 Stainless Steel to CF8 Stainless Steel	Welded then Annealed	54.6 (376)	147	44.2	Ductile

NF — No failure to date
IGSCC — Intergranular stress corrosion cracking
TGSCC — Transgranular stress corrosion cracking

Table 9

DEGREE OF SENSITIZATION MEASUREMENTS IN TEST WELDS DETERMINED ELECTROCHEMICALLY IN 0.5 M H_2SO_4 + 0.01 M KSCN AT 30°C (86°F)

Distance from Weld Fusion Line, mils (mm)	Weldment		
	TW-13	TW-4	TW-15
0	0.851*	0.091	0.119
50 (1.27)	0.532	0.270	0.108
100 (2.54)	0.170	0.057	0.034
As Received	0.009	—	—

---

*Units are C/cm²

4. TASK 2 — STATISTICAL PIPE TESTS — RESULTS AND DISCUSSION

4.1 INTRODUCTION AND TASK OBJECTIVES

A statistical approach is a requirement for analysis of stress corrosion cracking data for a number of reasons. First, inter-heat and intra-heat variability in the material being investigated must be recognized and accounted for. Variability in fabrication practices between different specimens, and variability in testing procedures must be accounted for. Variability in the corrosion mechanism under investigation must also be recognized and accounted for. Second, since some claim as to the improvement in stress corrosion cracking resistance will be made as a result of the investigation, an objective, rigorous test of that claim must be made and statistics is the only tool for making such a test. Third, in order to avoid excessively long test times, accelerated test conditions are required. However, even under these circumstances, a simple relative demonstration of a significant difference in behavior may involve very long test times. Statistics offers a means of further shortening the required test time on a rational basis.

4.2 ASSUMPTIONS

Only one assumption is involved in the statistical approach to be used for the demonstration of an improvement in stress corrosion cracking resistance of the desired magnitude. That assumption is that the effect in reducing specimen life of the accelerating factors chosen for these tests is proportional at all levels of all factors for both the reference material and the alternate, as illustrated by curve A compared to curve 304 in Figure 27. Those two curves identify time to first failure of an alternate and of Type-304 stainless steel as the levels of various accelerants are made more severe. It is recognized that this proportional reduction in life assumption may not be exactly correct, and that either of two other relationships may exist, as also shown in Figure 27. If the effect of one or more accelerating factors is less for the alternate than for the reference material then the situation illustrated by curve B in Figure 27 would exist. The result of this would be that any predictions made regarding the alternate under service conditions would be non-conservative; that is, the alternate would not perform as well as was predicted from the accelerated test. However, if the effect of one or more of the accelerating factors is *greater* for the alternate than for the reference material, then a situation illustrated by curve C in Figure 27 would exist. In this situation, the alternate would perform better in service than predicted from accelerated tests. It is difficult to imagine a mechanism by which the situation represented by curve B might exist within the same class of materials, and the probability of its occurrence is therefore considered to be insignificant. Since the situation represented by curve C results in conservative predictions, its occurrence does not cause an error in the wrong direction and it can be ignored for the purposes of this test program.

4.3 CRITERIA

Two criteria must be defined for the purposes of this investigation. The first is the criterion of a failure in the testing program, and the second is the criterion for acceptable improvement. For the purposes of this investigation, the criterion for failure will be complete severance of small specimens or a through-wall leaking crack in full-size pipe specimens. The criterion for acceptable improvement will be a factor of at least 20, at the 90% confidence level.

The selection of the criterion of failure was based on simple expediency; it is much easier to detect the two events chosen than any others associated with stress corrosion cracking, and their occurrence does not involve any interpretation on the part of an inspector or operator. The basis for the selection of a factor of 20 improvement was the median time to first failure for welded Type-304 stainless steel in boiling water reactor service among plants as of 1974 (approximately 5 years). While an increase by a factor of only about 8 would appear to be adequate to meet the requirements of a 40-year design life, some failures would still be anticipated in service. It was therefore decided to build conservatism into the alternate material by requiring that it exhibit at least a factor of 20 improvement in time to first failure in resistance to intergranular stress corrosion cracking.

4.4 TEST DESCRIPTION

Testing will consist of stressing welded 4-in.-diameter pipes in a cyclic tension mode, with the environment of interest on the inside of the pipe. Each pipe segment will contain 12 welds, and 11 pipe segments will be tested. Three different heats

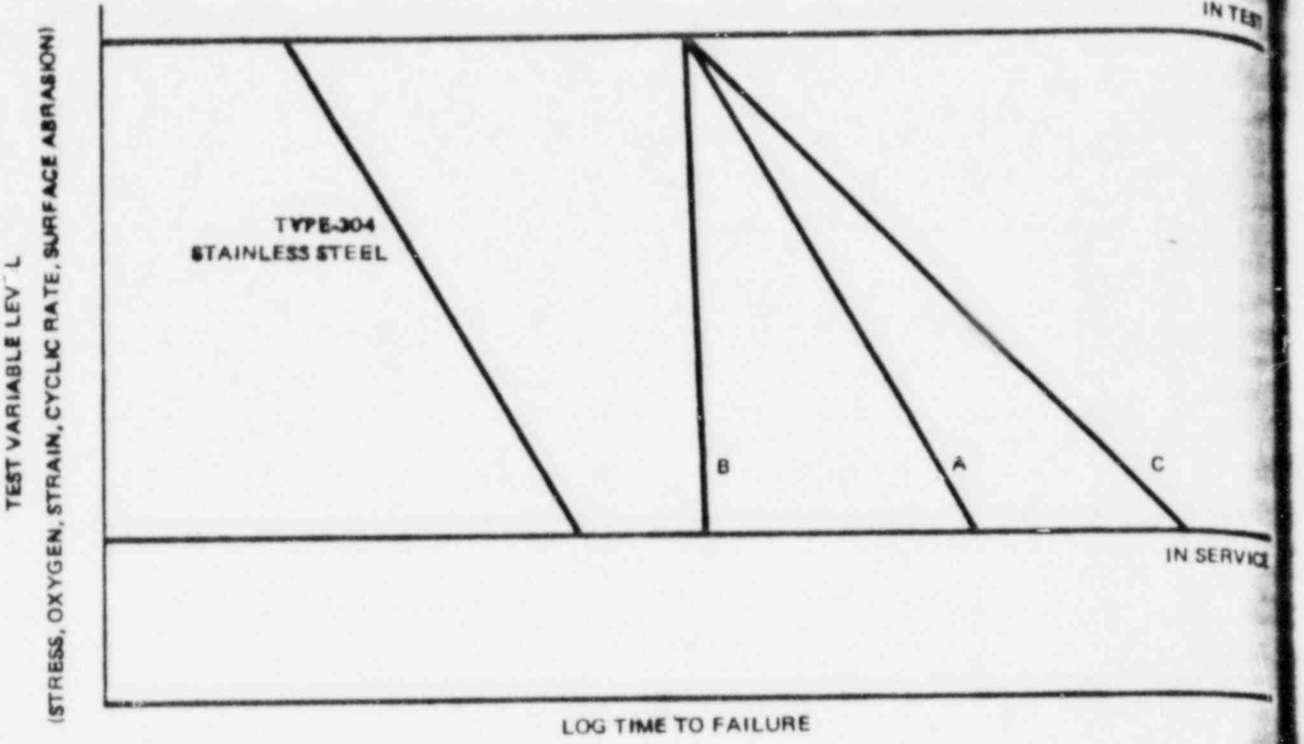

Figure 27. Possible Effect of Accelerants on Type-304 Stainless Steel and on an Alternate in Test and in Service

of each material of interest, or process, will be used in the evaluation in order to generate representative data. The accelerants will be dissolved oxygen and stress. The test matrix will include reference Type-304 stainless steel pipe welds and the three most promising candidate remedies determined from the screening tests.

4.5 TEST DURATION

The duration of the tests necessary to demonstrate some chosen factor improvement is a function of the following variables: the mean time to failure of the reference material; the variability in time to failure among reference welds; and (among alternate material welds) the number of reference welds tested, the number of alternate welds tested, and the desired factor improvement. If the mean time to failure for the materials was to be used as a test of the criterion of adequacy very long testing times would be involved. For example, if the mean time to failure for welded Type-304 stainless steel were 3 months, it would be necessary to test the alternate for more than 60 months in order to demonstrate an improvement of a factor of 20. It is possible, however, to greatly reduce the test time required for the demonstration by using time to first failure as the basis for comparison by using mean log time to failures of Type-304 stainless steel and time to first failure of the alternate.

Test duration of alternate materials will be set so that if no failures have occurred by a certain time, relative to the mean log time to failure of the Type-304 stainless steel specimens, the alternate material will be considered qualified. It is required that the time to first failure of the alternate be at least a factor of 20 times the time to first failure of the Type-304 stainless steel. But the time to first failure of the Type-304 stainless steel can be estimated with least error (smallest variance) by using the mean log time to failure, assuming that the variance among individuals is the historical variance for such testing of coupons among specimens and heats, and just confirming that the variance observed in this test does not differ significantly from that value, at the 5% level. It will be assumed that the variance of log time to fail of the alternate would not be greater than that assumed for Type-304 stainless steel; this assumption governs the variance of the time to first failure of the alternate

The waiting time is then found as the observed mean log time to fail of the Type-304 stainless steel, less the difference in the expected time to first failure of a log-normal distribution having the assumed variance and of sample size equal to the number of *alternate* material specimens, plus the log of factor improvement, to arrive at the minimum acceptable *expected* time to first failure of the alternate. To this is added an allowance for variability, the product of the normal distribution coefficient and standard deviation, and the variance of the first failure of the alternate. The last depends on the assumption that the variance of the alternate distribution of log time to failure should not be greater than that assumed for Type-304 stainless steel.

(Note that the *only* use of a *mean* log to failure is for the Type-304 stainless steel in test. Its variance depends on all Type-304 stainless steel specimens failing; if needed due to non-failure of a few Type-304 stainless steel specimens, new statistical technology now being developed may be available in time to permit suitable estimates of the mean for Type-304 stainless steel, and its variance, even with a few unfailed specimens.)

The variance of the distribution of log time to failures for small specimens of Type-304 stainless steel is known from previous test data, and can be used as the variance of welded pipe specimens for the purpose of planning the required test times. The corresponding observed variance in tests of Type-304 stainless steel will be compared to the value assumed in a statistical test of significance, and if not found significantly different the planned times will be used. Otherwise, the planned times will be adjusted. Using the variability in previous tests, Figure 28 was drawn to facilitate test planning in terms of factor improvement, numbers of specimens, and minimum required waiting time. This figure will be updated and adjusted to reflect any change in the standard deviation of the reference mean, if necessary, as the reference Type-304 stainless steel pipe failures occur.

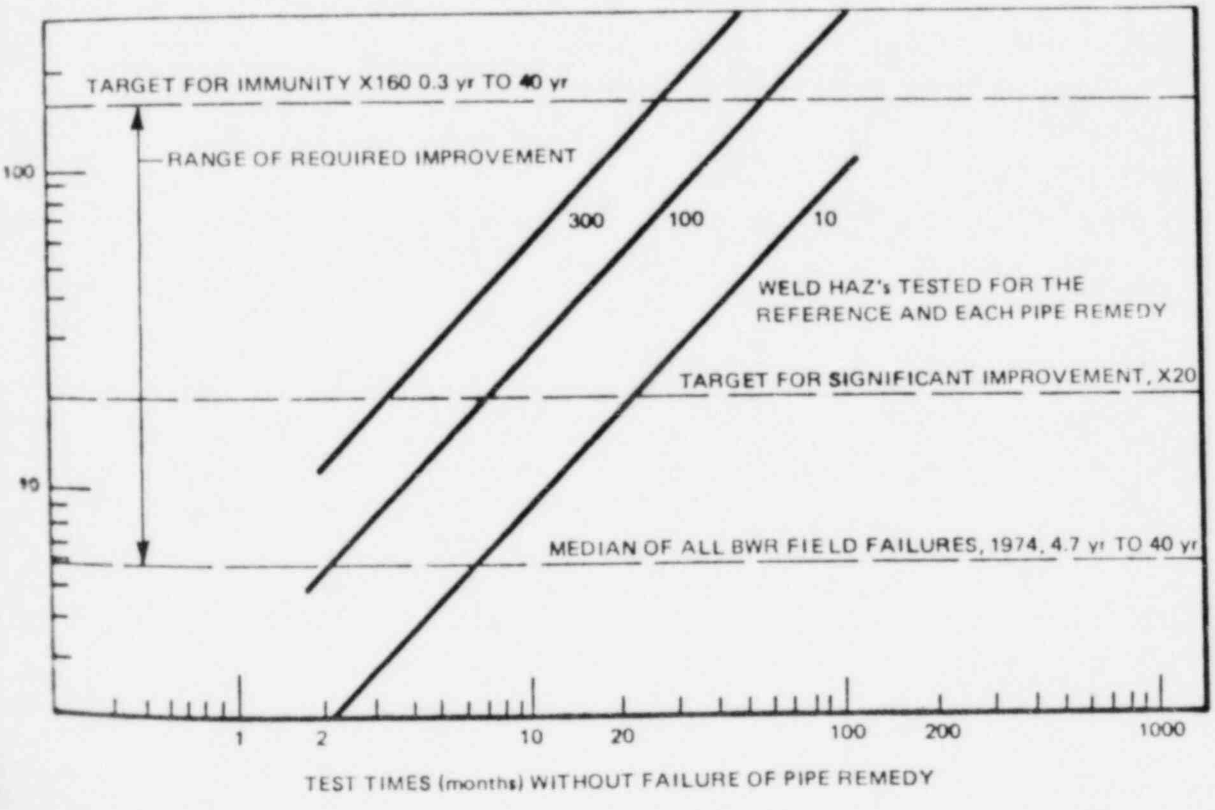

Figure 28 *Test Parameters for Statistical Qualification of Factor Improvement in Pipe Crack Remedies*

4.6 ANALYSIS OF CONSTRAINT NEAR PIPE WELDS — COMPARISON AMONG DIFFERENT DIAMETER P

4.6.1 Introduction

The General Electric Pipe Task Force report[1] presented discussion and experimental results showing that p deformation of Type-304 stainless steel near pipe welds is affected by the weld geometry and the neighboring higher st Type-308 stainless steel weld metal. This phenomenon has been called elastic constraint. The constraint effect on plastic flow is significant to the pipe cracking problem in that some plastic behavior is believed to be required for s corrosion cracking and constraint is believed to be a function of pipe size.

4.6.2 Test Objective

The objective of this task is to quantify the degree of elastic constraint on the pipe inside surface near butt welds in (10.16-cm) and 26-in. (66-cm) diameter Type-304 stainless steel pipes. The approach currently being pursued to qua this behavior is to develop elastic-plastic finite elements models of the weld joints.

The ANSYS computer program is being used to perform the finite element analysis. The grid arrangements for the pipe weld joint models are shown in Figures 29 and 30. The axisymmetric constant strain element STIF2 is being used preliminary calculations. Axial tensile loads are distributed along the end of the pipe away from the weld joint and increased in steps until the applied nominal stress exceeds twice the yield strength of the pipe material. Material proper are chosen to be typical of Type-304 stainless steel pipe and Type-308 stainless steel weld metal at operating temper (288°C).

4.6.3 Technical Summary of Constraint Modeling

Preliminary results from the 4-in. (10.16-cm) diameter pipe model (strain near the weld on the inside and s distance from the weld on the outside) did not agree with room temperature pipe test results obtained earlier.[1] Consequ before proceeding with the analysis of the larger pipe, a number of modeling changes were made. These incl lengthening the model, using a higher order finite element (STIF42) and applied displacement rather than load at the free of the pipe. A model of a simple tensile specimen was made to evaluate the adequacy of the STIF42 element and AN solution techniques for large plastic solutions.

Incorporation of all these modeling changes had little effect on the finite element local strain predictions. Predic strains near the weld on the inside of a pipe continue to be much higher than measured (at four locations) in the r temperature pipe test. For the model, these strains are due in large part to local bending near the weld.

Possible causes for the discrepancy between model and test include (1) the actual joint has deformed due to wel (weld shrinkage) and its geometry is not as modeled, (2) material properties in the weld heat affected zone are no modeled, and/or (3) residual stress (not included in the model) may play a bigger role in the plastic deformation near w joints than expected.

Recently the finite element model has been refined to include residual stress. This was accomplished introduc fictitious displacement of some elements as an initial condition. Preliminary results with this model variation show that ind residual stress affects the strain distribution at low loads. But, as the structure yields, the effect of residual stress is qu washed out.

Currently, the model geometry is being modified to more closely represent real welds such as the one shown in Figure Weld heat affected zone mechanical properties are also being measured. If they are shown to be significantly different fr the wrought pipe, the model will be changed accordingly.

In addition to modeling modifications, additional tests of full-size 10.16-cm (4-in.) and 66-cm (26-in.) diameter pi are planned. A 10.16-cm (4-in.) schedule 80 weld pipe will again be strain gaged and pulled in axial tension. A compar pipe will be sectioned, strain gaged, and pulled to determine whether results from a section are representative of the beha of a full pipe. If a section test is shown to be meaningful, a similar section of a 66-cm (26-in.) diameter pipe will be tested (ef of size on constraint), plus an annealed section (effect of residual stress) and a modified section (effect of local geometry) 10.16-cm (4-in.) diameter pipe will be tested.

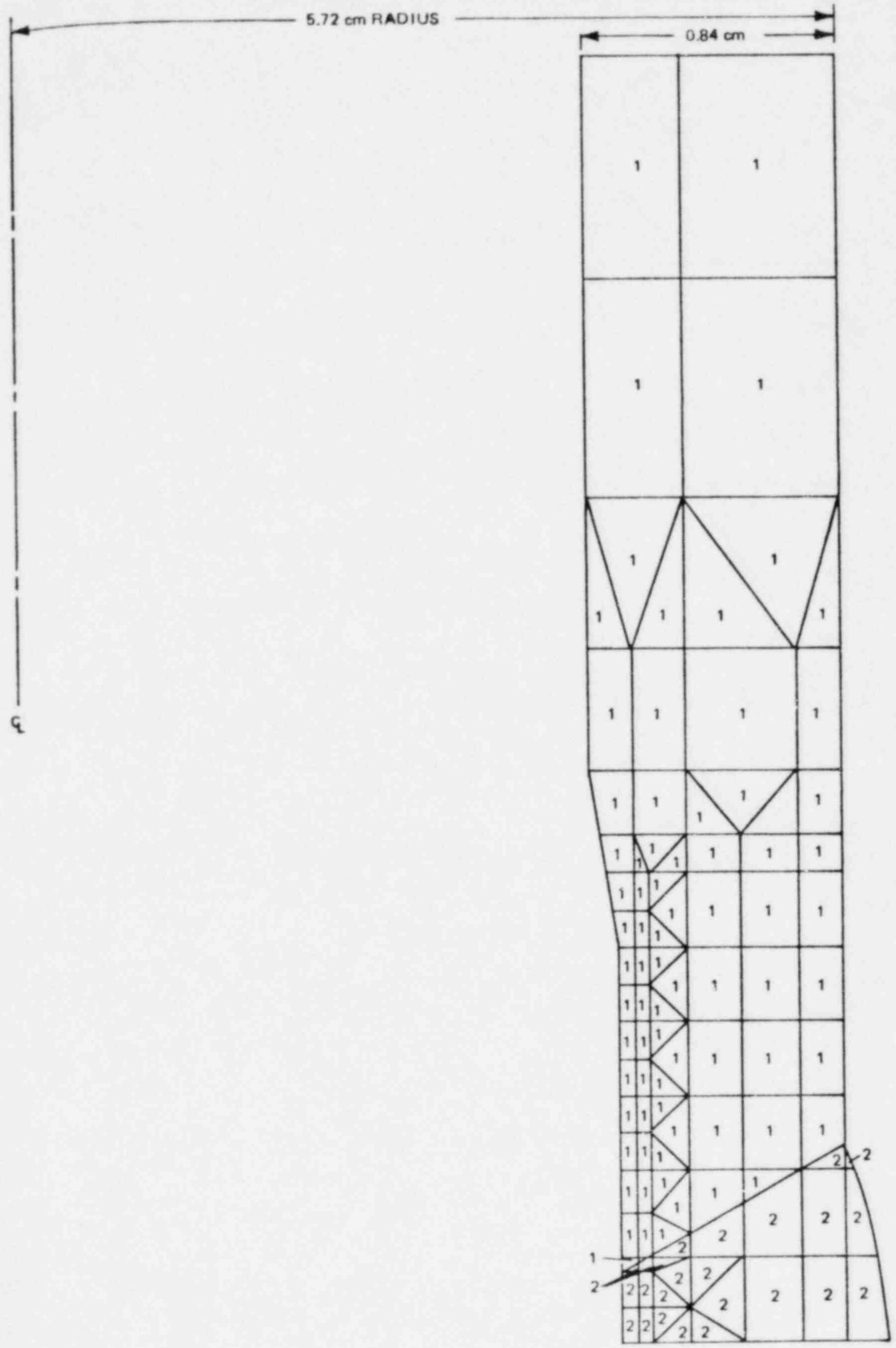

Figure 29. 10.16-cm-Diameter Schedule 80 Pipe Finite Element Weld Constraint Model

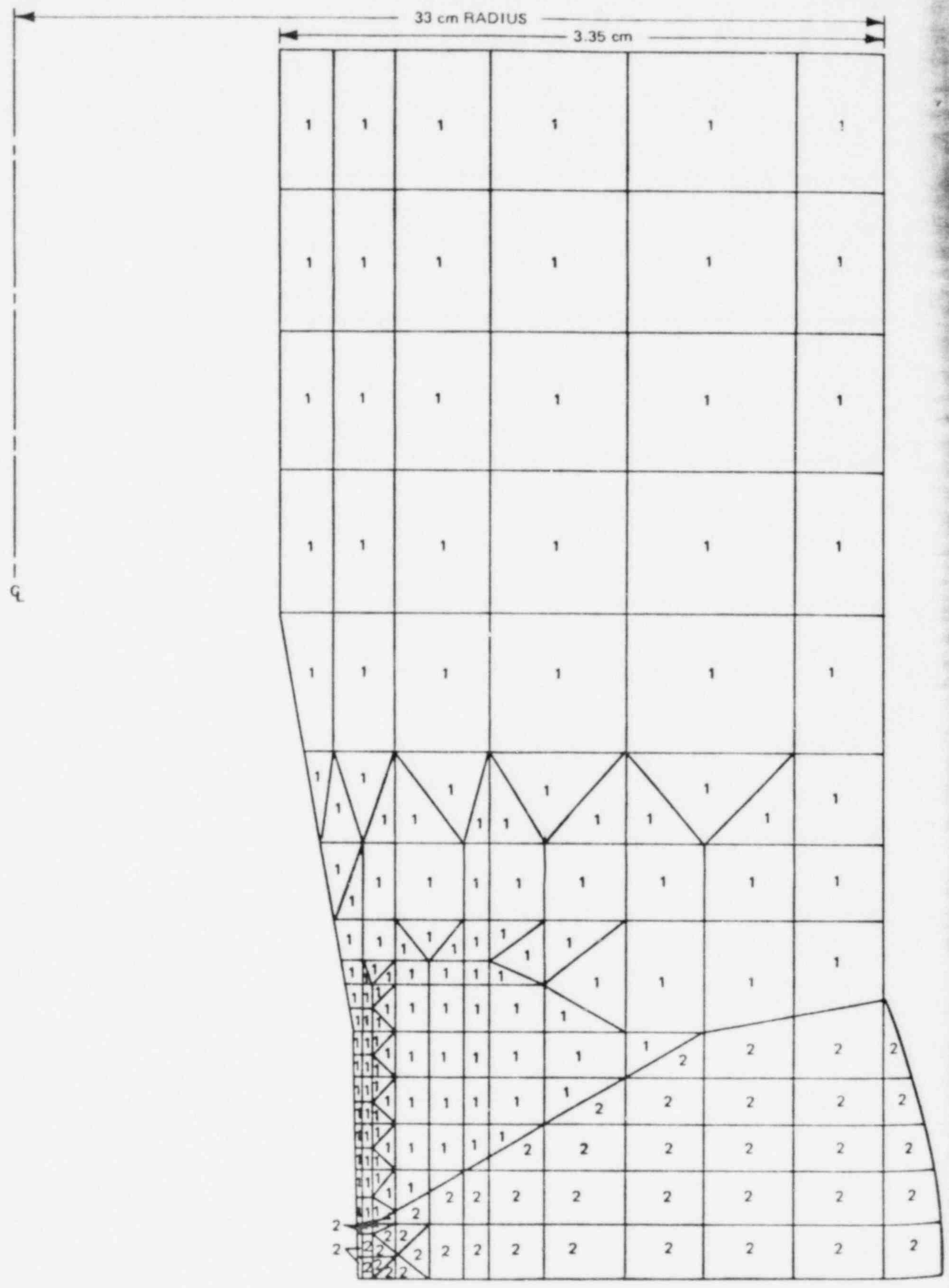

Figure 30. 66-cm-Diameter Schedule 80 Pipe Finite Element Weld Constraint Model

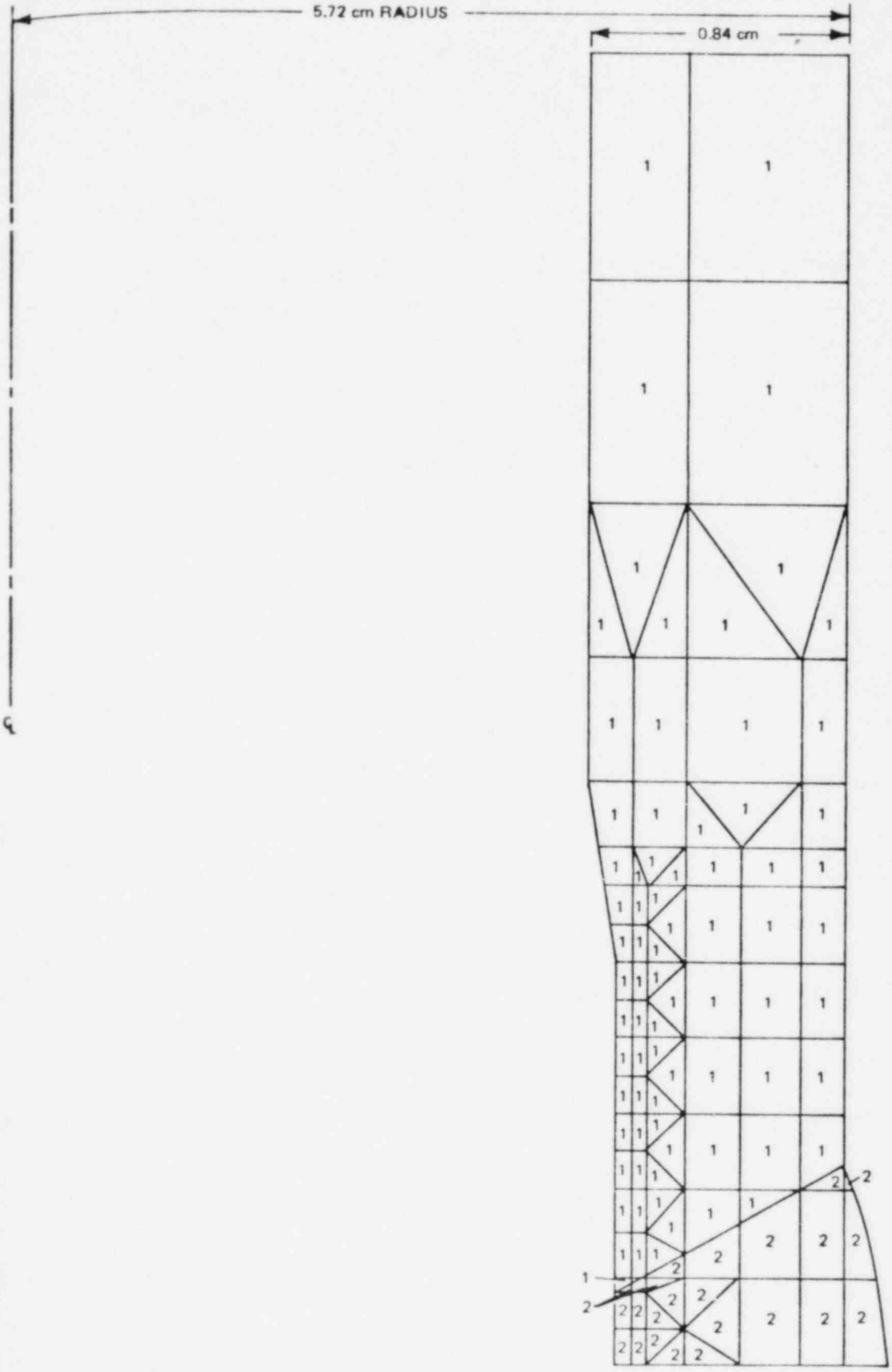

Figure 29. 10.16-cm-Diameter Schedule 80 Pipe Finite Element Weld Constraint Model

Figure 30. 66-cm-Diameter Schedule 80 Pipe Finite Element Weld Constraint Model

Figure 31. 10.16-cm-Diameter Schedule 80 Stainless Steel Pipe Butt Weld

5. TASK 3 — ELECTROCHEMICAL MEASUREMENTS — RESULTS AND DISCUSSION

5.1 INTRODUCTION AND TASK OBJECTIVES

For stress corrosion to occur a combination of stress, specific alloy metallurgical condition, and oxidizing potential must exist simultaneously. It is possible to affect the cracking phenomenon by a system change that alters any of these variables. In the present task an attempt is made to quantify the boiling water reactor system with respect to the electrochemical-environmental interactions that determine the oxidizing and corrosion potentials. The measured system oxidizing potentials will then be correlated to the intergranular stress corrosion cracking of welded Type-304 stainless steel. Initially the corrosion and oxidation potentials in actual and simulated boiling water reactor systems will be measured. In addition, potential kinetic curves will be determined in controlled environments that simulate the various operational conditions of a boiling water reactor system. Finally, the limiting potential for initiation and propagation of intergranular stress corrosion cracking will be determined in ex-reactor experiments and related to reactor operation. The correlation with reactor operation will include environmental factors from cold-standby to full power operation. Emanating from these studies will be a correlation between laboratory tests and reactor experience which will add to the understanding of the intergranular stress corrosion cracking of stainless steel piping systems.

5.2 TECHNICAL SUMMARY OF ELECTROCHEMICAL MEASUREMENTS

5.2.1 In-Reactor Experiments at Vermont Yankee

A critical part of this program is to obtain oxidation and corrosion potentials in operating boiling water reactors. The in-reactor potentials will then be related to potentials obtained in simulated boiling water reactor environments in the laboratory. The correlation of in- and ex-reactor potentials will allow the proper interpretation and design of laboratory experiments. The first in-reactor measurements were obtained in the "A" bypass line of the Dresden-2 Nuclear Power Station and are reported in the General Electric Pipe Task Force report.[1] In order to increase the data base and to follow the startup transient with chemical analyses of reactor O_2, H_2O_2, pH, and conductivity, an electrochemical test facility was installed in Vermont Yankee Nuclear Power Plant. The chemical analyses of the water were performed by Nuclear Water and Waste Technology. Figure 32 shows a diagram of the electrochemical test facility in Vermont Yankee. The test facility basically consists of a 1-liter stainless steel autoclave with four ports that contain specimen and reference electrodes. The specimen electrodes used were Type-304 mill-annealed stainless steel and platinum. Two silver/silver chloride electrodes were used for the references. Bottom penetrations in the autoclave were provided for continuous monitoring of temperature and flow. The temperature was measured with a chromel-alumel thermocouple and flow was determined from the output of a differential pressure transmitter. The autoclave with a reference and working electrode is shown in Figure 33. During operation, water from the "A" recirculation line is pumped to the reactor water cleanup system by the A and B reactor water cleanup pumps. A bypass installed across the cleanup pump delivered water to the autoclave at a rate of about 5 gpm. If required the bypass containing the autoclave can be isolated from the cleanup system by valves. The potentials, temperature, and flow rate were monitored remotely. Corrosion and oxidation potentials were monitored by a multi-station corrosion meter/recorder. Temperature and flow were monitored continuously with a dual-channel recorder.

The potentials at Vermont Yankee were monitored from cold startup to full temperature operation. All potentials have been converted to the standard hydrogen scale at all temperatures. After August 7, 1976, the monitoring station was set on automatic control. An operating procedure was written and Vermont Yankee personnel are providing coverage for the facility and periodically send the raw data to General Electric.

Figures 34 and 35 graphically present the corrosion and oxidation potentials and coincident temperatures up to August 11, 1976. At lower temperatures during cold standby the potentials were quite positive. The positive potentials reflect the conditions of oxygen saturated water with some hydrogen peroxide. Generally, as the temperature decreases the potential will increase. Thus, as the temperature dropped during the August 4 to August 5 period, positive spikes in the potential of platinum and stainless steel were observed. The greater increase of the stainless steel electrode potential can probably be explained by the greater sensitivity that stainless steel exhibits to H_2O_2. Presumably as the temperature decreases H_2O_2 concentration would increase. In ex-reactor experiments it has been shown that stainless steel responds to changes in H_2O_2 concentration far more than does platinum.

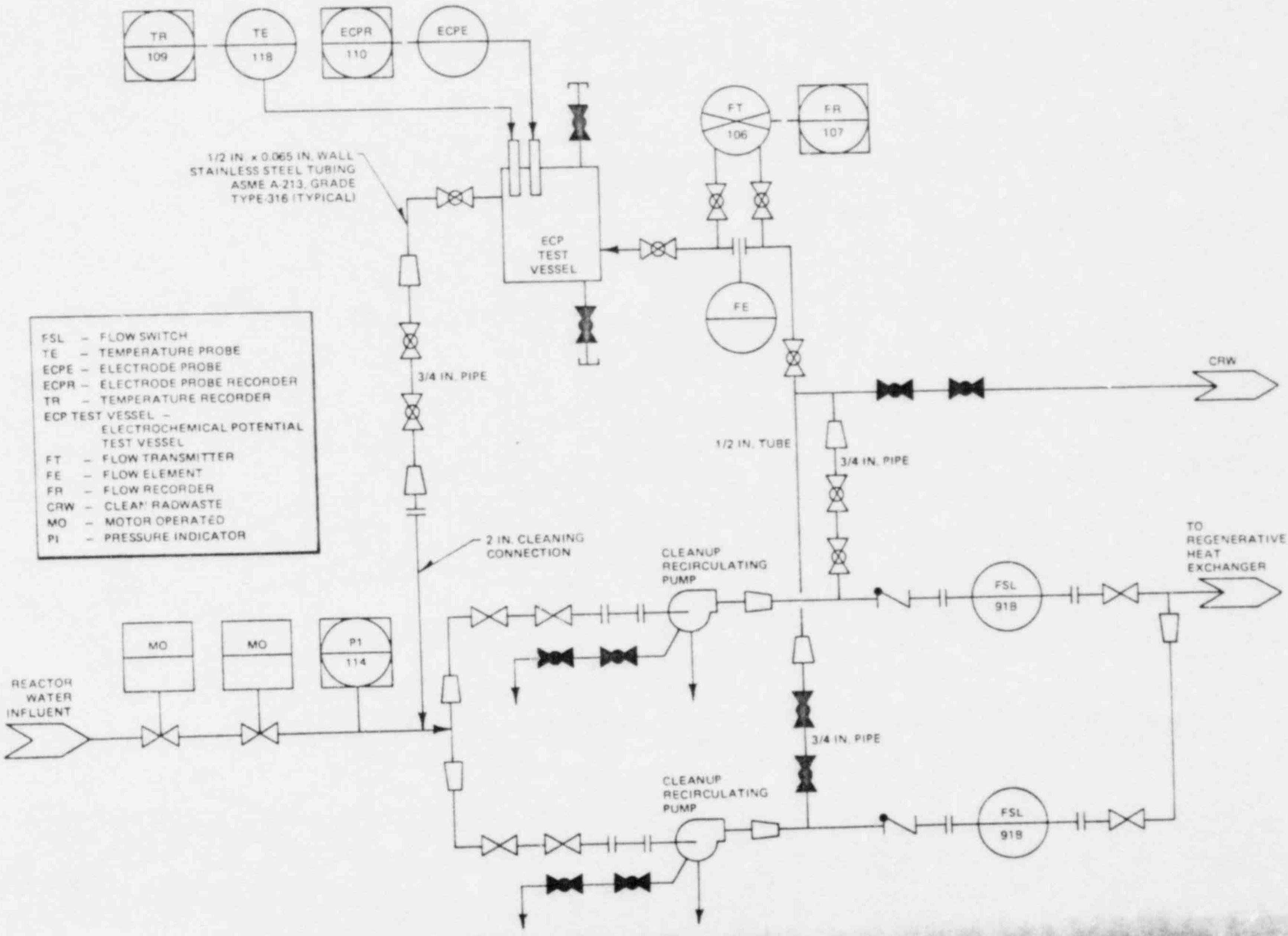

Figure [illegible] Flow Diagram of Electrochemical Potential Test Facility

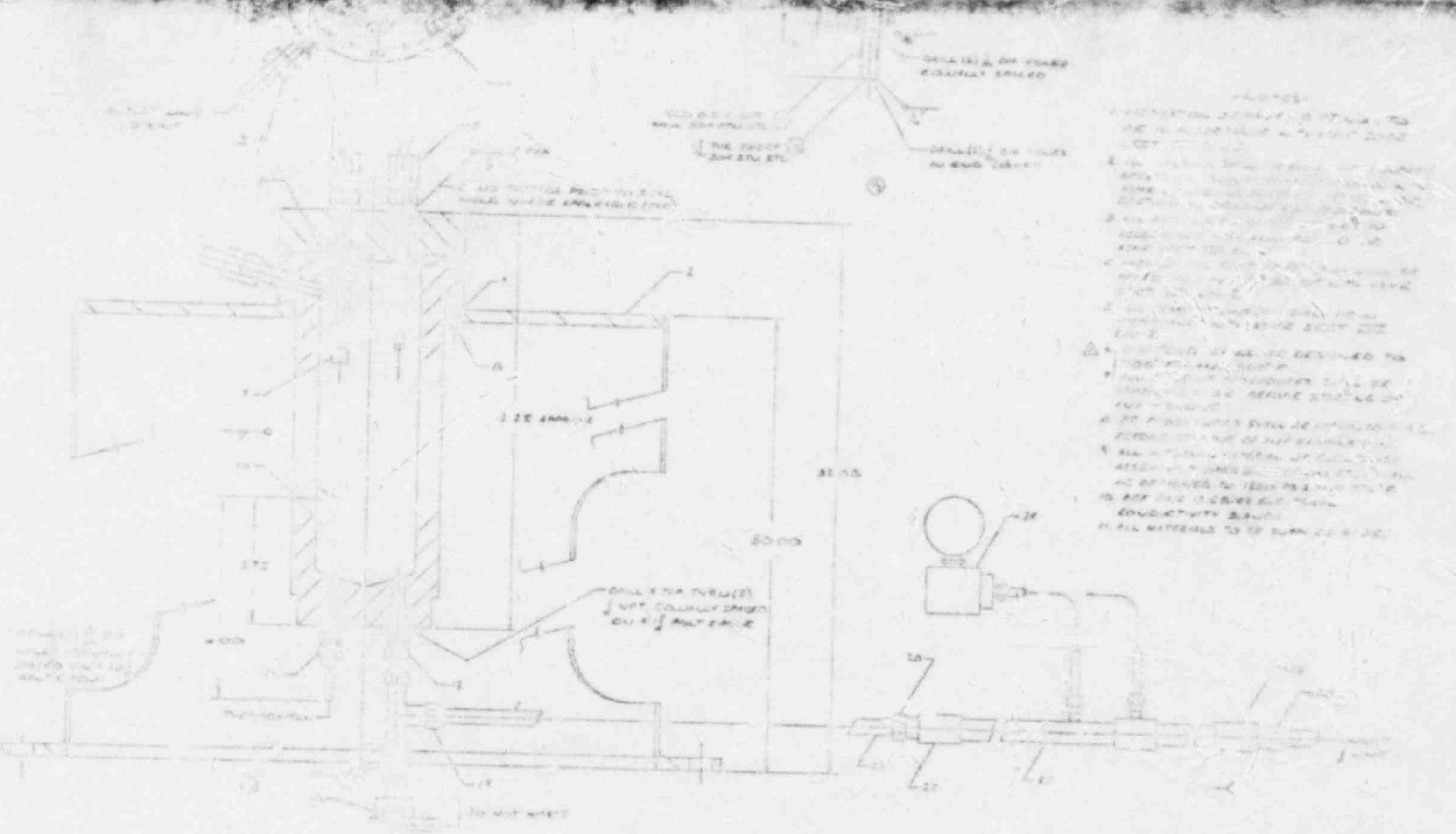
NOTES:
32.00
30.00
2.25 SPACING
DRILL 4 TIA THRU (2) NOT EQUALLY SPACED ON 4 1/2 BOLT CIRCLE
THERMOWELL
DO NOT WELD
10. SEE DWG 13 C8185 FOR CONDUCTIVITY BLANK
11. ALL MATERIALS TO BE

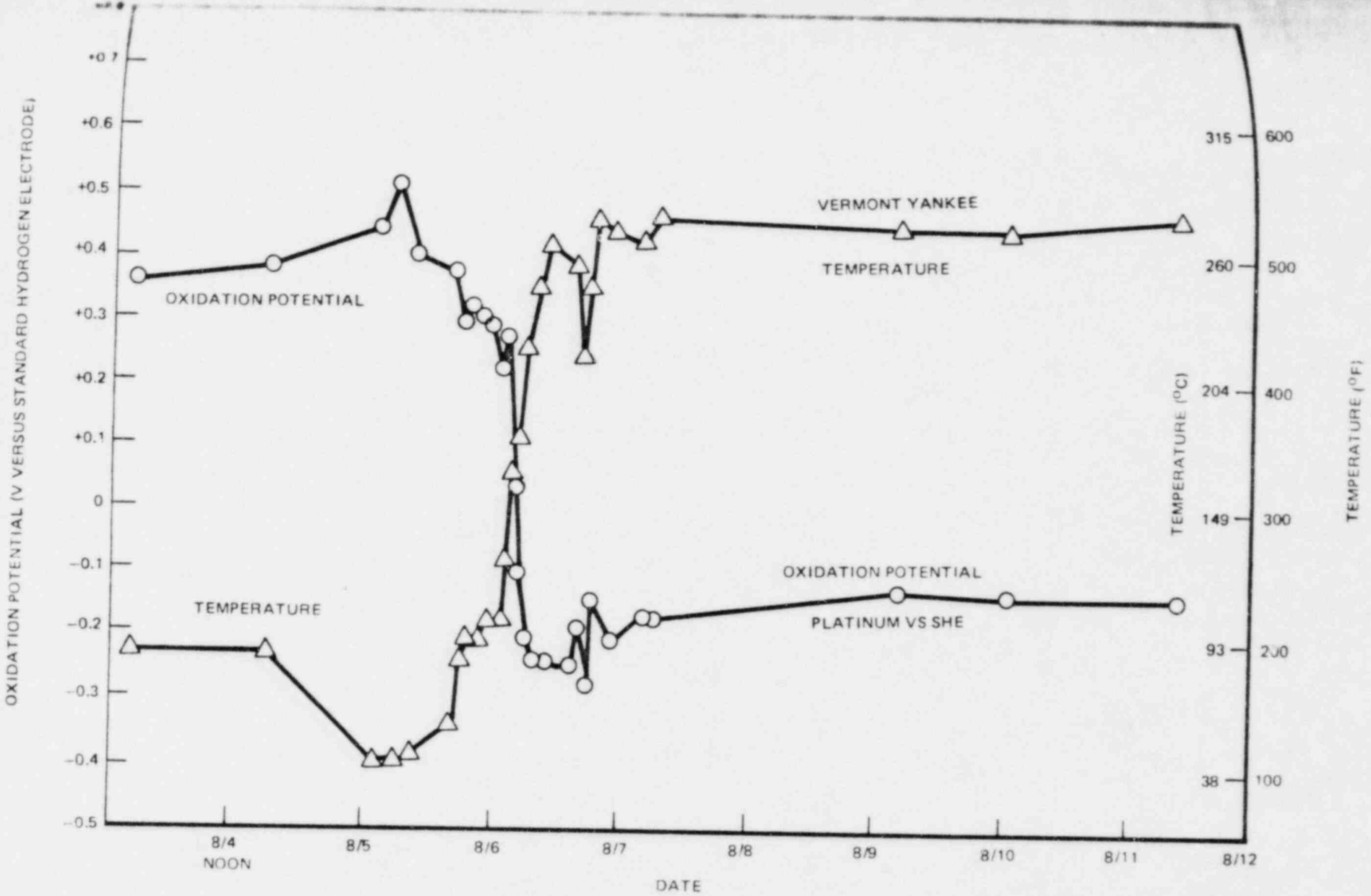

Figure 35   Oxidation Potential of Platinum During Reactor Startup

During heatup, as control rods are withdrawn from the reactor, a decrease of potential with increasing temperature was observed. A controlled degassing period at about the boiling point was conducted on August 6, 1976. During this period the potential decreased by 0.150 to 0.230 volt on the stainless steel electrode and about 0.100 volt on the platinum electrode. These decreases correspond to the drop in both oxygen and hydrogen peroxide as monitored by Nuclear Water and Waste Technology personnel. The stainless steel electrode responded to both O_2 and H_2O_2 changes, while the platinum probe responded to changes mainly in O_2 concentration. Normally at constant temperature a constant potential would be expected. However, the removal of the oxidizing agents lowers the potentials which should have a favorable effect on plant materials.

After the degassing period the potentials rose slightly even though the temperature increased. The slight rise was probably caused by the increased concentration of oxygen and hydrogen peroxide as recorded by Nuclear Water and Waste Technology. The continuous decrease in potential with increasing temperature was observed until a temperature of about 256°C (493°F) was achieved. At this point an increase in potential was measured which persisted several hours (from about 2100 to 0200, August 6 to August 7). This rise in potential was coincident with a decrease in the pH of the reactor water. The decrease in pH was caused by decomposition of ion exchange resins which had been dropped into the reactor vessel during shutdown. For this reason and because conductivity also rose, the reactor temperature was lowered to 215°C (420°F) and the reactor water cleanup system was run at maximum duty. During the cleanup period the pH and conductivity returned to acceptable values. In addition, the oxygen concentration dropped due to decrease in radiolysis with temperature. Normally the potential will rise with decreasing temperature; however, the *decreasing oxygen* and *increasing pH* more than compensated for the temperature effect and the potentials dropped. All of these chemical variations were measured by Nuclear Water and Waste Technology and coincided with the potential behavior. A second large positive spike was recorded after the heatup period was re-initiated. The potential of the stainless steel electrode rose to almost +0.1 volt versus the standard hydrogen electrode at 276°C (530°F). From previous studies it has been found that potentials above 0 volts can cause cracking of highly stressed sensitized Type-304 stainless steel. Coincident with the first positive spike of stainless steel at 256°C (493°F) and the second spike at 276°C (530°F), similar increases in potential were observed on the platinum electrode. However, the magnitude of the potential changes of the platinum was much less. It is postulated that the platinum electrode is more sensitive to hydrogen than the stainless steel and during the chemistry transient, the hydrogen concentration rose. At constant pH, increases in H_2 concentration in a hydrogen sensitive electrode result in a decrease in potential. Thus, on platinum the increase of potential caused by the decrease in pH was partly compensated by the increase in hydrogen which reduced the magnitude of the positive spike.

After the reactor chemistry returned to normal a steady-state potential of about −0.15 to −0.13 volt standard hydrogen scale was measured on the stainless steel and platinum electrode.

At the present time temperature, flow, corrosion, and oxidation potentials are being continuously recorded. To continue to obtain meaningful data all the electrodes described will be removed from the autoclave and new electrodes installed.

5.2.2 Ex-Reactor Electrochemical Measurements

Initial ex-reactor electrochemical studies performed in a recirculating water autoclave facility have yielded the oxidizing and corrosion potentials of stainless steel as affected by temperature, oxygen, and hydrogen peroxide. Initial polarization studies have shown active-passive behavior in water at 274°C (525°F) and a difference in polarization behavior between an initially filmed surface and a surface which has had its film altered by subsequent anodic polarization.

Electrochemical measurements were performed inside a Type-316 stainless steel autoclave using an Ag/AgCl reference electrode filled with 0.01 M KCl. The electrode was of Teflon construction and contained a silver wire and a fused silver chloride plug. A liquid-to-liquid junction was accomplished by an asbestos string encased in shrinkable Teflon.

Corrosion potentials of Type-304 stainless steel in high purity water were monitored from 66 to 288°C (150 to 550°F). It was observed that these potentials increased with sensitization, dissolved oxygen, and hydrogen peroxide, and decreased with increased temperature.

5.2.3 Effect of Heat Treatment and Temperature

Figure 36 and Table 10 give the data developed on the effect of heat treatment and temperature on the corrosion potential of stainless steel in air saturated water. Except for the single case for the as-cast CF3A condition at 66°C (150°F), specimens given a furnace sensitization treatment had higher corrosion potentials than material with a single treatment (mill annealed, solution annealed, or as cast). At present the reason for the apparent increase in potential with sensitization is not clear. However, the data in Figure 37 and Table 10 were developed during different runs and the apparent differences in corrosion potential might be due to experimental error. Further testing must be performed to determine whether these differences are significant.

At a lower oxygen content (0.1 — 0.2 ppm) the difference in the corrosion potential between treatments (mill annealed and sensitized) was much less (Figure 37). This was especially true at the higher temperatures. In tests of both high (9 ppm) and lower (0.1 — 0.2 ppm) oxygen levels, Figures 36 and 37, respectively, the effect of increased temperature was to decrease the corrosion potential. This is in agreement with previous in-reactor measurements made at Dresden and Vermont Yankee boiling water reactors.

Table 10

THE EFFECT OF HEAT TREATMENT ON THE CORROSION POTENTIALS OF TYPE-304 STAINLESS STEEL IN AIR SATURATED HIGH PURITY WATER[a]

	Open Circuit Corrosion Potential[b] (mV, Standard Hydrogen Electrode)				
Heat Treatment[c]	**66°C (150°F)**	**121°C (250°F)**	**178°C (350°F)**	**232°C (450°F)**	**288°C (550°F)**
MA	120	158	147	79	+2
MA + FS	188	201	188	113	69
SA	120	114	157	100	−90
SA + FS	129	*d*	*d*	*d*	*d*
Cast	311	159	118	—	−120
Cast + FS	171	205	191	107	63

---

[a] Resistivity 10 to 13 megohm-cm, neutral pH, O_2 = 9 ppm

[b] Potential determined after 1 hour at temperature

[c] MA – mill annealed
FS – furnace sensitization treatment of 40 hours at 621°C (1150°F), then air cooled
SA – solution annealed 1/2 hour at 1065°C (1950°F), then water quenched
Cast – cast CF3 stainless steel

[d] Not determined

5.2.4 Effect of Hydrogen Peroxide

An initial investigation into the effect of hydrogen peroxide was performed at 66°C (150°F) in air saturated water using Type 304 stainless steel and platinum specimens. As indicated in Figure 38, the addition of 10 ppm H_2O_2 increased the corrosion potential of stainless steel approximately 225 mV and lowered the corrosion potential of platinum 94 mV. The opposite response of the two materials to the additional hydrogen peroxide is probably due to platinum acting as an oxygen electrode and stainless steel acting as a peroxide electrode. With high levels of dissolved oxygen the potential of both platinum and stainless steel will be high. The platinum potential is higher than the stainless steel (time = 0 in Figure 38) since platinum behaves more as a reversible oxygen electrode according to the reaction

$$O_2 + 4H^+ + 4e^- \rightarrow 2\,H_2O \qquad E_o = 1.23 \text{ volts.}$$

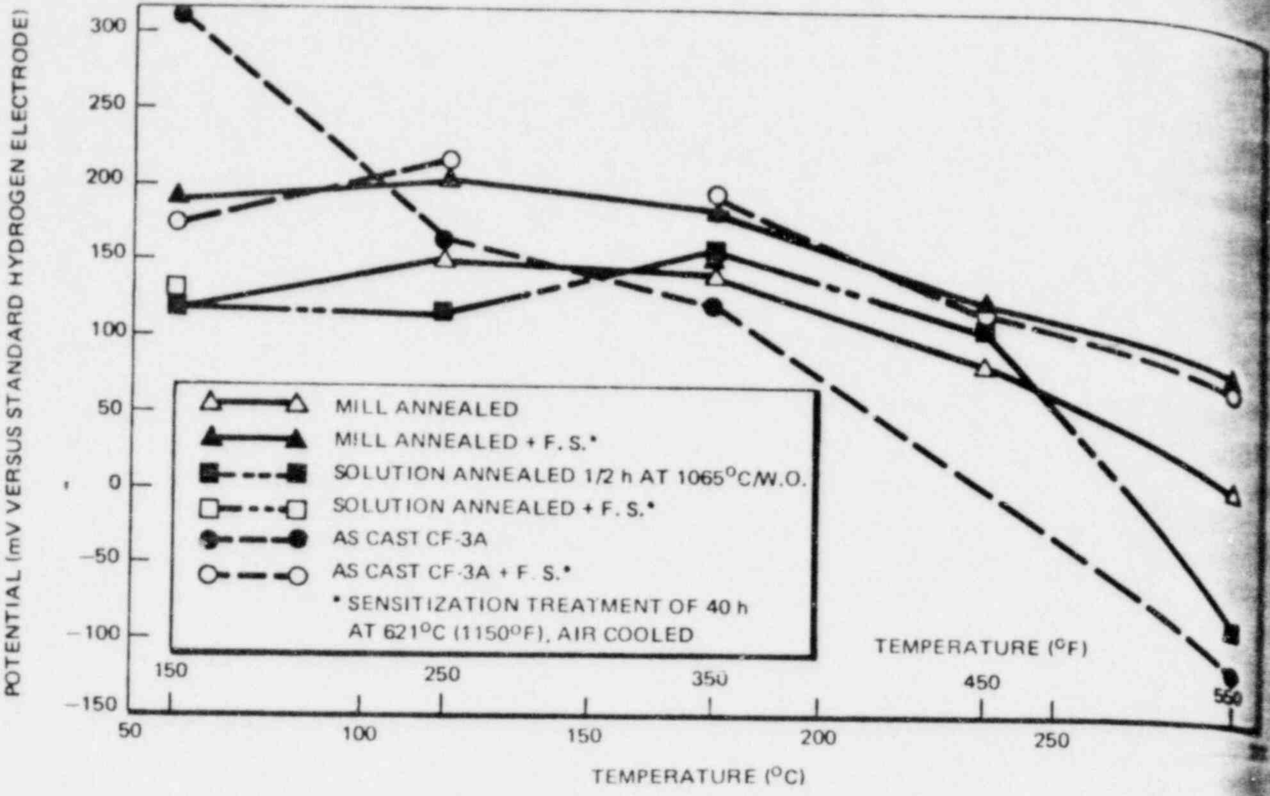

Figure 36. The Effect of Heat Treatment on the Corrosion Potential of Type-304 Stainless Steel in Air Saturated High Pu
Water

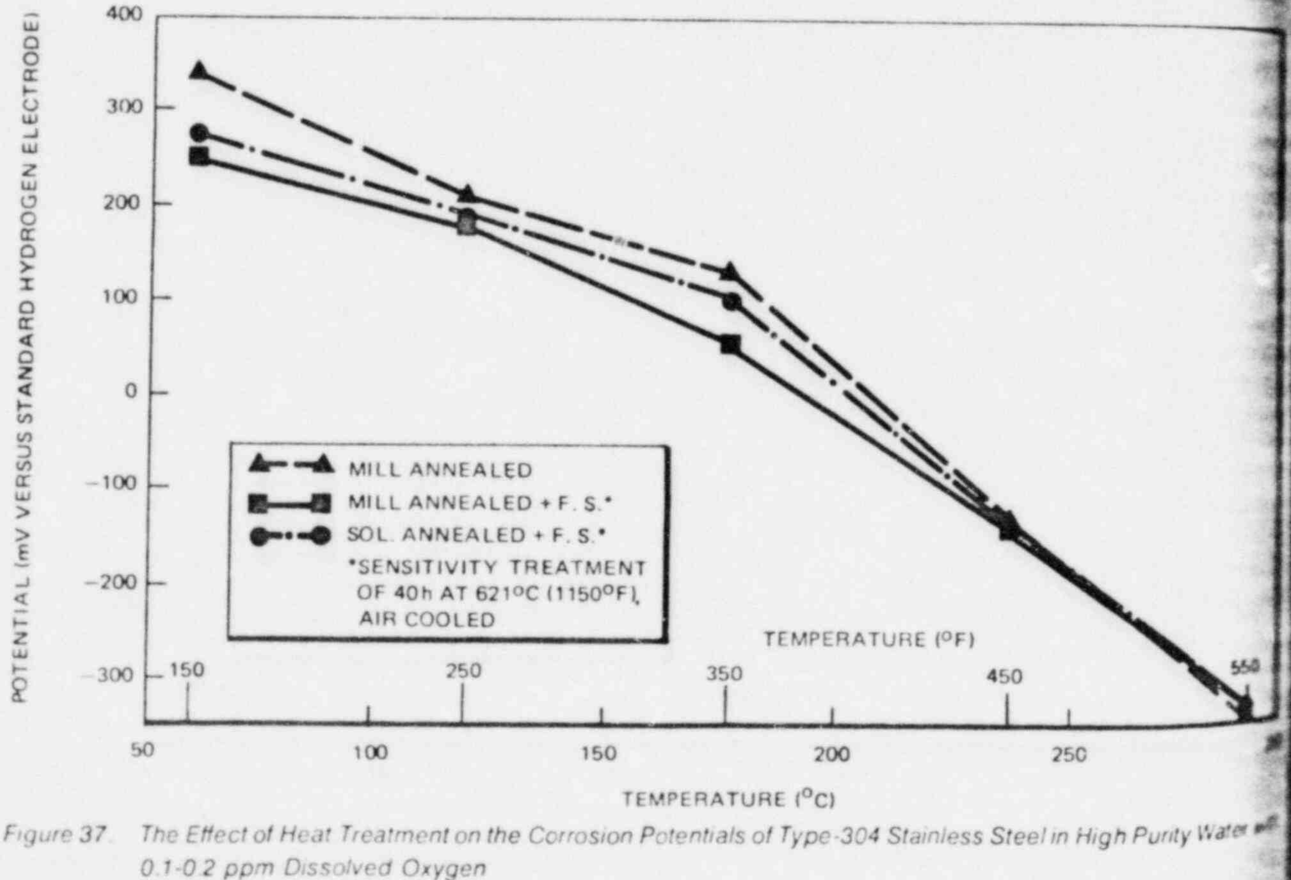

Figure 37. The Effect of Heat Treatment on the Corrosion Potentials of Type-304 Stainless Steel in High Purity Water
0.1-0.2 ppm Dissolved Oxygen

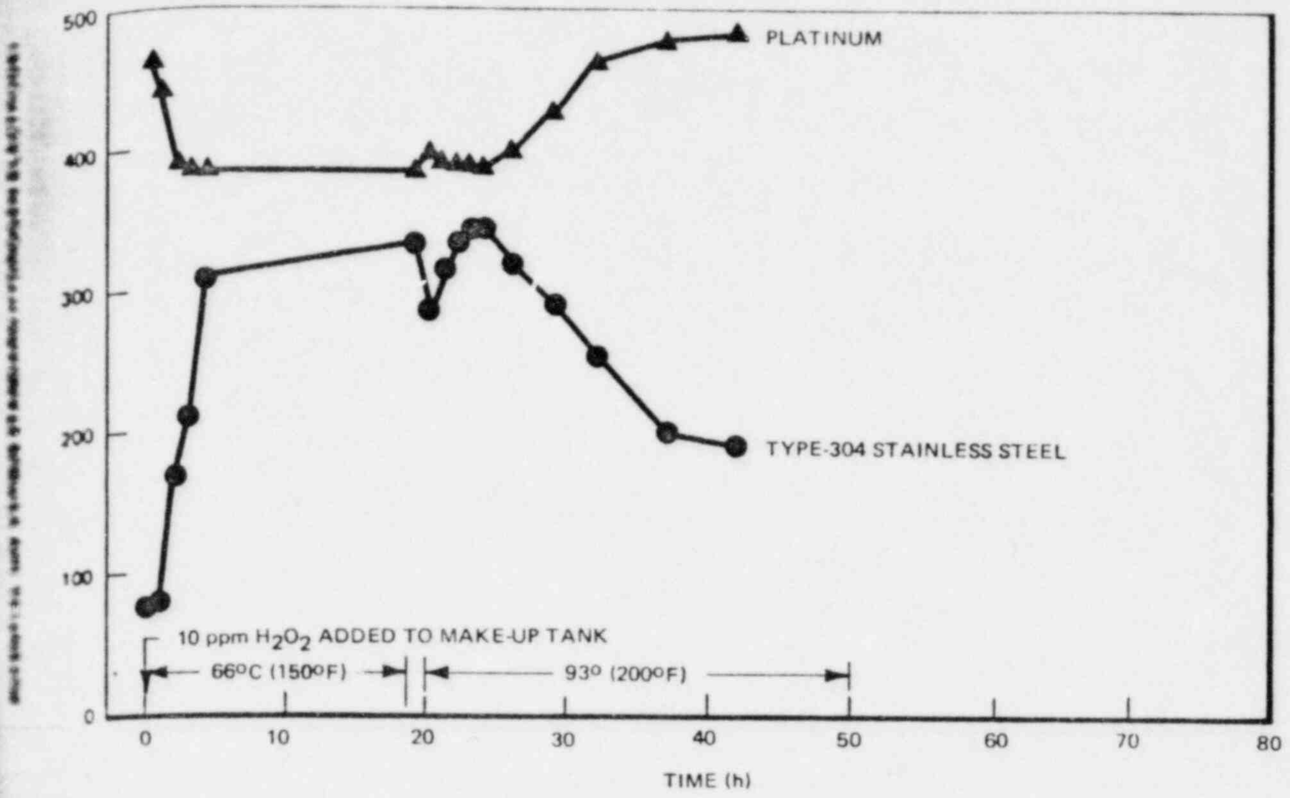

Figure 38 *Effect of Hydrogen Peroxide on Oxidation and Corrosion Potential of Platinum and Type-304 Stainless Steel in Aerated Water*

The reduction of oxygen to water does not occur directly as shown above but proceeds by a kinetic intermediate, H_2O_2, according to the reaction

$$O_2 + 2H^+ + 2e^- \rightarrow 2H_2O_2 \qquad E_o = 0.68 \text{ volt.}$$

The H_2O_2 subsequently disproportionates to water and oxygen. Since the intermediate reaction occurs at a lower potential, increasing the concentration of the kinetic intermediate (H_2O_2) will lower the potential of the platinum/oxygen electrode. On the other hand, the potential of stainless steel does not approach reversibility as an oxygen electrode, and in the presence of H_2O_2 it responded as a peroxide electrode according to the reaction

$$H_2O_2 + 2H^+ + 2e^- \rightarrow 2H_2O \qquad E_o = 1.77 \text{ volts.}$$

Since this reaction occurs at an extremely high potential, the potential of the stainless steel electrode increased significantly. The effects of hydrogen peroxide were realized only at 66°C (150°F) and for a short time (<4 hours) at 94°C (200°F). Holding at 94°C (200°F) eventually decomposed the H_2O_2 and the corrosion potentials of stainless steel and platinum approached their original values.

[illegible] Effect of Dissolved Oxygen

The effect of dissolved oxygen content on the corrosion potential of mill-annealed Type-304 stainless steel and platinum at 274°C (525°F) in high purity water is given in Table 11. The results given in Table 11 were determined during a run in which the water was deaerated at 94°C (200°F) by purging the feed tank with nitrogen gas and circulating the water in the

Table 11

EFFECT OF OXYGEN CONTENT ON THE CORROSION POTENTIAL OF MILL-ANNEALED TYPE-304 STAINLESS STEEL (HEAT NO. 7616) AND PLATINUM IN HIGH PURITY WATER[a] AT 274°C (525°F)

Oxygen Content[b] (ppm)	Hydrogen Content[d] (ppm)	Open Circuit Potential (mV Standard Hydrogen Electrode)	
		Type-304 Stainless Steel	Platinum
0	0	−705	−595
0.1	0.025	−355	−650
0.8[c]	0	−235	−200
5.0[c]	0	−103	+ 37
9.0	0	− 31	+ 49

---

[a] Resistivity CR.T = 10 to 13 megohm-cm, neutral pH

[b] Analysis taken on feed tank using CHEMets®

[c] Obtained during air bubbling transition from 0.1 ppb to 9.0 ppm

[d] Estimated from calibrated gas mixture used for overpressure

feed tank through a sulfite-resin bed. The deaerated water from the feed tank was then pumped into the autoclave and hea to 274°C (525°F). In water containing 0 ppb oxygen, the potentials of stainless steel and platinum dropped to the low values −705 and −595 mV standard hydrogen electrode, respectively. As the oxygen concentration was increased to 0.1 ppm bubbling with a N_2 - 0.5% O_2 - 1.6% H_2 gas mixture the corrosion potential of stainless steel increased to −355 mV and platinum potential decreased slightly to −650 mV. The decrease in platinum potential apparently was due to platin responding more as a hydrogen electrode than as an oxygen electrode. With 9 ppm oxygen, achieved by bubbling with the corrosion potential of both stainless steel and platinum increased significantly. Stainless steel increased to 31 mV platinum changed 700 mV to +49 mV. Corrosion potentials obtained during the transition between 0.1 and 9 ppm are given in Table 11 and have intermediate values.

5.2.6 Anodic Polarization Studies of Type-304 Stainless Steel

Anodic polarization studies could not be performed in the high purity water used for the corrosion potential measu ments because of the extremely high electrical resistance of the water. The resistance of the water was decreased by addition of sodium sulfate. Upon adding and thoroughly mixing the equivalent of 0.01 Na_2SO_4 the impedance between specimen electrode and the autoclave decreased by three orders of magnitude to approximately 30 ohms at 274°C (525 The resistance appeared low enough to allow polarization studies to be performed. Significant IR corrections in poten (>50 mV) would become necessary for current densities in excess of 260 μA/cm².

Figure 39 presents the polarization behavior observed for a mill-annealed Type-304 stainless steel specime 274°C (525°F). The curves were developed at a scan rate of 5 mV/sec (18 V/h) starting at −1200 mV, sweeping to +1 mV, and then reversing the scan back to −1200 mV. The curves given in Figure 39 are those developed during the second, and fourth through sixth scans.

During all forward scans (− to + direction) an active peak occurred around −500 mV (Figure 39a). The cur associated with this peak increased with successive scans. This increase in current is thought to be a result of the corro film being altered and probably thinned during the successive polarization cycles. In the forward scan direction over potential range of −500 mV to +600 mV there is a decrease in current with increased potential indicating a regio passivity. The first forward scan through this region yielded a complex curve with many inflections. As the number of sc increased, the complexity of the curve decreased. At potentials greater than +600 mV the current increased sharply with onset of oxygen evolution.

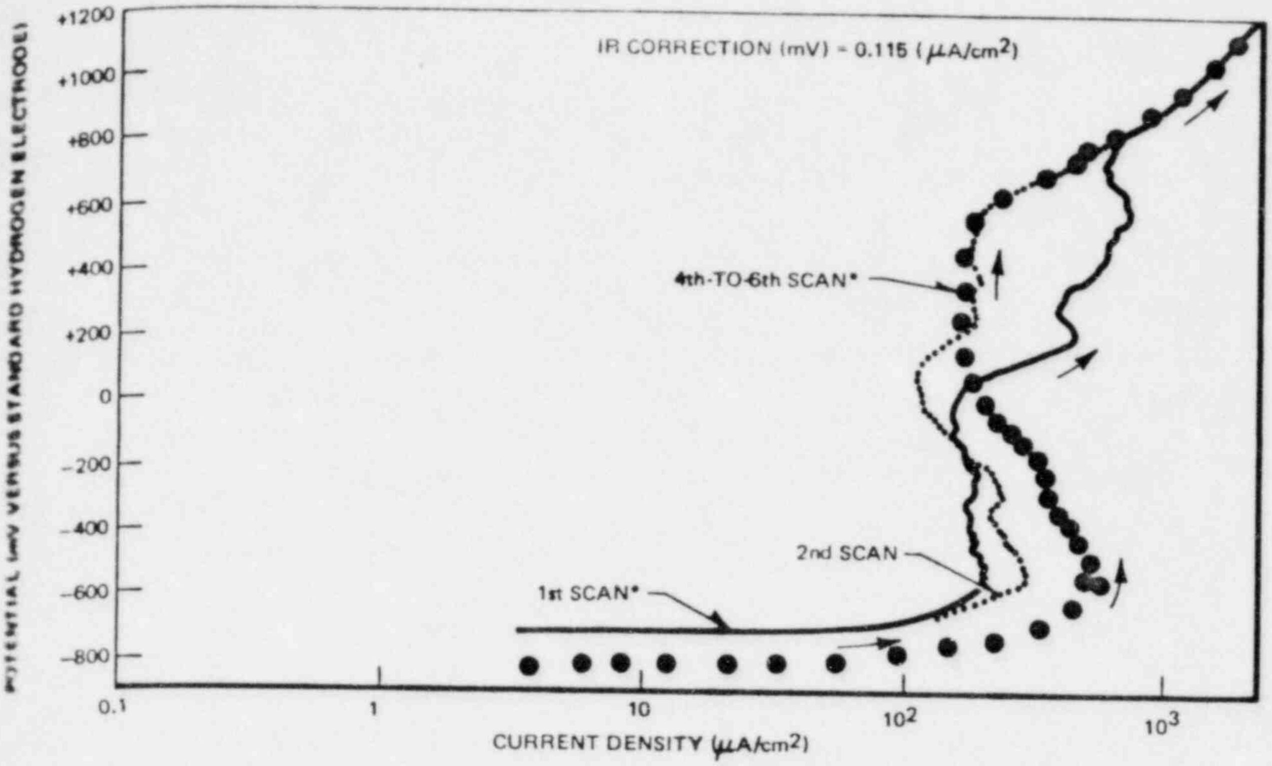

(a) FORWARD SCAN

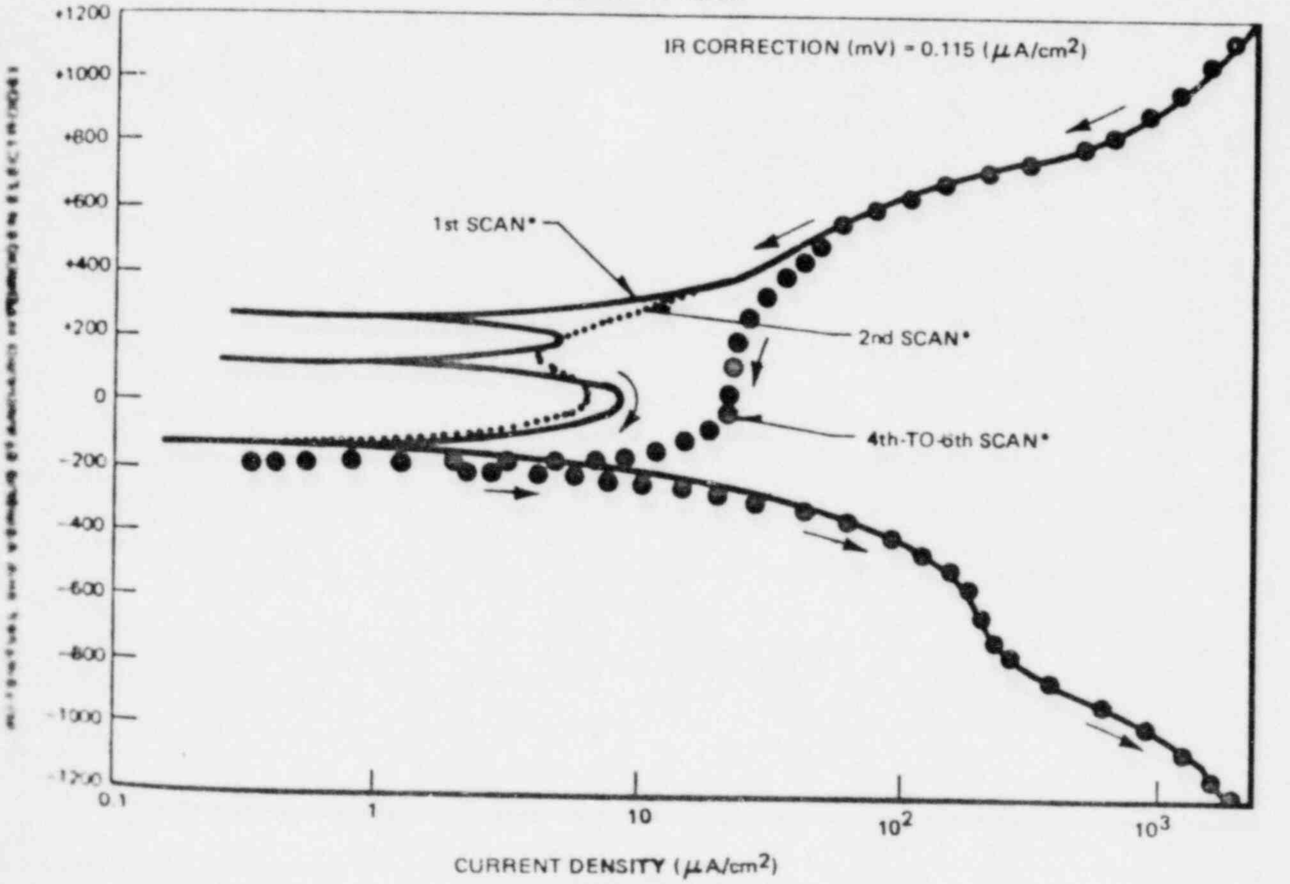

(b) REVERSE SCAN

Figure [illegible] Forward (A) and Reverse (B) Scan Polarization Curves of Mill Annealed Type-304 Stainless Steel at 274°C (525°F) in Deaerated Water Containing 0.01 N Na_2SO_4 (Scan Rate 5 mV/sec)

Upon reversing the scan direction (Figure 39b) the current fell to values less than that observed during the forward scan. During the first reverse scan the current dropped sharply and became cathodic around +250 mV. The cathodic current peaked at +200 mV and then changed to anodic at +140 mV. During successive scans this cathodic region eventually disappeared. The existence of the cathodic region is thought to be due to the reduction of Cr^{+6} to Cr^{+3} according to the reaction $6I^- + 2\,CrO_4^{2} + 5\,H_2O \rightarrow Cr_2O_3 + 10\,OH^-$.

As the potential was lowered below +140 mV the anodic current peaked around 0 mV and with further decrease in potential the current became cathodic around −120 to −200 mV. This second cathodic region persisted to −1200 mV. However, at potentials corresponding to the initial active peak (−500 mV) observed during the forward scan the cathodic curve flattened out slightly indicating that an anodic reaction (active metal dissolution) was competing for the current. Below approximately −700 mV the back scan curve became the same as the forward scan curve (not shown in Figure 39a).

In future reports a more detailed discussion will be presented on the significance of the various changes in current with potential observed in the polarization curves and their correlation to possible stress corrosion cracking. At present, interpretation of these polarization curves is made difficult by interferences by other reactions. These interfering reactions occur over the potential of interest and are due primarily to the oxidation-reduction reactions associated with the materials used in the autoclave construction. For example, the oxidation of Fe^{+2} to Fe^{+3} has been shown by Indig and Vermilyea[2] to contribute substantially to the oxidation current in active-passive regions. Such reactions can significantly obscure important regions. Future plans include obtaining a Ti-6Al-4V autoclave and improving water purification methods which will minimize currents associated with reactions not relevant to the stainless steel corrosion process.

6. FUNDAMENTAL STUDIES OF FERRITE EFFECTS IN DUPLEX STAINLESS STEELS ON RESISTANCE TO INTERGRANULAR STRESS CORROSION CRACKING IN BOILING WATER REACTOR ENVIRONMENT — RESULTS AND DISCUSSION

6.1 INTRODUCTION AND TASK OBJECTIVE

In-reactor experience and numerous laboratory studies conducted in simulated boiling water reactor environments have indicated duplex stainless steels to be much more resistant to intergranular stress corrosion cracking than austenitic stainless steels. It is the goal of this program to determine the metallurgical conditions responsible for this resistance to stress corrosion cracking in the various boiling water reactor environments. The minimum amount of ferrite, the required chemical composition of the ferrite, and the morphology of the ferrite required to inhibit intergranular stress corrosion cracking in simulated boiling water reactor environments will be determined. The effect of cold work as well as the effect of second phase particles such as carbides, σ phase and α' phase on the stress corrosion cracking of duplex stainless steels will also be investigated. To expedite testing of the large number of alloys and heat treatments to be examined in this study, a screening test will be developed to detect and screen out alloys and/or heat treatments highly susceptible to stress corrosion cracking. These alloys and/or heat treatments would not be tested in the simulated boiling water reactor stress corrosion cracking apparatus, freeing the latter for tests on more resistant materials.

6.2 SUMMARY OF RESULTS

The present results indicate that several screening tests used in the past to evaluate the stress corrosion cracking susceptibility of austenitic stainless steels do not correctly predict the stress corrosion cracking behavior of duplex stainless steels. An accelerated corrosion test which measures the pitting potential in chloride ion media and which accurately predicts the stress corrosion cracking behavior of both austenitic and duplex stainless steels in 0.01 N H_2SO_4 at room temperature was developed. Stress corrosion cracking tests have been initiated on specimens in simulated boiling water reactor environments. As part of the screening test program, stress corrosion cracking tests were conducted at room temperature in 0.01 N H_2SO_4.

The pitting potential test was also shown to be very sensitive to changes in microstructural features detecting, for example, the presence of $M_{23}C_6$ precipitates formed at austenite grain boundaries and along austenite-ferrite phase boundaries as well as α' phase (475°C embrittlement) which forms in and embrittles the ferrite phase. Should future stress corrosion crack testing in simulated boiling water reactor environments show such microstructural features to be deleterious to stress corrosion cracking resistance, then the pitting potential test will be useful in screening duplex stainless steels containing these harmful phases.

Although this study is solely interested in the stress corrosion cracking behavior of duplex stainless steels, corrosion work conducted on fully austenitic stainless steel (which was used as a benchmark during the development of a stress corrosion cracking screening test) revealed an interesting effect deemed worthy of disclosure in this report. The results of the accelerated intergranular corrosion tests, the pitting tests, and the stress corrosion cracking tests indicate that prior annealing treatments have a marked effect on the corrosion and stress corrosion cracking behavior of sensitized austenitic stainless steel. Preliminary transmission electron microscopy indicates that intergranular precipitation of M_xC_y during annealing at 1000°C inhibits intergranular precipitation of $Cr_{23}C_6$ during lower temperature anneals and the material is resistant to intergranular stress corrosion cracking. Annealing at the usual temperature of 1100°C does not result in intergranular carbide precipitation and the material is sensitized and susceptible to intergranular stress corrosion cracking when subsequently heat treated at 600°C for 24 hours.

Casting and thermomechanical processing were initiated on 51 alloys to be used in this program to study the effect of volume fraction, morphology, and chemical composition of the ferrite phase, the effect of secondary phases, and the effect of cold work on the stress corrosion cracking behavior of duplex stainless steels.

6.3 SUBTASK 1 DEVELOP A TESTING PROCEDURE TO ASSESS THE STRESS CORROSION CRACKING SUSCEPTIBILITY OF DUPLEX STAINLESS STEELS IN THE BOILING WATER REACTOR ENVIRONMENT

6.3.1 Introduction

The primary test employed in this program to assess an alloy's susceptibility to stress corrosion cracking in the boiling water reactor environment will consist of constant extension rate test 1/4-in.-diameter tensile-type specimens immersed in air saturated high purity water at 289°C and measuring the stress and strain at failure and determining the amount of brittle intergranular fracture. Because of the limited number of facilities capable of performing the above test, an extensive ongoing effort is being made in this program to develop a screening test capable of assessing an alloy's susceptibility to stress corrosion cracking in the constant extension rate test. Such a test could be used to detect and screen out alloys and/or heat treatments with a high degree of susceptibility to stress corrosion cracking. These alloys and/or heat treatments would not be tested in the constant extension rate test facility, freeing the latter for tests on more resistant material.

The initial screening tests to be evaluated are A262C, A262E, and the pitting potential measured in near-neutral and low pH chloride ion solutions. Initially all alloys studied will be subjected to the above short-time screening tests as well as the constant extension rate test. These initial results will establish the credibility of the various short-time screening tests. Those which do not correctly predict the stress corrosion cracking behavior in the constant extension rate test will be eliminated from future use. Those which adequately describe the stress corrosion cracking behavior will be used for initial screening tests in alloy evaluation work and in fundamental mechanistic studies.

The A262C and A262E tests were selected because of the long history of their use in assessing the intergranular stress corrosion cracking susceptibility of austenitic stainless steels. The pitting potential test was selected principally because the pitting potential is a strong function of the chromium content of the alloy. Regions of a material which are low in chromium will pit first and at a lower applied potential than regions higher in chromium. This is very important for two reasons. First, a strong correlation exists between intergranular stress corrosion cracking susceptibility in the boiling water reactor environment of austenitic stainless steel and the presence of chromium-depleted zones adjacent to grain boundaries. Because of the dependency of pitting susceptibility on the chromium content, the presence of chromium-depleted grain boundaries in austenitic and in any other type of stainless steel would be detected by the pitting potential tests. Second, many microstructural features in duplex stainless steels are accompanied by chromium-depleted regions. Consequently, the pitting potential test could be used to detect the presence of these microstructural features. For example, σ phase which can form in single phase as well as duplex stainless steels is a chromium-rich intermetallic compound of transition elements and is surrounded by a chromium-depleted zone. Similarly, the intermetallic compounds known as R phase and χ phase, both are formed in molybdenum-containing stainless steels, are rich in chromium, and their formation results in the creation of chromium-depleted zones. Finally, α' phase is a chromium-rich phase formed within a miscibility gap existing at low temperatures in the ferrite phase. The α' precipitates contain as much as 90% chromium and result in severe chromium depletion of the ferrite phase as well as embrittlement of the ferrite. Should stress corrosion crack testing show such microstructural features to be deleterious to stress corrosion cracking resistance, then the pitting potential test will be useful in screening duplex stainless steels containing these harmful phases.

Constant extension rate test facilities for determining the stress corrosion cracking susceptibility of duplex stainless steels in simulated boiling water reactor environments have just recently been completed. Results of stress corrosion cracking tests on duplex stainless steel in simulated boiling water reactor environments will be obtained in the constant extension rate test facilities. During the period, screening stress corrosion cracking tests were conducted at room temperature in 0.01 N H_2SO_4. These results are of interest for several reasons. First, the pH of the test solution models the pH which exists at the tip of a crack even in a sample immersed in a solution with bulk pH 7. Second, preliminary results show a wide easily discernible difference in behavior between material known to be resistant to stress corrosion cracking in boiling water reactor environments (e.g., fully annealed austenitic stainless steel) and material known to be highly susceptible to stress corrosion cracking (e.g., sensitized austenitic stainless steel). Third, failure times are relatively short. Fourth and foremost, since the tests are conducted in an electrolyte, potentiostatic control of the test specimen is possible providing information useful in studying the mechanism of cracking. Expanding further on this last point, if intergranular stress corrosion cracking is indeed related to intergranular corrosion caused by chromium depletion at grain boundaries, then it should be possible to anodically polarize even a fully sensitized austenitic stainless steel sample to a sufficiently noble potential so that even the chromium-depleted zones are passivated and no longer susceptible to localized accelerated corrosion attack so that stress corrosion cracking should no longer occur.

6.3.2 Materials and Processing

To date thermomechanical processing has been completed on Heat S0099 of Type-308 stainless steel whose composition is listed in Table 12. The as-received 3/32-in. (0.24-cm) diameter welding rods of this alloy were given an initial 1-hour anneal at one of four temperatures — 1350°C, 1100°C, 1050°C, 1000°C — followed by a water quench. Annealing at 1350°C for 1 hour and water quenching produces a duplex microstructure consisting of approximately 25 vol % ferrite. The other three heat treatments produce a single-phase austenitic matrix. The austenitic material was tested to produce a benchmark for the intergranular corrosion screening tests. The annealed rods were cold drawn to 0.030-in. (0.075-cm) diameter wire using intermediate anneals after reductions of ~40% at the same initial temperature for 1 hour followed by water quenching. After the last drawing pass, the wire was sectioned into 1-1/2-in. (3.8-cm) lengths for corrosion testing and 10-3/4-in. (27.3-cm) lengths for stress corrosion crack testing. The specimens were then given a final 1-hour anneal and water quench. Half the number of specimens given each annealing treatment were subsequently heat treated at 600°C for 24 hours and water quenched.

Table 12
COMPOSITIONS OF TYPE-308 STAINLESS STEEL

Form	Heat No.	C	Si	P	Wt % Ni	Mn	S	Cr	Ferrite Number
As Cold Drawn 1/16 in. x 36 in. welding rod (0.16 cm x 91.4 cm)	13405013	Analysis not completed							9.5
As Cold Drawn 3/32 in. x 36 in. welding rod (0.24 cm x 91.4 cm)	S0099	0.014	0.32	0.005	9.62	1.92	0.011	20.37	11.5

6.3.3 Testing Procedure

Prior to corrosion and stress corrosion crack testing all specimens were electropolished in a solution of 60% H_3PO_4 + 40% H_2SO_4 at 60°C at 1 amp/cm² for 5 minutes. Samples for anodic polarization tests were soldered to an electrical test lead. The soldered joint was subsequently marked off with Glyptal® paint. Accelerated intergranular corrosion tests were performed according to ASTM specifications A262C and A262E. Prior to anodic polarization and accelerated intergranular corrosion testing, samples were ultrasonically cleaned in acetone and rinsed in distilled water.

6.3.4 Results

6.3.4.1 Corrosion Tests

Figure 40 summarizes the results of A262E testing of as-annealed and sensitized Type-308 stainless steel. The specimens were nominally 0.025 inch (0.063-cm) in diameter and 1.5 inches (3.8-cm) in length. A rating of zero indicates no etching of the specimen following 3 days of immersion. A rating of 1 indicates grain boundary etching. A rating of 2 indicates grain boundary cracking following bending of the specimen. A rating of 3 indicates severe intergranular penetration characterized by nearly zero ductility. In the four as-annealed conditions no attack of any kind occurred. Following a 600°C for 24-hour heat treatment, the sample which had been annealed at 1100°C for 1 hour suffered 100% intergranular penetration.

Table 13
RESULTS OF A262C TESTS ON TYPE-308 STAINLESS STEEL

Heat Treatment	2-day Weight Change[a]	4-day Weight Change[a]	6-day Weight Change[a]
1350°C/1 h, W.Q.	−0.0703	*b*	*b*
1100°C/1 h, W.Q.	+0.0018	−0.0163	−0.0401
1050°C/1 h, W.Q.	+0.0015	−0.0097	−0.0135
1000°C/1 h, W.Q.	+0.0040	−0.0123	−0.0083
1350°C/1 h, W. Q. + 600°C/24 h, W.Q.	−0.0088	*b*	*b*
1100°C/1 h, W.Q. + 600°C/24 h, W.Q.	−0.3018	S.D.	
1050°C/1 h, W.Q. + 600°C/24 h, W.Q.	−0.0388	*b*	*b*
1000°C/1 h, W.Q. + 600°C/24 h, W.Q.	−0.0240	*b*	*b*

---

[a] gms/cm^2

[b] test not completed

S.D. — Specimen dissolved during test

W.Q. — Water Quench

boundaries. Although the value of the pitting potential in 0.16 M NaCl of the material heat treated to produce a single phase austenitic matrix did not change substantially with sensitization, the pitting morphology of the material annealed at 1100°C changed markedly with sensitization. Samples as-annealed at 1100, 1050, and 1000°C to produce an all-austenite matrix exhibited a relatively low pit density of 2-4 pits/cm^2 following anodic polarization. The pits were large and not clearly associated with any particular microstructural feature. Heat treating at 600°C for 24 hours samples which were annealed at 1050 and 1000°C for 1 hour resulted in the same pit morphology following anodic polarization as in the fully annealed austenitic material — namely, very low pit density (2-4 pits/cm^2), with the pits not clearly associated with any particular microstructural feature. As illustrated in Figure 47, the sample annealed at 1100°C and sensitized at 600°C for 24 hours exhibited a vastly different pitting morphology. Here pit nucleation is very much greater and clearly occurs at grain boundaries which are outlined by rows of tiny pits. Thus, in agreement with the results of the A262C and A262E tests, the pitting behavior in 0.16 M NaCl of austenitic Type-308 stainless steel annealed at 1000°C and 1050°C is relatively insensitive to sensitization. The pitting behavior of austenitic Type-308 stainless steel annealed at 1100°C is drastically altered by a sensitization anneal.

Figure 48 depicts the pitting potential of Type-308 stainless steel in 0.16 M HCl as a function of annealing temperature. The solid points represent the pitting potentials of materials given a subsequent 600°C for 24 hours heat treatment following the 1-hour anneal. The pitting potential of the material annealed at 1100°C is reduced by over 1 volt by a sensitization anneal. The pitting potential of the material annealed at 1050°C is also lowered by a sensitizing anneal although not nearly as drastically. The pitting potentials of the material annealed at 1350°C and 1000°C were unaffected by the sensitizing anneal.

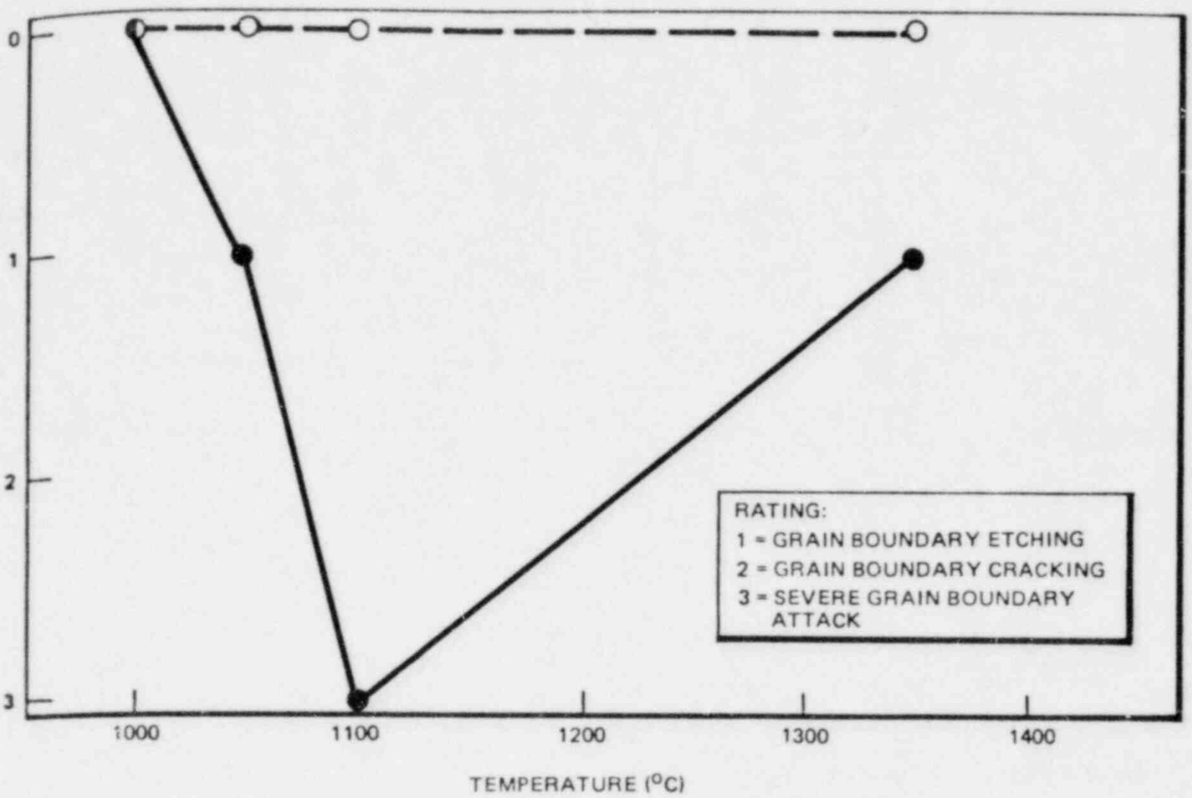

Figure 40. Effect of Heat Treatment on the Corrosion of Type-308 Stainless Steel in A262 Practice E Test

The appearance of this specimen is depicted in Figure 41. The sample given a prior anneal of 1050°C for 1 hour and 1350°C for 1 hour underwent grain boundary etching as shown in Figures 42 and 43, respectively. The attack is greater in the duplex structure with the austenite-ferrite boundaries heavily etched. The samples which had been annealed at 1000°C for 1 hour prior to 600°C for 24 hours were completely free of corrosion attack.

Table 13 lists the weight losses of Type-308 stainless steel specimens in the as-annealed and annealed-plus-sensitized conditions following multiple 48-hour periods of immersion in boiling 65% nitric acid. Intergranular attack occurred even in specimens in the fully annealed condition. In agreement with the results of A262E, the material annealed at 1100°C and then sensitized suffered the greatest attack in A262C. Additionally, the material annealed at 1000°C and 1050°C for 1 hour prior to sensitization are not severely attacked in A262C.

[illegible] Anodic Polarization in Chloride-Ion Media

Anodic polarization tests were conducted in 0.16 M HCl and 0.16 M NaCl to determine the anodic polarization characteristics and the pitting potential of Type-308 stainless steel in chloride-ion media as a function of heat treatment. Tests were conducted in deaerated solutions at room temperature and the potential was swept at a rate of 1 mV/sec starting at the corrosion potential. Figure 44 depicts the pitting potentials measured in 0.16 M NaCl as a function of annealing temperature. The solid points represent the pitting potentials of material subsequently sensitized at 600°C for 24 hours. Sensitization did not greatly reduce the pitting potential in 0.16 M NaCl. The material annealed at 1350°C for 1 hour possesses a duplex microstructure and did not pit during anodic polarization in 0.16 M NaCl. Following a sensitizing treatment of 600°C for 24 hours the material annealed at 1350°C for 1 hour pitted in 0.16 M NaCl at a potential of 955 mV. The appearance of the latter specimen is depicted in Figure 45. As illustrated in the higher magnification photograph in Figure 46, pits in the sensitized duplex alloy were confined to the austenite phase and appeared to nucleate at the austenite-ferrite

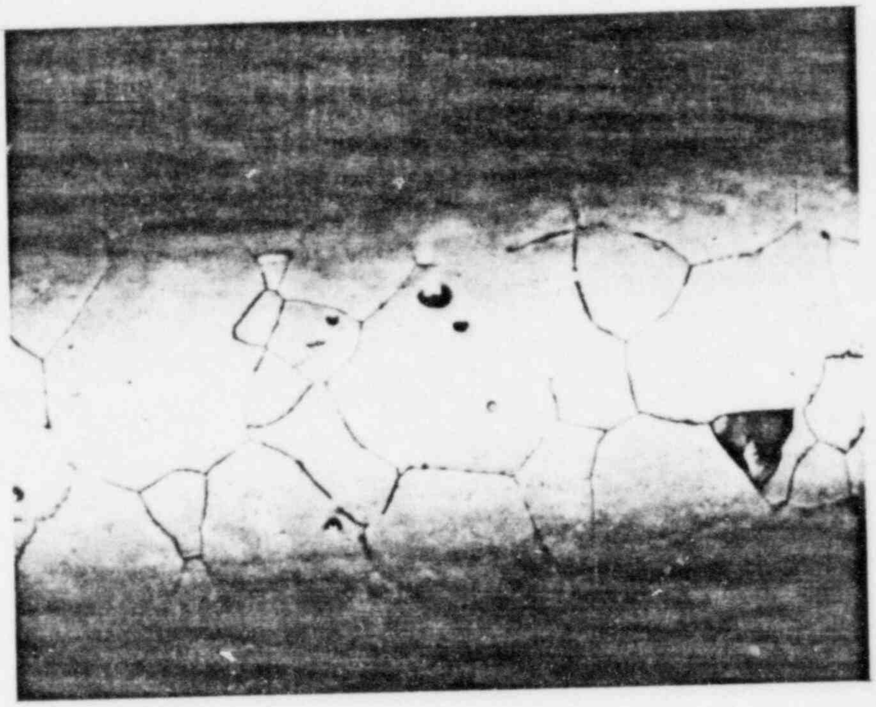

Figure 41. Photomicrograph of Type-308 Stainless Steel Heat Treated at 1100°C for 1 Hour, Water Quenched Followed by 600°C for 24 Hours, Water Quenched, then Followed by 3 Days in A262 Practice E Solution. 250X

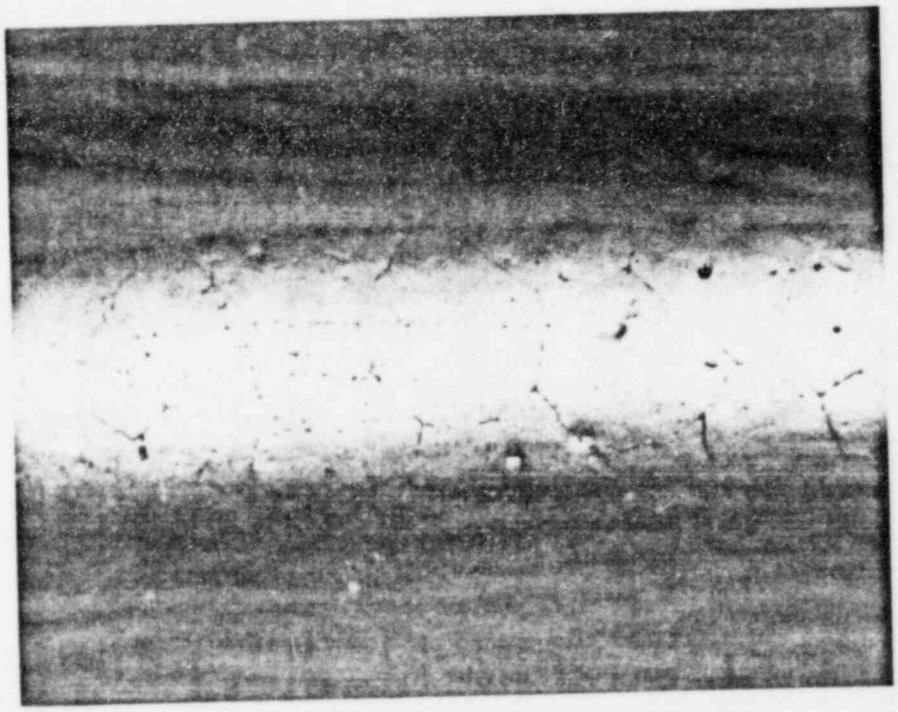

Figure 42. Photomicrograph of Type-308 Stainless Steel Heat Treated at 1050°C for 1 Hour, Water Quenched Followed by 600°C for 24 Hours, Water Quenched, then Followed by 3 Days in A262 Practice E Solution. 250X

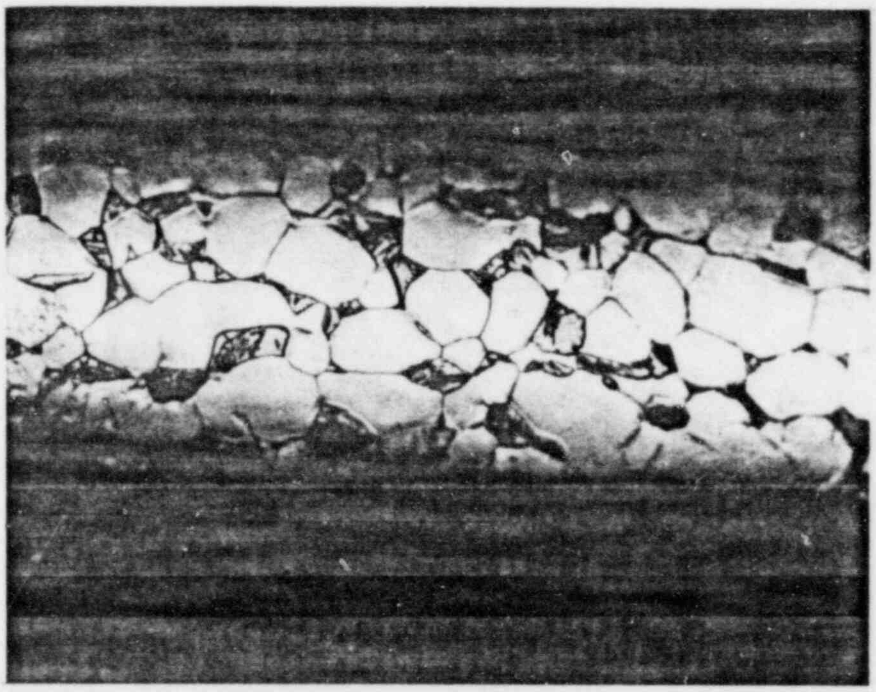

Figure 43. Photomicrograph of Type-308 Stainless Steel Heat Treated at 1350°C for 1 Hour, Water Quenched Followed by 600°C for 24 Hours, Water Quenched, then Followed by 3 Days in A262 Practice E Solution. 250X

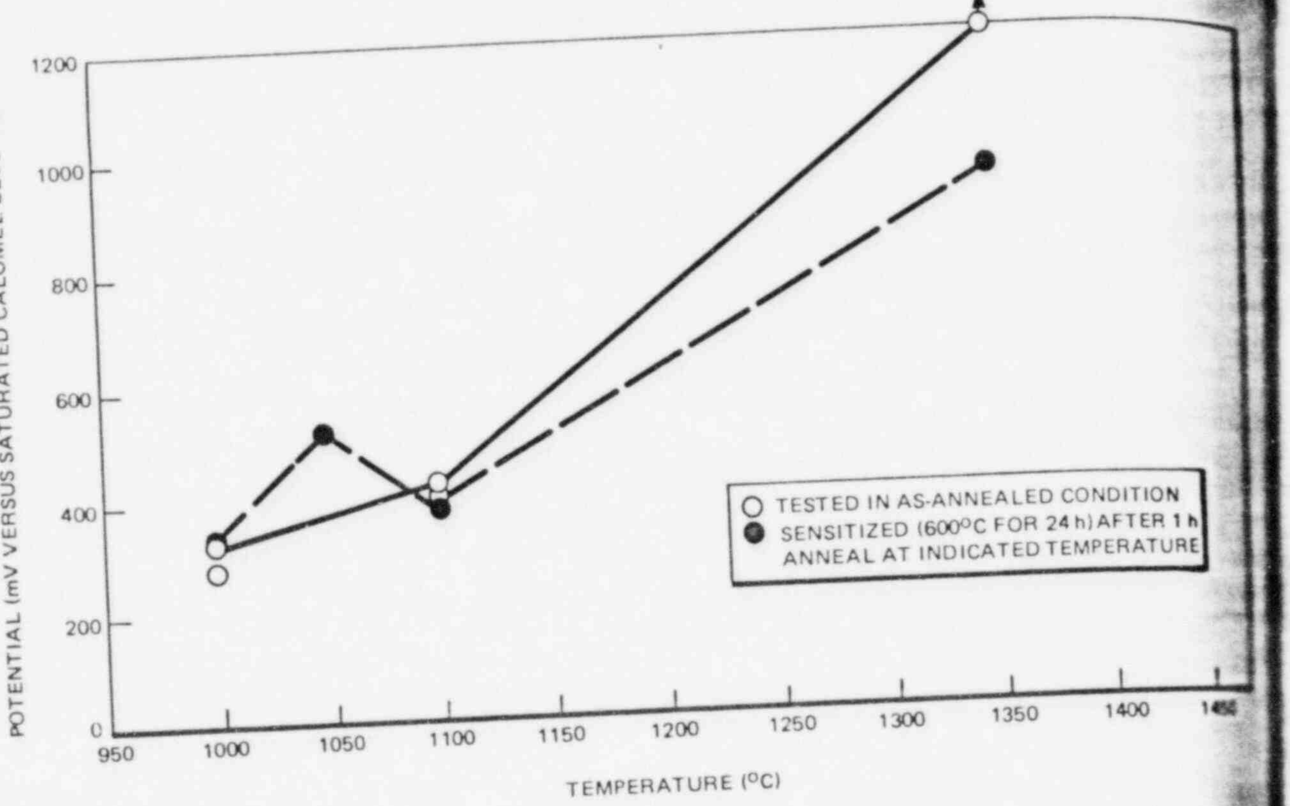

Figure 44. Pitting Potential of Type-308 Stainless Steel in 0.16 M NaCl

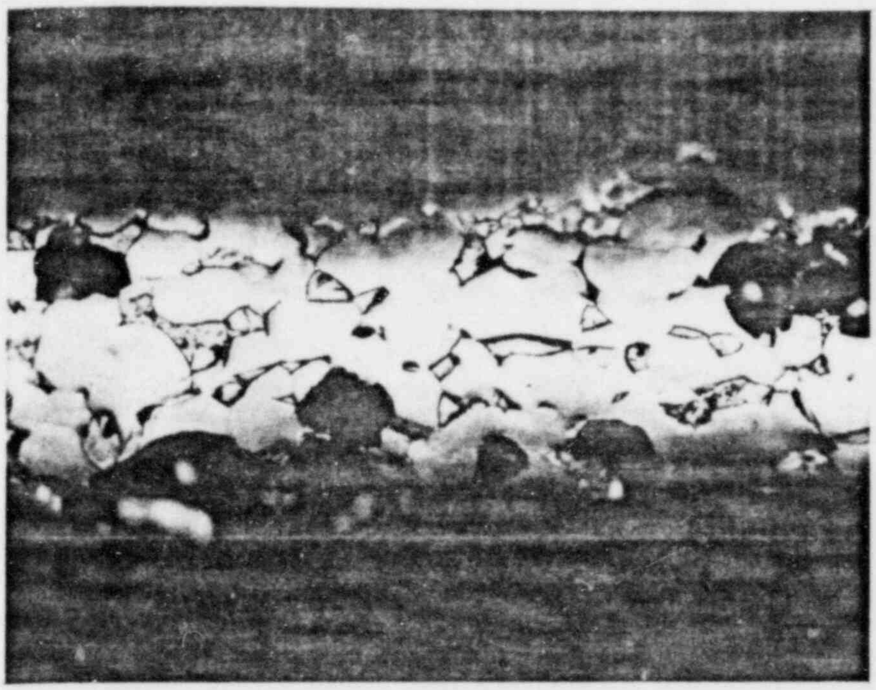

Figure 45. Photomicrograph of Type-308 Stainless Steel Heat Treated at 1350°C for 1 Hour, Water Quenched Followed by 600°C for 24 Hours, Water Quenched and Anodically Polarized in 0.16 M NaCl. 250X

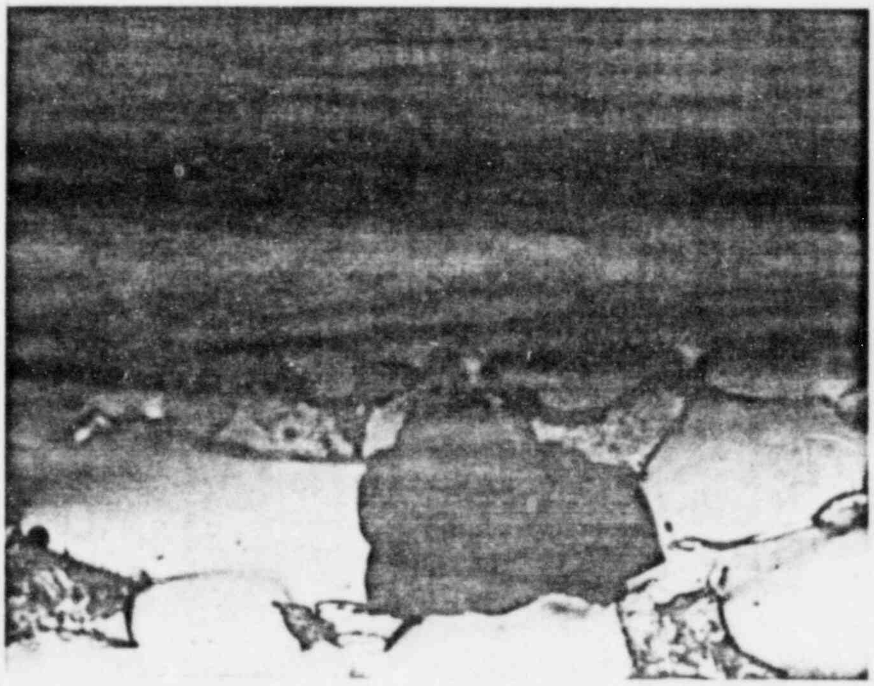

Figure 46. Photomicrograph of Type-308 Stainless Steel Heat Treated at 1350°C for 1 Hour, Water Quenched Followed by 600°C for 24 Hours, Water Quenched and Anodically Polarized in 0.16 M NaCl. 750X

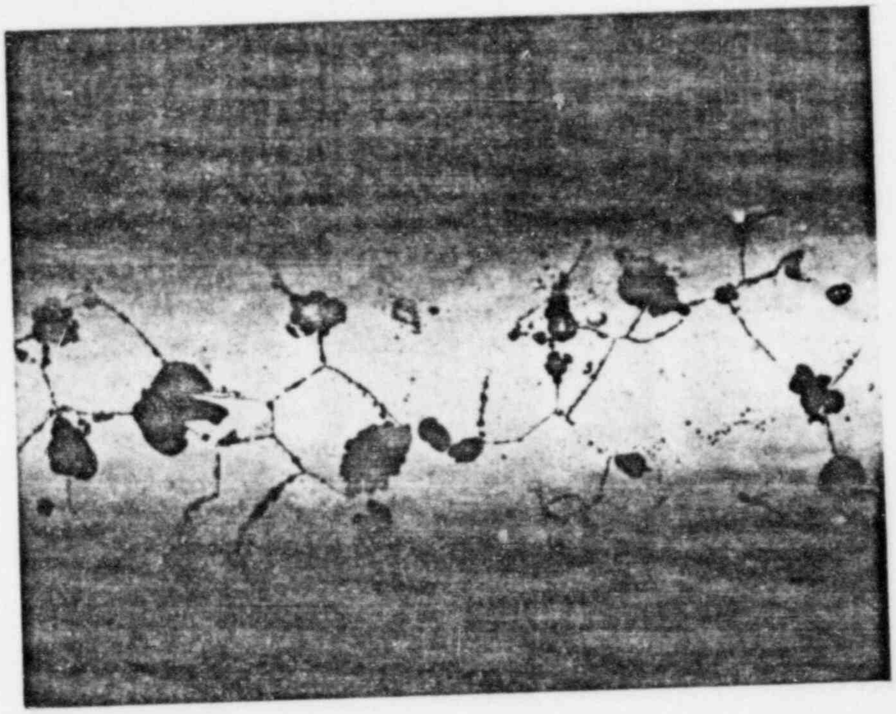

Figure 47. Photomicrograph of Type-308 Stainless Steel Heat Treated at 1100°C for 1 Hour, Water Quenched Followed by 600°C for 24 Hours, Water Quenched and Anodically Polarized in 0.16 M NaCl. 250X

As in tests conducted in 0.16 M NaCl, the as-annealed single phase austenitic Type-308 stainless steel exhibited a very low pit density of 2-4 pits/cm² following anodic polarization in 0.16 M HCl. Again the few pits formed were not clearly associated with any particular microstructural feature. The pitting morphology of samples annealed at 1350°C to produce a duplex microstructure and that of samples annealed at 1350°C plus heat treated at 600°C for 24 hours was identical to that obtained for the latter in 0.16 M NaCl and depicted in Figures 45 and 46, namely, pits nucleated at the austenite-ferrite interface and propagated into the austenite phase. The all-austenitic material annealed at 1050°C plus sensitized (600°C for 24 hours exhibited numerous pit nuclei as illustrated in Figure 49. Recall from Figure 48 that this sample had a significantly reduced pitting potential as a result of the sensitizing anneal. The all-austenitic material annealed at 1000°C plus 600°C for 24 hours exhibited a very low pit density (2-4 pits/cm²) and the pits were not clearly associated with any particular microstructural feature. As indicated in Figure 50, the material annealed at 1100°C and sensitized exhibited a peculiar type of pitting attack. Rows of tiny pits formed along certain grain boundaries, accenting the appearance of these grain boundaries. All the grain boundaries of this material were in relief following electropolishing. Figure 51 shows a high magnification view of an early stage in the formation of these pits along the grain boundaries. In this photomicrograph, a large pit is extending into a grain. The growth of these fine pits down into the material along the grain boundary resulted in numerous grain pullouts such as depicted in Figure 52.

In summary, the pitting potential tests in 0.16 M NaCl and 0.16 M HCl both result in minor pitting not associated with any particular microstructural feature of the as-annealed austenitic Type-308 stainless steel, as well as of the sensitized austenitic material which had first been annealed at 1000°C for 1 hour. Recall from above that these same heat treatments resulted in only minor weight losses during A262C testing and resulted in no localized attack of any kind during A262C testing. Very severe pitting confined to the grain boundaries occurred in the 100% austenitic material which was sensitized following a 1-hour anneal at 1100°C. This heat treatment resulted in severe attack in the A262C test — the material completely dissolved during the second 48-hour period of immersion. Similarly, this heat treatment resulted in

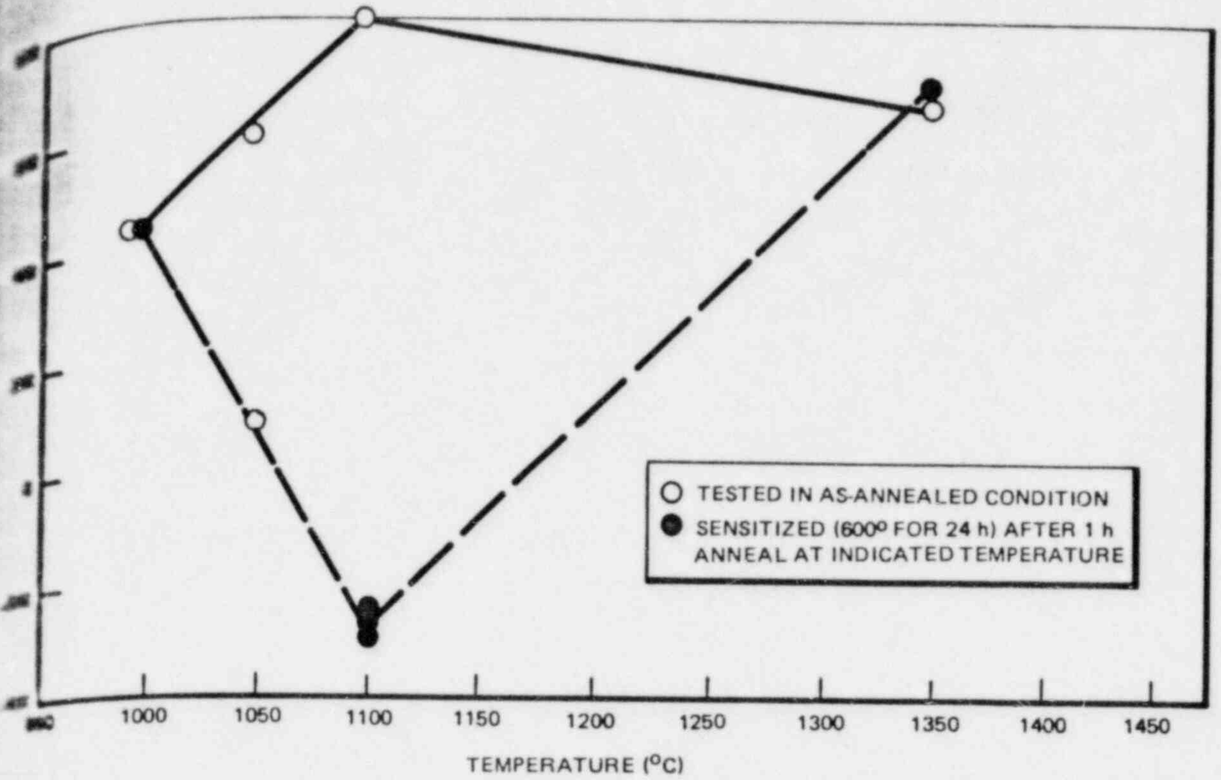

Figure 48. Pitting Potential of Type-308 Stainless Steel in 0.16 M HCl.

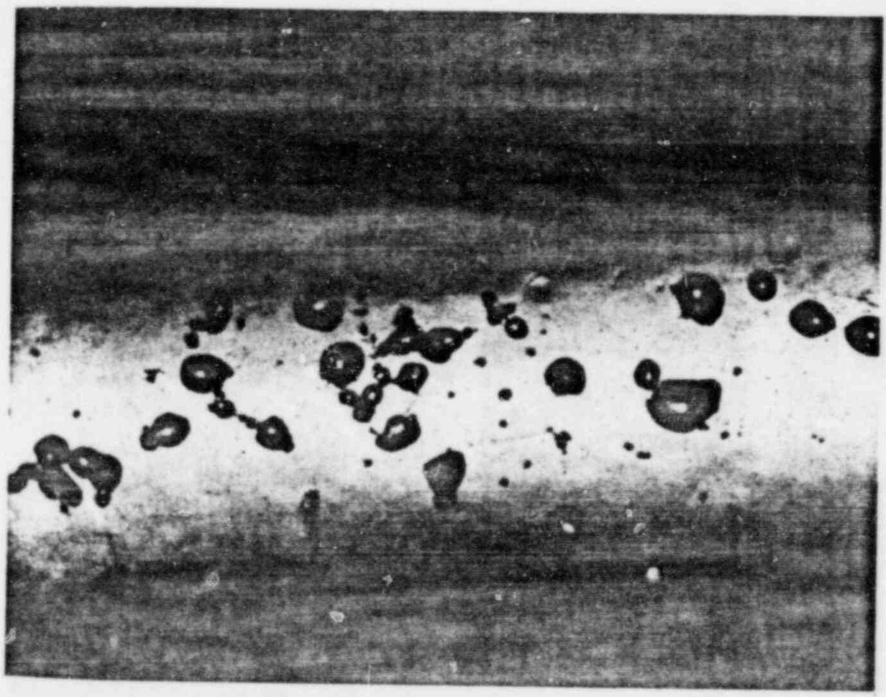

Figure 49. Photomicrograph of Type-308 Stainless Steel Heat Treated at 1050°C for 1 Hour, Water Quenched, Followed by 600°C for 24 Hours, Water Quenched and Anodically Polarized in 0.16 M HCl. 250X

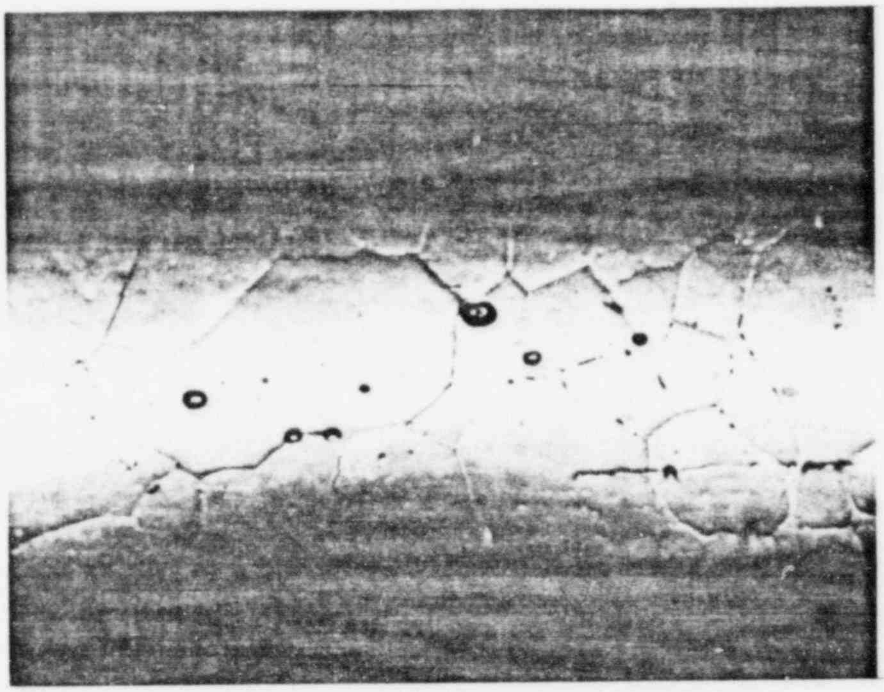

Figure 50. Photomicrograph of Type-308 Stainless Steel Heat Treated at 1100°C for 1 Hour, Water Quenched, Followed by 600°C for 24 Hours, Water Quenched and Anodically Polarized in 0.16 M HCl. 250X

Figure 51. Photomicrograph of Type-308 Stainless Steel Heat Treated at 1100°C for 1 Hour, Water Quenched Followed by 600°C for 24 Hours, Water Quenched and Anodically Polarized in 0.16 M HCl. 750X

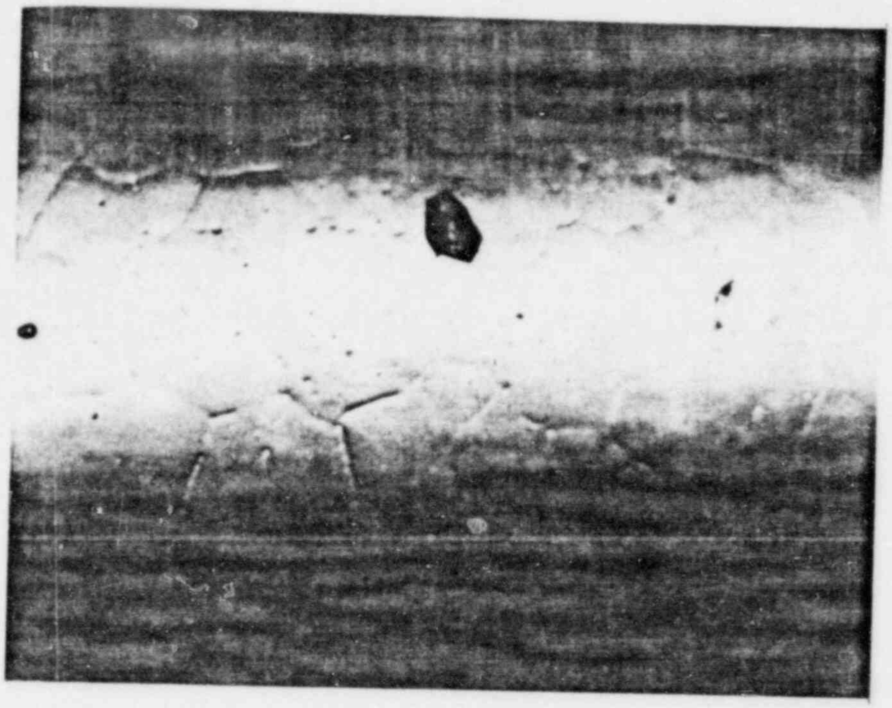

Figure 52. Photomicrograph of Type-308 Stainless Steel Heat Treated at 1100°C for 1 Hour, Water Quenched Followed by 600°C for 24 Hours, Water Quenched and Anodically Polarized in 0.16 M HCl. 250X

[illegible] granular penetration in the A262E test. Pits nucleated at the austenite-ferrite boundaries in sensitized duplex Type-308 stainless steel in both chloride-ion test solutions. This material suffered localized attack of the austenite-ferrite boundaries during the A262E test but no penetration down the boundary was detected. In the as-annealed duplex Type-308 stainless steel which was water quenched from 1350°C, pitting attack nucleated at the austenite-ferrite boundaries in 0.16 M HCl solutions but no pitting attack occurred in the 0.16 M NaCl solution. No attack of any kind occurred in the as-annealed duplex Type 308 stainless steel during A262E testing.

Summarizing, the results of the A262C tests, A262E tests, and pitting potential tests on annealed and sensitized austenitic Type-308 stainless steel all agreed. The results of such tests conducted on annealed and sensitized *duplex* Type 308 stainless steel resulted in pitting along the austenite-ferrite boundaries but little or no attack of such boundaries in the A262E test.

[illegible] Stress Corrosion Cracking Tests

Constant load, constant applied potential stress corrosion crack tests in 0.01 N H_2SO_4 at room temperature are being conducted on Type-308 stainless steel as a function of heat treatment. The all-Teflon polarization cell in which the stress corrosion crack tests are being conducted is schematically illustrated in Figure 53. The main features of the cell are the wire tensile specimen which is under a tensile load during testing, two platinum mesh screens which serve as counter electrodes, and a Luggin-Haber probe which provides a low-resistance path between the specimen and a saturated calomel reference electrode. Deaeration of the test electrolyte is accomplished by bubbling ultra-high purity nitrogen through the cell for a minimum of 4 hours prior to testing.

Three applied potentials are being used, +1200 mV (transpassive region), +700 mV (passive region), and +200 mV (active region). To date, results have been obtained for samples heat treated at 1350°C for 1 hour and 1100°C for 1 hour as

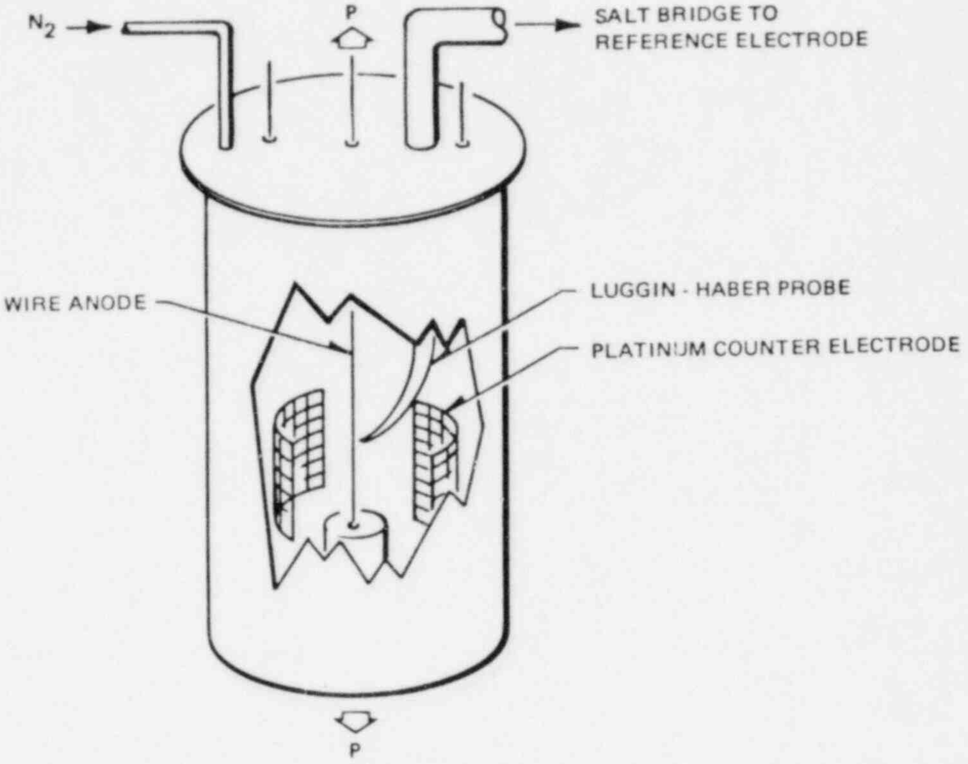

Figure 53. Schematic Drawing of Stress Corrosion Cracking Polarization Cell

well as on samples annealed at those temperatures and then heat treated at 600°C for 24 hours. Specimens consist of 0.030-in. (0.075-cm) diameter wires, 10.75 inches (27.3 cm) in length. Prior to testing, each specimen is electropolished in a solution of 60% H_3PO_4 + 40% H_2SO_4 at 60°C and 1 amp/cm² for 5 minutes. The specimen test length is then masked off with Glyptal® paint. Each specimen is dead-weight loaded to an initial tensile strain of 10%. The results are presented in Figure 54. Both annealed samples were tested at an applied potential of +1200 mV fractured in a ductile fashion. Failure was due to corrosion which reduced the cross-sectional area to the point at which the room temperature fracture strength was exceeded. This is as expected since transpassivity initiates on the annealed samples in this solution at +850 mV. Samples annealed at 1350°C and polarized in the passive region at +700 mV and +200 mV failed in a ductile manner. Microstructural observations on the surface of the failed wires indicate planar slip along a single slip system within the austenite grains. Evidence of slip in the ferrite could not be found by optical microscopy.

Figure 55 depicts the surface appearance of the specimen annealed at 1350°C for 1 hour and tested at an applied potential of +700 mV. The ferrite phase has been preferentially removed. It would appear that failure in specimens annealed at 1350°C for 1 hour was due to the preferential loss of ferrite which resulted in intensification of the applied stress. Both the samples annealed at 1100°C which produced a 100% austenitic matrix and the samples annealed at 1350°C which produced a duplex microstructure were highly susceptible to stress corrosion cracking in 0.01 N H_2SO_4, after a 600°C heat treatment for 24 hours. Both heat treatments resulted in failure in less than 2 minutes. Figure 56 is an optical micrograph of the surface of a sample annealed at 1100°C for 1 hour prior to a 600°C heat treatment for 24 hours. The test was stopped before failure occurred. In addition to the planar nature of the slip, several intergranular cracks can be seen. The fracture surfaces of samples tested to complete failure consisted of an inner core of ductile, cup-cone fracture and an outer region of intergranular fracture. Apparently intergranular cracks initiate at the surface of the specimen as shown in Figure 56 and propagate into the sample until the applied stress exceeds the fracture strength of the alloy and ductile fracture of the remaining material occurs.

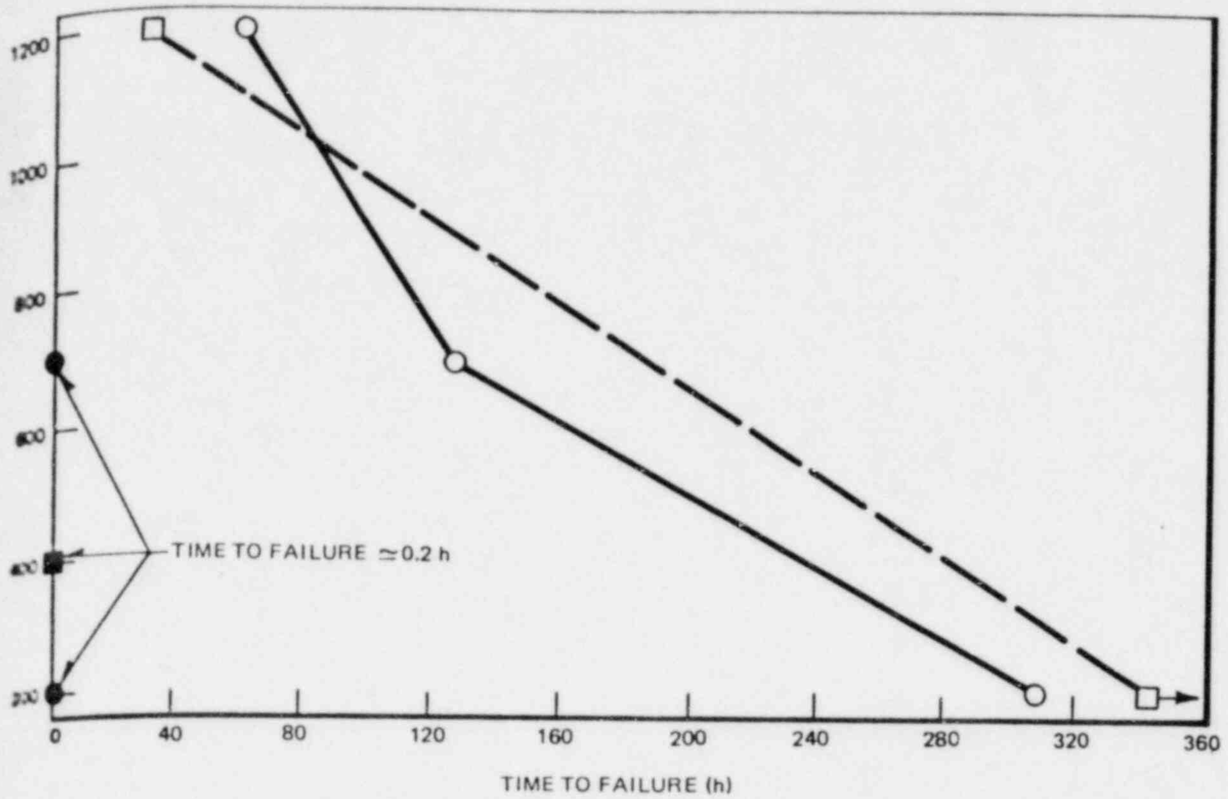

Time to Failure as a Function of Applied Potential in 0.01 N H_2SO_4 of Type-308 Stainless Steel Dead-Weight Loaded to an Initial Tensile Strain of 10%

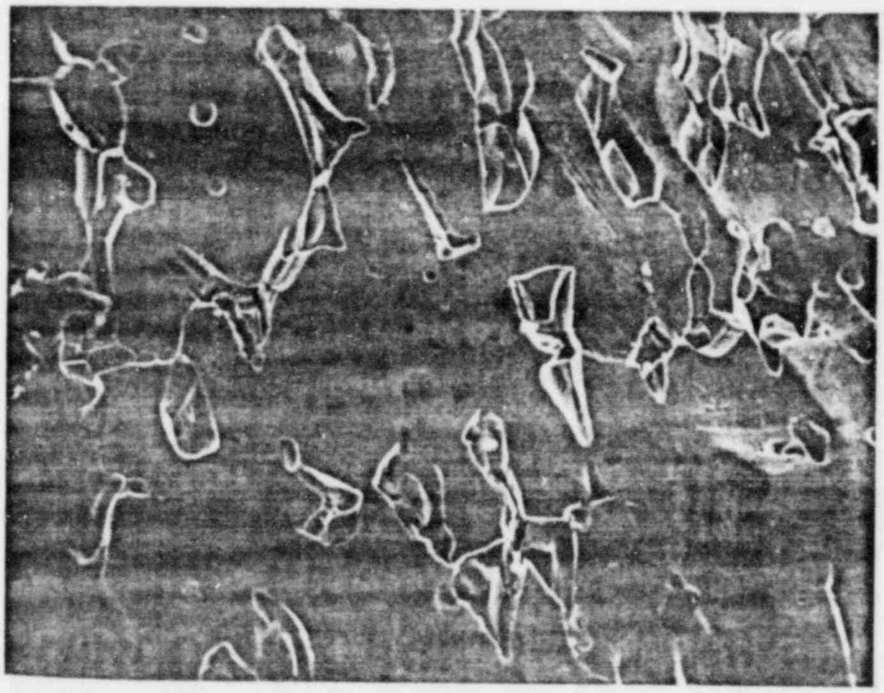

Figure 55. Scanning Electron Micrograph of Type-308 Stainless Steel Heat Treated at 1350°C for 1 Hour, Water Quenched, and Tested to Failure in 0.01 N H_2SO_4 at an Applied Potential of +700 mV. 400X

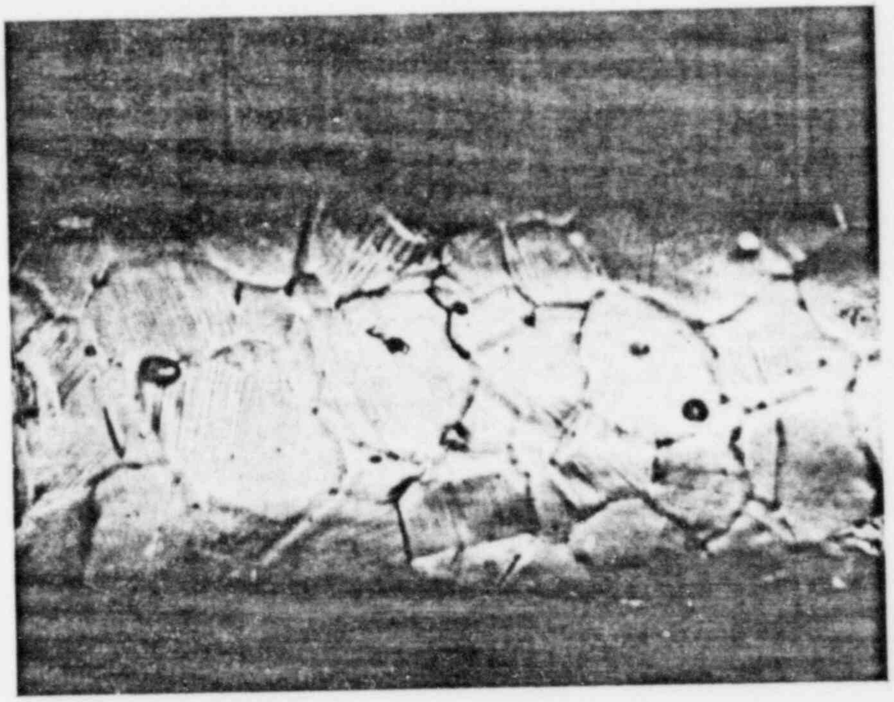

Figure 56. Photomicrograph of Type-308 Stainless Steel Heat Treated at 1100°C for 1 Hour, Water Quenched, Followed by 600°C for 24 Hours, Water Quenched and Stress Corrosion Cracked in 0.01 N H_2SO_4 at an Applied Potential of +400 mV. 250X

Figure 57 is a scanning electron micrograph of a failed sample heat treated at 1350°C for 1 hour plus 600°C for 24 hours which was potentiostatically polarized to +700mV. Again the fracture surface consists of an inner region of ductile cup-core fracture and an outer zone of intergranular fracture. Figure 58 is a higher magnification view of the outer region of intergranular fracture.

6.3.5 Discussion

All discussion of the mechanisms and causes for the localized corrosion and stress corrosion cracking in the Type-308 stainless steel reported above are presented below. The present task is concerned only with the ability of the various tests to assess the stress corrosion cracking susceptibility of duplex stainless steels in the constant extension rate test. The latter test will be performed so that a final discussion of the validity of the various screening tests will be possible.

The results of the A262E tests and the A262C tests conducted to date on annealed and annealed-plus-sensitized duplex and single-phase austenitic Type-308 stainless steel agree reasonably well. Unfortunately, although the weight losses in A262C tests of samples which have been annealed plus sensitized are much greater than those for as-annealed samples, both as-annealed and as-annealed-plus-sensitized samples undergo localized grain boundary attack. Consequently, the micro-appearance of the sample *per se* following A262C tests cannot be used to indicate the susceptibility to intergranular stress corrosion cracking. The results of the A262C tests, A262E tests, and the pitting potential tests in 0.16 M NaCl and 0.16 M HCl of as-annealed and annealed-plus-sensitized *austenitic* Type-308 stainless steel showed excellent agreement. The as-annealed austenitic Type-308 stainless steel exhibited no attack at all during the 3-day immersion in A262E and minimum weight loss in A262C tests. In both the NaCl and HCl solutions the as-annealed austenitic Type-308 stainless steel exhibited a low pit density of 2-4 pits/cm². The pitting potentials of these were high and pits probably nucleated at inclusions such as sulfides. Following a 600°C anneal for 24 hours the materials austenitized by a prior anneal at 1000°C

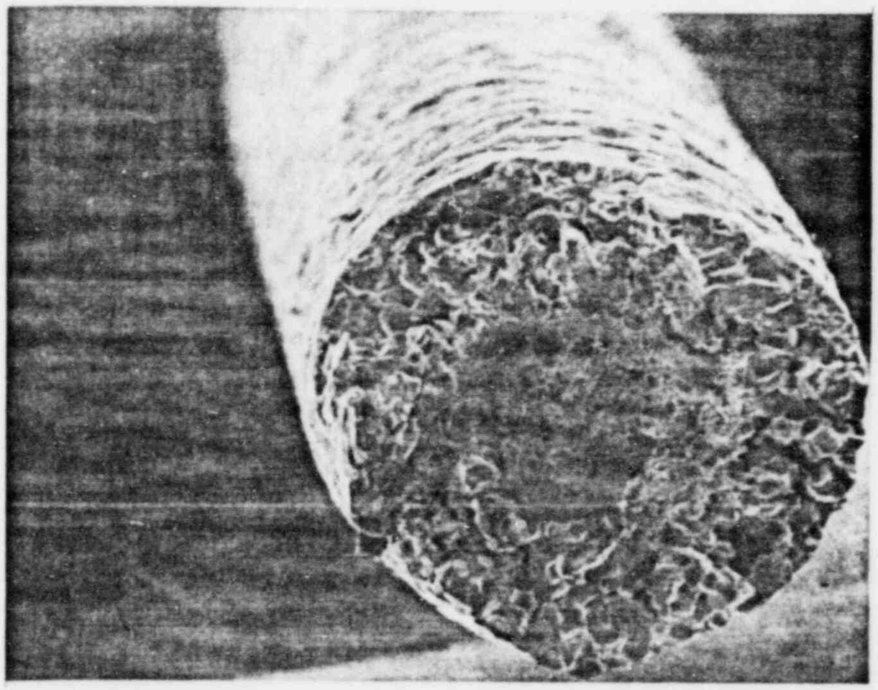

Figure 57. *Scanning Electron Micrograph of Fracture Surface of Type-308 Stainless Steel Heat Treated at 1350°C for 1 Hour, Water Quenched, Followed by 600°C for 24 Hours, Water Quenched and Tested to Failure in 0.01 N H_2SO_4 at an Applied Potential of +700 mV. 100X*

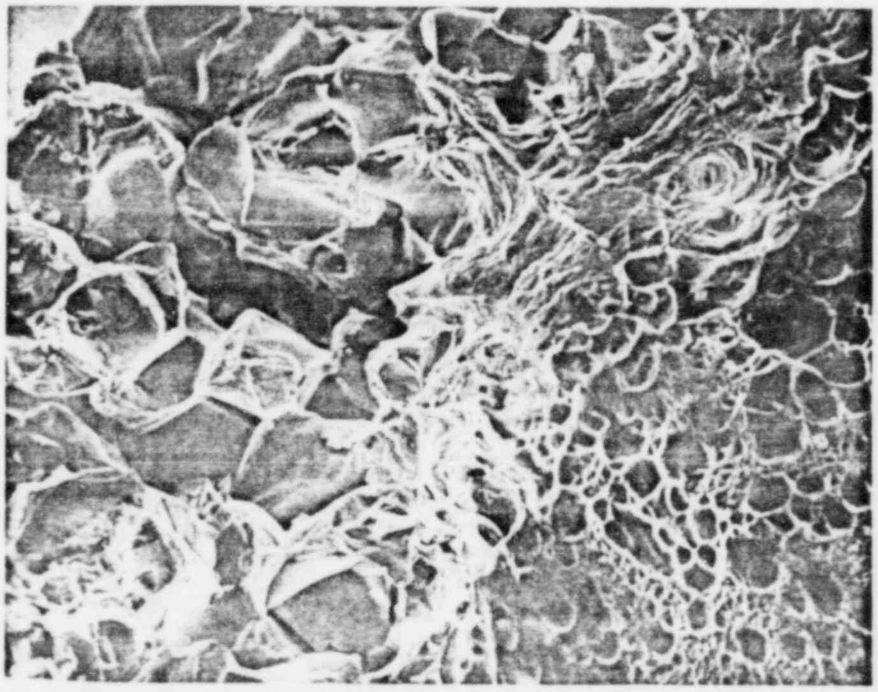

Figure 58. *Scanning Electron Micrograph of Fracture Surface of Type-308 Stainless Steel Heat Treated at 1350°C for 1 Hour, Water Quenched, Followed by 600°C for 24 Hours, Water Quenched and Tested to Failure in 0.01 N H_2SO_4 at an Applied Potential of +700 mV. 250X*

exhibited no grain boundary attack during A262E testing and material given a prior anneal of 1050°C exhibited very slight grain boundary etching. Similarly, samples which had been first annealed at 1000°C prior to heat treating at 600°C exhibited a much lower corrosion rate in A262C tests. When anodically polarized in 0.16 M NaCl and 0.16 M HCl, the specimens annealed at 1000°C for 1 hour plus 600°C for 24 hours exhibited minor pitting attack and the pits could not be associated with any particular microstructural feature. The samples which had been annealed at 1100°C for 1 hour plus 600°C for 24 hours exhibited localized grain boundary pitting corrosion in 0.16 M NaCl and 0.16 M HCl. The pits initiated at and propagated along grain boundaries as well as into the grain interiors. In the 0.16 M HCl solution, the pitting potential of austenitic Type-308 stainless steel was drastically lowered by sensitization so that the magnitude of the pitting potential as well as the appearance of the specimen following testing could be used as an indicator of sensitization.

Poor agreement existed between the results of A262E tests and pitting potential tests for duplex Type-308 stainless steel. Although samples heat treated at 1350°C for 1 hour plus 600°C for 24 hours showed preferential etching of austenite-ferrite boundaries following 3 days of A262E immersion, such samples exhibited no cracking at any boundaries when bent to an angle of ~180 degrees. Consequently, such material would be said to have passed the conventional A262E test. However, pitting did occur during anodic polarization in 0.16 M NaCl and 0.16 M HCl and such pits initiated at austenite-ferrite boundaries. Also, the as-annealed duplex Type-308 stainless steel samples (1350°C for 1 hour and water quenched) pitted at a potential of 750 mV and the pits initiated at austenite-ferrite boundaries. However, when this material was tested in the A262E test no selective attack occurred along the austenite-ferrite boundaries; in fact, no attack of any kind was observed. Also the material did not pit during anodic polarization in 0.16 M NaCl.

Since samples of as-annealed duplex Type-308 stainless steel (heat treated at 1350°C for 1 hour) and samples of sensitized duplex Type-308 stainless steel (heat treated at 1350°C for 1 hour plus 600°C for 24 hours) suffered time-delayed failure and underwent preferential corrosion and/or cracking along austenite-ferrite boundaries during potentiostatic stress corrosion cracking testing in 0.01 N H_2SO_4, and since pits initiated preferentially along austenite-ferrite boundaries during anodic polarization in 0.16 M HCl while such samples passed the A262E test, the pitting potential test in 0.16 M HCl may be a more accurate indicator of the intergranular stress corrosion cracking susceptibility in 0.01 N H_2SO_4 of a duplex stainless steel than A262E. The pitting potential test in 0.16 M HCl and the A262E test indicate the intergranular stress corrosion cracking susceptibility of austenitic stainless steels equally well. Whether the pitting potential test indicates the stress corrosion cracking susceptibility of austenitic and duplex stainless steels in the constant extension rate test remains to be determined. It should be emphasized that the results of the constant potential stress corrosion cracking tests in 0.01 N H_2SO_4 do not necessarily indicate the stress corrosion cracking susceptibility of a material in the boiling water reactor environment. Recall that the stress corrosion cracking tests in 0.01 N H_2SO_4 are primarily being conducted to study the mechanism of stress corrosion cracking by observing the potential dependency of cracking. The relationship, if any, between the stress corrosion cracking behavior in 0.01 N H_2SO_4 and in the constant extension rate test will be determined.

Assuming that intergranular stress corrosion cracking is related to intergranular corrosion caused by chromium depletion at grain boundaries, the fact that intergranular stress corrosion cracking occurred in the sensitized austenitic and duplex stainless steels polarized to as high a potential as +700mV would indicate that the combined effect of chromium depletion and low solution pH was too severe to permit passivation of the chromium-depleted grain boundary regions and prevent stress corrosion cracking. Whether this is the case will be determined by conducting the constant potential stress corrosion cracking tests in a near-neutral pH solution such as 0.01 N Na_2SO_4.

6.3.6 Conclusions

1. The pitting test conducted in 0.16 M HCl is an accurate indicator of the sensitivity of austenitic and duplex stainless steels to stress corrosion cracking in 0.01 N H_2SO_4 caused by chromium depletion due to $Cr_{23}C_6$ precipitation along high angle boundaries. Whether the pitting test can successfully predict the stress corrosion cracking susceptibility of austenitic and duplex stainless steels in the simulated boiling water reactor environment constant extension rate test remains to be determined.

2. The results of the A262C tests, A262E tests, and pitting potential tests in 0.16 M NaCl and 0.16 M HCl of as-annealed and annealed-plus-sensitized *austenitic* Type-308 stainless steel show excellent agreement and accurately predict the stress corrosion cracking susceptibility of the material in 0.01 N H_2SO_4 at room temperature.

3. Pitting corrosion of sensitized, austenitic Type-304 stainless steel in 0.16 M NaCl and 0.16 M HCl initiates at the grain boundaries. Pits propagate down the grain boundaries leading to grain pull-outs and, to some extent, pits propagate into the grain interiors.

4. 0.16 M HCl is a more effective solution than 0.16 M NaCl for determining the degree of carbide sensitization by pitting. Not only does pitting appear to be localized at grain boundaries in the 0.16 M HCl solution as in the 0.16 M NaCl solution, thereby permitting surface examination of tested specimens as a method of rating intergranular corrosion susceptibility, but the magnitude of the pitting potential obtained in 0.16 M HCl also permits a measure of the degree of sensitization.

5. Annealed-and-quenched and annealed-plus-sensitized duplex Type-308 stainless steels passed the A262E test yet were susceptible to stress corrosion cracking in 0.01 N H_2SO_4 at room temperature. Only the pitting tests conducted in 0.16 M HCl accurately predicted the stress corrosion cracking behavior of duplex Type-308 stainless steel in 0.01 N H_2SO_4.

6. The results of the constant potential stress corrosion cracking tests in 0.01 N H_2SO_4 do not necessarily indicate the stress corrosion cracking susceptibility of a material in the constant extension rate test.

7. Stress corrosion cracking tests were conducted in 0.01 N H_2SO_4 to study the mechanism of intergranular stress corrosion cracking by observing the potential dependency of cracking and comparing it to the potential dependency of intergranular corrosion. More tests must be performed before this study is complete.

6.4 SUBTASK 2 — DETERMINE THE EFFECT OF VOLUME PERCENT FERRITE ON THE STRESS CORROSION CRACKING SUSCEPTIBILITY OF DUPLEX STAINLESS STEELS

6.4.1 Introduction

The stress corrosion cracking behavior of 16 alloys all lying along one of two tie lines at 927°C will be determined in the constant extension rate test. These alloys will permit studying the effect of volume fraction of ferrite on the stress corrosion cracking behavior of alloys all containing the same chemical composition of austenite and ferrite.

6.4.2 Materials and Processing

Sixteen alloys lying along one of two tie lines at 927°C were melted into ~25-lb cylindrical ingots measuring 2-1/2 inches x 10 inches (6.3 cm x 25.4 cm). The nominal compositions of these alloys are given in Table 14. A 3-in.-thick section of each ingot was hammer forged at ~1250°C to a rectangular shape 4 x 4 x 1 inches (10 x 10 x 2.5 cm). These were then surface ground, soaked at 1250°C, and hot rolled in four passes to 1/4-in.-thick plate and water quenched. These will next be annealed at 927°C and hot rolled to ≃0.0[illegible]-in. thickness, reannealed at 927°C and water quenched. Each alloy sheet will then be cold rolled to ≃40% RA. One-half of each sheet will then be reannealed at 927°C and water quenched.

In addition, a 3-1/2-in. (8.8-cm) long section of each alloy was jacketed in a mild steel container and extruded at [illegible] to 5/8-in. (1.5-cm) diameter rod. Each rod will then be hot swaged at 927°C to ≃1/8-in. (0.35-cm) diameter and then cold drawn to 0.030-in. (0.075-cm) diameter wire.

Four additional duplex alloys whose compositions are given in Table 15 were cast and forged to rounds at 1175°C. These were then extruded at 1175°C to 5/8-in. (1.56-cm) diameter rod. These will be hot swaged and finally cold drawn to 0.030-in. (0.075-cm) diameter wire.

Seven heats of Type-308 stainless steel welding rod with ferrite numbers ranging from 2.0 to 13 were obtained. The compositions of these heats are listed in Table 16.

Table 14
NOMINAL COMPOSITIONS (wt %) OF DUPLEX STAINLESS STEELS LYING ALONG 927°C TIE LINES

Heat No.	Mn	Si	C	Ti	Ni	Cr	Comments
FF 147	0.4	0.4	0.02	0.16	3.2	31.8	All ferrite (α)
FF 148	↓	↓	↓	↓	4.8	28.9	Duplex (α+γ)
FF 150	↓	↓	↓	↓	5.8	25.2	
FF 151	↓	↓	↓	↓	7.6	21.9	
FF 152	↓	↓	↓	↓	8.8	19.5	
FF 153	↓	↓	↓	↓	9.0	19.0	All austenite (γ)
FF 154	0.4	0.4	0.02	0.16	2.9	23.9	α
FF 155	↓	↓	↓	↓	3.5	21.9	α+γ+M
FF 156	↓	↓	↓	↓	4.2	20.2	
FF 157	↓	↓	↓	↓	4.7	18.8	
FF 158	↓	↓	↓	↓	5.4	17.2	
FF 159	↓	↓	↓	↓	5.5	16.5	Martensite (M) + austenite (γ)
FF 163	0.4	0.4	<0.005	—	6.0	25.0	Low carbon α+γ
FF 164	↓	↓	<0.005	—	4.2	20.0	Low carbon α+γ+M
FF 165	↓	↓	0.02	—	6.0	25.0	Ti free α+γ
FF 166	↓	↓	0.02	—	4.2	20.0	Ti-free α+γ+M

Table 15
NOMINAL COMPOSITIONS (wt %) OF URANUS-50 TYPE ALLOYS*

Heat No.	Mn	Si	Cu	N	C	Mo	Ni	Cr	Comments
3461	0.5	0.5	1.8	0.06	0.04	2.4	0.0	20.0	Lower volume fraction of ferrite than found in Uranus 50
3462	↓	↓	↓	↓	0.035	2.4	7.0	22.0	Higher volume fraction of ferrite than found in Uranus 50
3463	↓	↓	↓	↓	0.04	2.45	8.2	20.25	Contains ≃20 vol% ferrite
3464	↓	↓	↓	↓	0.035	2.5	6.0	23.5	Contains ≃60 vol% ferrite

---

* Ingots obtained from H. D. Solomon of Corporate Research and Development, General Electric Company, Schenectady, New York

Table 16
COMPOSITIONS (wt %) OF 7 LIBRARY HEATS OF TYPE-308 STAINLESS STEEL[a]

Heat No.	C	Mn	P	S	Si	Cr	Ni	Ferrite Number
1N10B	0.056	1.71	0.020	0.018	0.32	18.92	10.30	2.0
5410	0.05	1.65	0.027	0.015	0.33	20.97	9.52	6.2
G 6976	0.053	1.70	0.019	0.017	0.20	20.65	9.83	6.6
2E7L	0.044	1.69	0.015	0.019	0.31	20.23	9.32	7.0
45983	0.04	1.76	0.016	0.008	0.41	20.95	9.82	8.3
05518	0.02	1.63	0.010	0.018	0.72	20.72	10.18	—
2E11L	0.036	1.84	0.019	0.019	1.05	20.03	8.88	1.3

---

[a] Obtained through D. Bertossa, Nuclear Energy Division, General Electric Company, San Jose, California

6.5 SUBTASK 3 — DETERMINE THE EFFECT OF THE COMPOSITION OF THE AUSTENITE AND FERRITE PHASES ON THE STRESS CORROSION CRACKING RESISTANCE OF DUPLEX STAINLESS STEEL

The alloys mentioned in Subtask 2 and listed in Tables 14 and 15 will be used for this study also.

6.6 SUBTASK 4 — DETERMINE THE EFFECT OF FERRITE MORPHOLOGY ON THE STRESS CORROSION CRACKING SUSCEPTIBILITY OF DUPLEX STAINLESS STEELS

In addition to the alloys mentioned in Subtasks 2 and 3, a centrifugal casting of CF3 whose composition is listed in Table 17 has been obtained and will be used in this study.

6.7 SUBTASK 5 — DETERMINE THE EFFECT OF SECOND PHASE PARTICLES ON THE STRESS CORROSION CRACKING SUSCEPTIBILITY OF DUPLEX STAINLESS STEELS

6.7.1 Materials and Processing

The materials used in this task are identical to those used in Subtask 1. The reader is referred to subsection 6.3.2 for a description of the fabrication schedule of these materials. In addition, 3/32-in. (0.24-cm) diameter rod of Type-308 stainless steel from Heat S0099 (see Table 12) was cold drawn to 0.030-in. (0.075-cm) diameter rod using intermediate anneals at [illegible]°C for 1 hour followed by a water quench. At the final diameter of 0.030 inch (0.075 cm) the alloy contained 38.9% RA cold work. It was then sectioned into 1-1/2-in. (3.8-cm) lengths and heat treated at various temperatures and times as described below.

The first 5 of the 24 stainless steel alloys whose compositions are listed in Table 17 have been melted into 25-lb cylindrical ingots measuring 2-1/2 inches x 10 inches (6.3 cm x 25.4 cm) long. These alloys will be used to study the relative importance of phosphorous, sulfur, and carbon in determining the susceptibility of stainless steels to stress corrosion cracking.

6.7.2 Experimental Procedure

Prior to corrosion and stress corrosion crack testing, all specimens were electropolished in a solution of 60% H_3PO_4 + [illegible]% H_2SO_4 at 60°C and 1 amp/cm² for 5 minutes. Samples for anodic polarization tests were prepared as described previously in subsection 6.3.3. Accelerated intergranular corrosion tests were performed according to ASTM specifications [illegible] and A262E.

Table 17

NOMINAL COMPOSITIONS (wt %) OF STAINLESS STEELS DOPED WITH SULFUR, PHOSPHOROUS, AND CARBON

Heat No.	S	P	C	Ni	Cr	Comments
FF 186					5	*
FF 189				10	5	*
FF 187					10	*
FF 195				10	10	*
FF 188					13	*
	0.03				13	
		0.08			13	
			0.08		13	
	0.03	0.08	0.08		13	
				3	13	*
	0.03			3	13	
		0.08		3	13	
			0.08	3	13	
	0.03	0.08	0.08	3	13	
	0.03			10	13	*
		0.08		10	13	
			0.08	10	13	
	0.03	0.08	0.08	10	13	
				6	25	*
	0.03			6	25	
		0.08		6	25	
			0.08	6	25	

---

* Sulfur, phosphorous, and carbon contents will be as low as possible.

6.7.3 Results

The results of A262C, A262E, and pitting corrosion tests conducted on annealed and sensitized austenitic and duplex Type-308 stainless steel have already been presented above in Subtask 1. These results are summarized in Table 13 and Figures 41, 45, and 49. The relevance of these results in terms of predicting the stress corrosion cracking behavior of duplex stainless steel has already been discussed in Subtask 1. An additional reason for conducting the pitting potential test was to determine if microstructural changes which occurred during heat treatment of duplex stainless steels could be followed and their presence indicated with measurements of the pitting potential. In subsection 6.7.4, these results are discussed in terms of the mechanisms responsible for the localized corrosion and stress corrosion cracking.

The A262E and A262C tests are being conducted on heat treated specimens of 0.030-in.-diameter duplex Type-308 stainless steel wire which, as mentioned in subsection 6.7.1, was produced by several repetitions of 40% cold reductions in area by wire drawing plus 1 hour anneals at 1350°C and water quenching. Heat treatments consisted of 600, 700, 800, and 900°C anneals for times of 1, 10, and 100 hours on specimens in the as-drawn condition (containing 38.9% reduction in area cold work). Additionally, samples were also heat treated at 475°C for times of 10, 100, and 1000 hours. The results of A262C and A262E tests are not yet completed and will be disclosed in the next reporting period.

Anodic polarization tests in 0.1 M HCl have been completed on these samples and the measured pitting potentials are reported in Figure 59. No pitting corrosion occurred as a result of annealing at 900°C for times of up to 100 hours. Microstructurally, the volume fraction ferrite decreased from ≃20% after 1 hour at 900°C to ≃5% after 100 hours at 900°C. Samples annealed up to 100 hours at 800°C were immune to pitting. After annealing for 100 hours at 800°C the pitting potential was reduced to 380 mV. Annealing for even 1 hour at 700°C resulted in pitting corrosion. Maximum pitting attack occurred after a 10-hour anneal. Annealing for 100 hours at 700°C increased the pitting resistance. Figure 60 depicts the morphology of pitting in samples heat treated at 700°C. The pits nucleated at austenite-ferrite boundaries and propagated into the austenite phase. While no pitting occurred during anodic polarization in 0.1 M HCl of specimens annealed at 600°C for 1 hour, longer anneals resulted in pitting attack. As in the case of samples heat treated at 700°C, maximum susceptibility occurred after 10 hours. Pits nucleated at the austenite-ferrite boundaries and propagated into the austenite phase. The greatest susceptibility to pitting corrosion occurred after 100- and 1000-hour anneals at 475°C. The appearance of these specimens following anodic polarization is shown in Figures 61 and 62. A marked difference in pitting morphology can be seen between samples annealed at 475°C and those annealed at 600 and 700°C. In the latter the pits nucleated at the austenite-ferrite interface and propagated into the austenite. In the former case, pits nucleated and grew within the ferrite phase.

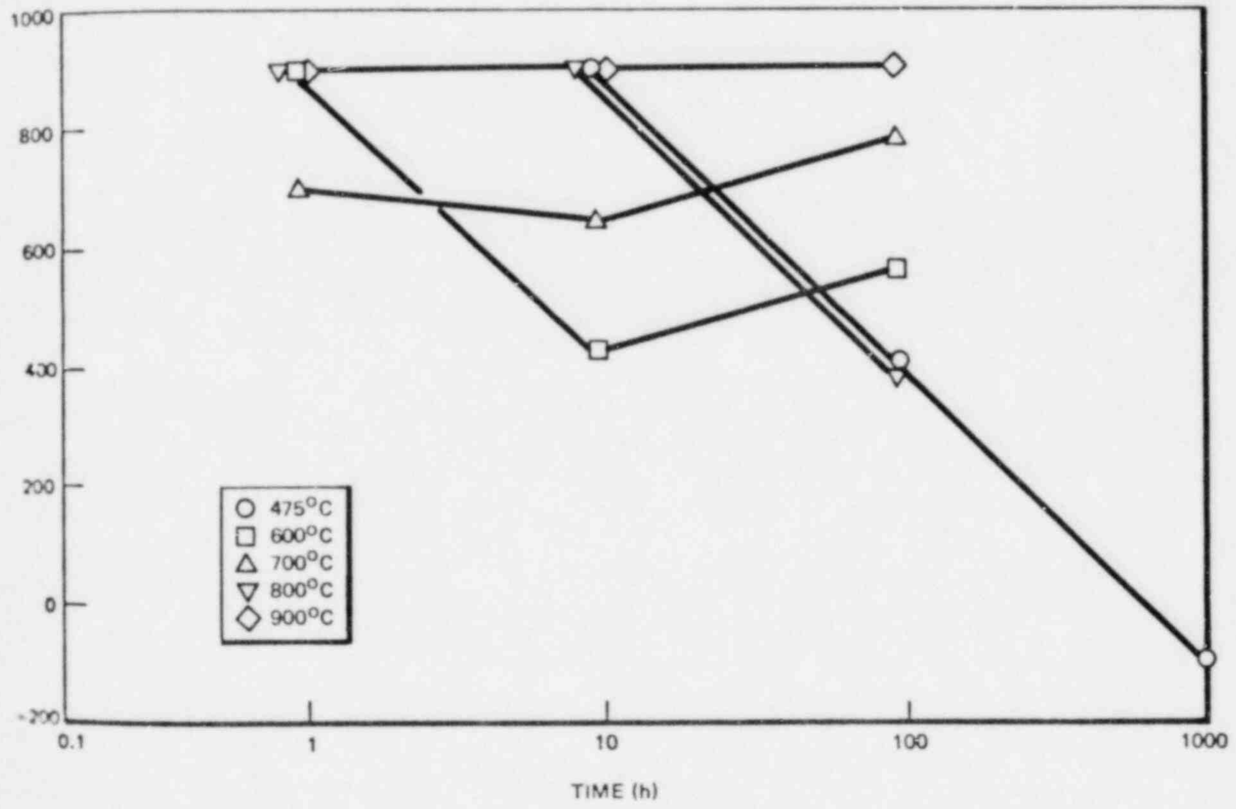

Figure 59. *Effect of Heat Treatment on the Pitting Potential in 0.01 M HCl of Type-308 Stainless Steel*

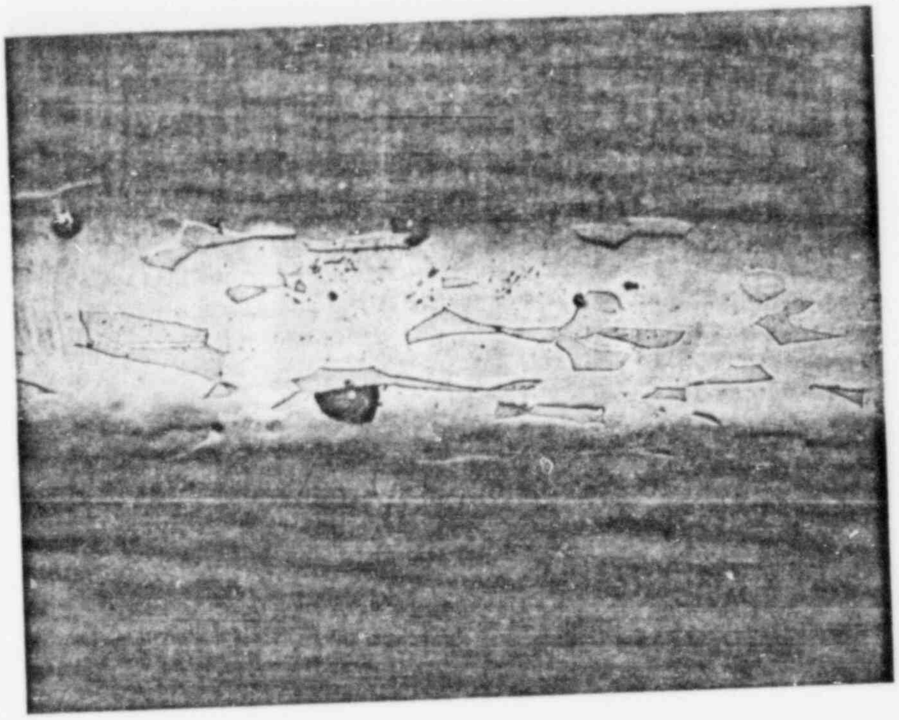

Figure 60. Photomicrograph of Type-308 Stainless Steel Heat Treated at 1350°C for 1 Hour, Water Quenched, Cold Drawn to 38.9% Reduction of Area, Heat Treated at 700°C for 1 Hour, Water Quenched and Anodically Polarized in 0.1 M HCl. 250X

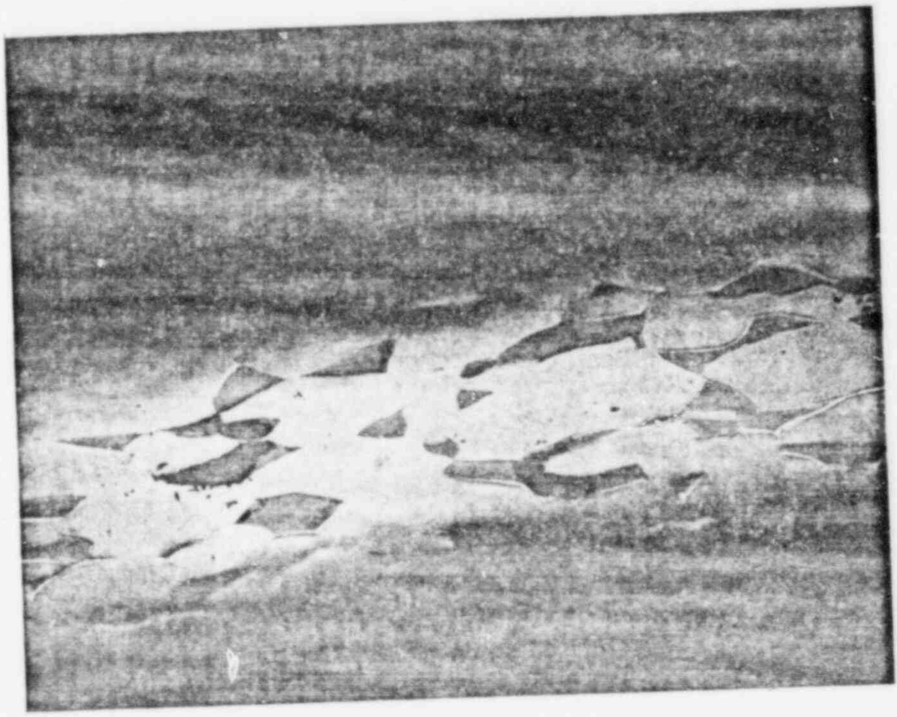

Figure 61. Photomicrograph of Type-308 Stainless Steel Heat Treated at 1350°C for 1 Hour, Water Quenched, Cold Drawn to 38.9% Reduction of Area, Heat Treated at 475°C for 100 Hours, Water Quenched and Anodically Polarized in 0.1 M HCl. 250X

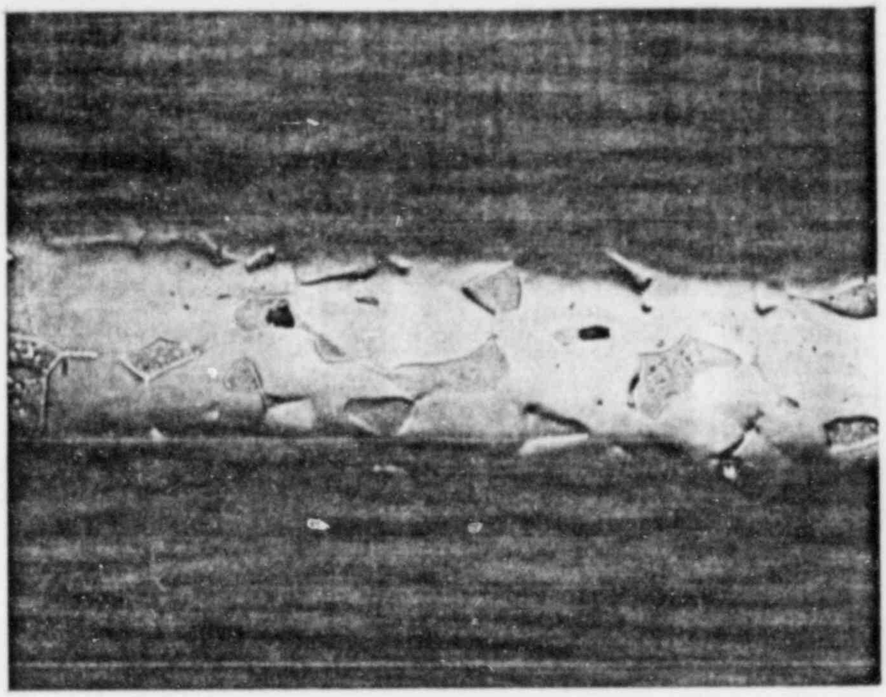

Figure 62. Photomicrograph of Type-308 Stainless Steel Heat Treated at 1350°C for 1 Hour, Water Quenched, Cold Drawn to 38.9% Reduction of Area, Heat Treated at 475°C for 1000 Hours, Water Quenched and Anodically Polarized in 0.1 M HCl. 250X

Discussion

The severe intergranular corrosion in A262C and A262E tests of austenitic Type-308 stainless steel annealed at for 1 hour plus 600°C for 24 hours as reported in Figure 40 and Table 13 can undoubtedly be attributed to attack of depleted regions adjacent to $Cr_{23}C_6$ precipitates at grain boundaries. The susceptibility of this material to pitting at grain boundaries is due to the less-protective nature of the passive film formed over those areas depleted in Approximately 12% chromium is required in ferrous alloys to ensure ease of passivation and stability of the state. The rapid intergranular stress corrosion cracking in 0.01 N H_2SO_4 of samples annealed at 1100°C for 1 hour for 24 hours reported in Figure 54 and the resistance to stress corrosion cracking of material as annealed at would indicate the chromium-depleted zones adjacent to grain boundaries are responsible for intergranular stress cracking.

inary transmission electron microscopy has indicated a possible explanation for the remarkable immunity Subtask 1 (see Figures 40, 44, and 48 and Table 13) of austenitic Type-308 stainless steel annealed at 1000°C for ntergranular attack following a 600°C anneal for 24 hours. Foils from samples annealed at 1100°C for 1 hour were be completely solutionized. Samples heat treated at 600°C for 24 hours following a 1100°C anneal for 1 hour extensive grain boundary precipitation. The precipitates were too small to obtain a diffraction pattern but based on ity of the material to intergranular corrosion are presumed to be $Cr_{23}C_6$. Samples solutionized at 1100°C for 1 hen annealed at 1000°C for 1 hour exhibited large intragranular precipitates preliminarily identified as $(Cr, Fe)_7C_3$. onized at 1100°C for 1 hour, annealed at 1000°C for 1 hour, and heat treated at 600°C for 24 hours contained boundary precipitates but did exhibit intragranular precipitates also preliminarily identified as $(Cr, Fe)_7C_3$. The the material annealed at 1000°C to sensitization might be due to the intragranular precipitation of $(Cr, Fe)_7C_3$ y lowers the carbon content of the matrix to prevent the formation of $Cr_{23}C_6$ during annealing at 600°C.

Pitting corrosion in as-annealed duplex Type-308 stainless steel (1350°C for 1 hour, water quenched) nucleates at austenite-ferrite interfaces and might possibly be explained by chromium depletion adjacent to $Cr_{23}C_6$ precipitates formed in the ferrite at the austenite-ferrite interface on rapid cooling from 1350°C. The presence of a chromium-depleted interface would also explain the preferential loss of ferrite in as-annealed duplex Type-308 stainless steel during potentiostatic stress corrosion crack testing in 0.01 $\underline{N}$ H_2SO_4 as illustrated in Figure 55. Similarly, pitting in Chlorideion media of sensitized duplex Type-308 stainless steel (heat treated at 1350°C for 1 hour plus 600°C for 24 hours) initiates at the austenite-ferrite interface; stress corrosion cracking in 0.01 $\underline{N}$ H_2SO_4 of sensitized duplex stainless steel is characterized by cracking of the austenite-ferrite interface. Both phenomena probably result from the preferential precipitation of $Cr_{23}C_6$ along the austenite-ferrite phase boundary such as reported in the duplex stainless steel IN744. It would appear, therefore, that sensitization results in the duplex microstructure in two distinct manners. First, on rapid cooling from 1350°C, $Cr_{23}C_6$ forms in the ferrite at the austenite-ferrite interface because of the extremely low solubility of carbon in ferrite below ~800°C and because of the very rapid diffusivity of carbon and chromium in the ferrite phase. Upon heat treating the as-annealed and quenched duplex structure at 600°C for 24 hours, the high diffusivity of chromium in the ferrite quickly deletes the chromium-depleted zones around the $Cr_{23}C_6$ particles created on water quenching from 1350°C. However, during this heat treatment $Cr_{23}C_6$ now precipitates in the austenite phase in which the carbon has a higher solubility and the chromium has a lower diffusivity. Chromium-depleted zones are now created around $Cr_{23}C_6$ precipitates formed in the austenite phase at the austenite-ferrite boundary.

Although the hypothesized chromium-depleted zones formed in the as-annealed duplex Type-308 stainless steel and in the annealed-plus-sensitized duplex Type-308 stainless steel are sufficient to cause pitting in HCl solutions and stress corrosion cracking in 0.01 N H_2SO_4 it is interesting that both materials pass the A262E test. This might be explained by the formation of noncontinuous chromium-depleted zones along the boundaries which are sufficient to cause localized pitting but insufficient in extent to cause extensive intergranular penetration by intergranular corrosion alone. With the application of a stress, intergranular penetration is achieved by intergranular corrosion and/or cracking along chromium-depleted paths adjacent to boundaries and the stress can rupture the chromium-rich sections of the boundaries separating the chromium-depleted portions.

The results presented in Figure 59 indicate cold worked duplex Type-308 stainless steel annealed up to 100 hours at 900°C to be immune to pitting in 0.1 M HCl. The only microstructural change, in addition to recrystallization, observed during annealing at 900°C was a steady decrease in volume fraction ferrite. After 100 hours at 900°C the ferrite had decreased to ~5 vol%. Likewise, the only optically observed microstructural change occurring during heat treating of cold worked duplex Type-308 stainless steel, other than recrystallization, was a decrease in the volume fraction of ferrite. However, pitting did occur after a 100-hour anneal at 800°C. The pitting could be the result of chromium depletion caused by $Cr_{23}C_6$ precipitation in the austenite. This, however, is yet to be determined. Pitting initiated at the austenite-ferrite boundaries of cold worked duplex Type-308 stainless steel following annealing at 700°C for as short a time as 1 hour and at 600°C after a 10-hour anneal. This can be attributed to the formation of chromium-depleted zones adjacent to $Cr_{23}C_6$ precipitates at the austenite-ferrite boundary. Following 100- and 1000-hour heat treatments at 475°C, pits no longer initiated at the austenite-ferrite interface of cold worked duplex Type-308 stainless steel but instead initiated within the ferrite phase. Such pits probably form at chromium-depleted zones adjacent to α' particles. The detection of these α' particles by the pitting potential test is of great interest since the formation of α' is certain to embrittle the alloy at the least and other workers have been unable to detect the presence of α' by the A262E test. This would further point to the efficacy of using the pitting potential test for assessing the applicability of duplex stainless steels for use as boiling water reactor structural material.

6.7.5 Conclusions

1. Heat treating Type-308 stainless steel at 1100°C for 1 hour and water quenching produced a solution annealed austenitic material. When subsequently heat treated at 600°C for 24 hours and water quenched, the material annealed for 1 hour at 1100°C contained grain boundary precipitates presumed to be $M_{23}C_6$. The alloy failed the A262C and A262E tests, exhibited a very low pitting potential in 0.1 M HCl, and was highly susceptible to intergranular stress corrosion cracking in 0.01 $\underline{N}$ H_2SO_4.

2. Heat treating Type-308 stainless steel at 1100°C for 1 hour followed by a 1000°C for 1 hour anneal produced an austenitic alloy containing intragranular carbide precipitates. When subsequently heat treated at 600°C for 24 hours, the material remained free of intergranular precipitates and the alloy passed A262E test and exhibited a high pitting potential in 0.1 M HCl.

3. Presumably the lack of sensitization in the austenitic Type-308 stainless steel first annealed at 1000°C is due to the intragranular carbide precipitates which lower the carbon content of the matrix and inhibit low-temperature (600°C) grain boundary carbide precipitation.

4. The pitting potential was able to follow the various changes in microstructural features produced by the heat treatments given to duplex Type-308 stainless steel.

    a. No pitting occurred in 0.1 M HCl in duplex Type-308 stainless steel annealed at 800 and 900°C for times of 1 to 100 hours. Correspondingly, no microstructural changes occurred in the alloy other than a decrease in the ferrite content.

    b. Pitting occurred at the primary austenite-ferrite phase boundaries and along the austenite-ferrite phase boundaries created by the precipitation of Widmanstätten austenite within the ferrite. Presumably this pitting is associated with chromium depletion along austenite-ferrite phase boundaries due to $M_{23}C_6$ precipitation.

    c. Pitting occurred within the ferrite phase of duplex Type-308 stainless steel annealed at 475°C for 100 and 1000 hours. This pitting is undoubtedly due to the formation of the chromium-rich (up to ~90% Cr) α' phase which results in severe chromium depletion of the ferrite phase.

SUBTASK 6 — DETERMINE THE EFFECT OF COLD WORK ON THE STRESS CORROSION CRACK SUSCEPTIBILITY OF DUPLEX STAINLESS STEEL

The 20 duplex stainless steels listed in Tables 14 and 15 will be employed in studying the effect of cold work on the [illegible] corrosion cracking susceptibility of duplex stainless steels. The thermomechanical processing of these alloys has [illegible] been described in subsection 6.4.2. Additionally, 0.030-in. (0.075-cm) wire of Type-308 stainless steel from Heat [illegible] exists in the as-cold-reduced (38.97% reduction in area) state. A portion of this wire will be recrystallized and then the [illegible] intergranular corrosion, and stress corrosion cracking behavior of each will be studied as a function of subsequent [illegible] treatment.

7. REFERENCES

1. *Investigation of Cause of Cracking in Austenitic Stainless Steel Piping*, General Electric Company, July 1, 1975 (NEDO-21000-1, NEDO-21000-2).

2. M. E. Indig and D. A. Vermilyea, *Corrosion*, **31**, 51 (1975).

APPENDIX A

MATERIAL CERTIFICATION FOR PIPING MATERIALS USED IN PIPE TESTS

SANDVIK STEEL INC.
P. O. Box 52
Clarks Summit, Pa. 18411

SANDVIK

CC-414
J-

Material Certificate

KILSBY TUBE SUPPLY

OK 2/14/75

RECEIVED
FEB 26 1975
D. C. Bertozza

Your order	Your spec.	Our order	Our invoice	Certificate
55 37916	ASTM A-312 ASME SA-312 74 EDITION	60823		95676

Material

4" SCH 80 39'3"
SANDVIK TYPE 304 SEAMLESS STAINLESS STEEL ANNEALED PIPE

Analysis

Heat	C %	Si %	Mn %	P %	S %	Cr %	Ni %	Mo %	Ti %
454659	.043 ✓	.59	1.22 ✓	.018 ✓	.010 ✓	18.4 ✓	10.0 ✓		

Check Analysis

Heat									

Mechanical tests

Heat	Yield strength psi	Tensile strength psi	Elongation 2", %	Hardness	Hydr. pressure test psi
454659	42,000 ✓	84,800 ✓	60 ✓		2390

FLATTENING TEST: OK

January 15, 1975

Bengt H. Berg
Quality Assurance M

ALLIANCE, OHIO-1

TUBULAR PRODUCTS DIVISION
BEAVER FALLS, PA.-2

MILWAUKEE, WISCONSIN-3

TEST REPORT

CUSTOMER ORDER NO. 4A05080

DATE [illegible]

GUYON ALLOYS INC
950 S FOURTH ST
HARRISON NJ 07029

NUCLEAR

Material was given a heat treatment consisting of heating to a min of 1900°F for a min of 10 minutes & water quenched

STEEL WAS MELTED IN THE USA

SMLS CROLOY 304 EF CD AW PIPE TO ASTM A 312-73 & ASME SA 312 W/CK ANAL
2 PIPES EA LOT & HT PER PARA 8 OF ASTM A 312-73 AND 7 OF ASME SA 312
NO OIL PICKLED & PASSIVATED

Reconverd thickness CC-
5-20-75

9040257-361722000350911 0000

ITEM	O.D.	WALL	LENGTH	SPECIAL MARKS	P/C	PCS.	FOOTAGE	HYDRO TEST LBS. PER SQ. INCH	TESTS MADE	
01	4500	337	RL 17-24		C	32	656 61	2247	ETCH	
									BEND	
									FLATTENING	C.S.
									FLANGE	
									EXPANSION	
									FLARE	
									CORROSION	
									MICRO	
									ULTRASONIC	
									DYE PENETRANT	

Acme Piping Eng. Co.
41452

APPROVED
A.P.E.
Q.C. DEPT.
DATE 3/14/75
SIGNED

Q. A. APPROVED
BY: DATE 3/27/75
GUYON ALLOYS, INC.

HEAT NO.	CARB.	MANG.	SUL.	PHOS.	SIL.	CHROM.	NI.	MO.	CU.	CB.	TI.
17616	.060	1.70	.012	.023	.55	18.80	10.34				
Tube CK	.066	1.71	.012	.025	.53	18.85	10.41			-	
"	.064	1.72	.012	.025	.54	18.81	10.44				
~~17772~~	~~[illegible]~~	~~[illegible]~~	~~.014~~	~~.028~~	~~[illegible]~~	~~18.8[illegible]~~	~~[illegible]~~				
~~Tube CK~~	~~.057~~	~~1.8[illegible]~~	~~.014~~	~~.028~~	~~[illegible]~~	~~18.8[illegible]~~	~~[illegible]~~				
~~"~~	~~.058~~	~~1.83~~	~~.014~~	~~.028~~	~~[illegible]~~	~~18.83~~	~~10.42~~				

HEAT NO.	ULTIMATE STRENGTH	YIELD POINT	% ELONG. IN 2"	% RED. AREA	HARDNESS
17616	83700	45800	58	CC-775	
~~17772~~	~~86100~~	~~40500~~	~~57~~	~~CC~~-776	

STRIP ☒ STD. RD. ☐ FULL SECTION ☐

Job #18645

SWORN TO AND SUBSCRIBED BEFORE ME 12/18/73

RITA C. [illegible] NOTARY PUBLIC
W. [illegible], PA.
MY COMMISSION EXPIRES
COMMISSION EXPIRES OCT. [illegible]

THIS IS TO CERTIFY THE ABOVE TUBES AND PIPE HAVE BEEN INSPECTED AND TESTED IN ACCORDANCE WITH AND HAVE MET ALL THE REQUIREMENTS OF THE SPECIFICATIONS.

THE BABCOCK & WILCOX COMPANY BY C.C. [illegible]

TUBULAR PRODUCTS DIVISION

ALLIANCE, OHIO-1 BEAVER FALLS, PA.-2 MILWAUKEE, WISCONSIN-3

TEST REPORT

CUSTOMER ORDER NO. AA05060

DATE SHIPPED 12 10 73

GUYON ALLOYS INC
950 S FOURTH ST
HARRISON NJ 07029

NUCLEAR

Material was given a heat treatment consisting of heating to a min of 1900°F for a min of 10 minutes & water quenched

STEEL WAS MELTED IN THE USA

SMLS CROLOY 304 EF CD AW PIPE TO ASTM A 312-73 & ASME SA 312 W/CK ANAL
2 PIPES EA LOT & HT PER PARA 8 OF ASTM A 312-73 AND 7 OF ASME SA 312

RECORDED INV-NTRY/CC-
3-24-75

NO OIL PICKLED & PASSIVATED

B & W ORDER NO. — CODE NO — "P" PARTIAL — "C" COMPLETE

ITEM	O.D.	WALL	LENGTH	SPECIAL MARKS		PCS.	FOOTAGE	HYDRO TEST LBS. PER SQ. INCH	TESTS MADE	
S040257-351722000350911000O									ETCH	
01	4500	337 RL	17-24		C	32	656 61	2247	BEND	
									FLATTENING	CK.
									FLANGE	
									EXPANSION	
									FLARE	
									CORROSION	
									MICRO	
									ULTRASONIC	
									DYE PENETRANT	

1/50

Acme Piping & Eng. Co.
41452

APPROVED
APCE
QC DEPT.
DATE 3/24/75
SIGNED

Q. A. APPROVED
BY: DATE 3/21/74
GUYON ALLOYS, INC

ITEM	HEAT NO.	CARBON	MANG.	SUL.	PHOS.	SIL.	CHROM.	NI.	MO.	CU.	CB.	TI.
	~~M7616~~	~~.060~~	~~1.70~~	~~.012~~	~~.023~~	~~.55~~	~~18.86~~	~~10.34~~				
	~~Tube ck~~	~~.066~~	~~1.71~~	~~.012~~	~~.025~~	~~.53~~	~~18.85~~	~~10.41~~			-	
	~~"~~	~~.064~~	~~1.72~~	~~.012~~	~~.025~~	~~.54~~	~~18.81~~	~~10.44~~				
	M7772	.058	1.67	.014	.028	.40	18.85	10.38				
	Tube ck	.057	1.85	.014	.029	.43	18.80	10.40				
	"	.058	1.83	.014	.028	.42	18.83	10.42				

ITEM	HEAT NO.	ULTIMATE STRENGTH	YIELD POINT	% ELONG IN 2"	% REDUCT. AREA	HARDNESS
	~~M7616~~	~~83900~~	~~45000~~	~~53~~	~~CC-~~	~~775~~
	M7772	86100	40500	57	CC-	776

Job #18645

STRIP ☒ STD. RD ☐ FULL SECTION ☐

SWORN TO AND SUBSCRIBED BEFORE ME 12/18/73

RITA A. ... Notary Public
W. Mayfield Borough, Beaver County, Pa.
MY COMMISSION EXPIRES OCT ... 19..
COMMISSION EXPIRES

THIS IS TO CERTIFY THE ABOVE TUBES AND PIPE HAVE BEEN INSPECTED AND TESTED IN ACCORDANCE WITH AND HAVE MET ALL THE REQUIREMENTS OF THE SPECIFICATIONS.

dea

A-4

THE BABCOCK & WILCOX COMPANY BY

700-04550 № 2,763 76 2P6424

⑦

RECEIVED JUN 6 1974

United States Steel Corporation

ELLWOOD
METALLURGICAL DEPT WORKS

STANDARD CERTIFIED TEST REPORT
TUBULAR PRODUCTS

3/

CUSTOMER KEYSTONE TUBULAR SERVICE CORP	CUSTOMER'S ORDER NUMBER 80-S-4183	INVOICE NO. 43357		DATE 5/29/74 U.S. STEEL ORDER NO. LC 60515
ADDRESS PO BOX 992	MATERIAL CF SMLS STAINLESS PRESSURE PIPE			GRADE TP 304
CITY STATE BUTLER, PA. 16001	HEAT TREATMENT		SIZES 4.500"OD X .337"AW	
SPECIFICATION OR PRODUCT DESCRIPTION ASTM A 312 AND ASME SA 312	RECORDED INVENTORY 3-20-75		ITEM 04 4/15/86	

HEAT NUMBER	CODE ITEM OR LOT	CHEMICAL ANALYSIS (%) C	MN	P	S	SI	NI	CR	MO			HYDRO TEST PRESSURE PSI MIN	MECHANICAL PROPERTIES YIELD STRENGTH POINT PSI	ULTIMATE STRENGTH PSI	ELONG. 2"	RED OF A OR HARDNESS	OTHER DATA	
2P6396		.057	1.69	.028	.023	.59	10.31	18.74				2250	47500	82185	55.0		CC-778	
2P6424		.070	1.63	.024	.013	.46	9.66	18.53				2250	48419	85446	53.0		CC-777	

A-5

Accc. Piping & Engr. Co.

Bergen alloy 4145 CP

Job 18645

FLATTENING TESTS SATISFACTORY

Q.C. ACCEPTED
5/29/74

APPROVED
AP&E
Q.C. DEPT.
DATE 3/14/75
SIGNED

R. A. SETTLE

800-01550 1 2,7 63 96 2P6424

①

JUN 6 1974

United States Steel Corporation

STANDARD CERTIFIED TEST REPORT

TUBULAR PRODUCTS

ELLWOOD

METALLURGICAL DEPT

DATE 5/29/74

CUSTOMER KEYSTONE TUBULAR SERVICE CORP	CUSTOMER'S ORDER NUMBER 80-S-4183	INVOICE NO 43357	U.S. STEEL ORDER NO. LC 60515
ADDRESS PO BOX 992	MATERIAL CF SMLS STAINLESS PRESSURE PIPE		GRADE TP 304
CITY STATE BUTLER, PA. 16001	HEAT TREATMENT	SIZES 4.500"OD X .337"AW ITEM 04 4/15/75	
SPECIFICATION OR PRODUCT DESCRIPTION ASTM A 312 AND ASME SA 312	RECORDED INVENTORY 3-20-75		

		CHEMICAL ANALYSIS (%)										MECHANICAL PROPERTIES				OTHER DATA	
HEAT NUMBER	CODE ITEM OR LOT	C	MN	P	S	SI	NI	CR	MO			HYDRO TEST PRESSURE PSI	YIELD STRENGTH POINT PSI	ULTIMATE STRENGTH PSI	ELONG % 2"	RED OF A OR HARDNESS	
2P6396		.057	1.69	.028	.023	.59	10.31	18.74				2250	47500	82185	55.0		[illegible]-777
2P6424		.074	1.63	.024	.013	.46	9.66	18.55				2250	40419	85446	53.0		CC-777

A-6

Job 18645

Gen. Piping & Eng. Co.

Dugan alloy 41455

FLATTENING TESTS SATISFACTORY

Q.C. ACCEPTED

7/24/74

APPROVED
AP&E
Q.C. DEPT.
DATE 3/14/75
SIGNED

R A SETTLE

NEDC-21463-1

MILL TEST REPORT APPLIES TO: GENERAL ELECTRIC PO# 205-J1P77

TEST REPORT

CHECKED

SWEPCO TUBE CORPORATION

Swepco

ONE CLIFTON BOULEVARD • P.O. BOX 328 • CLIFTON, NEW JERSEY 07015

REMIT TO: P. O. BOX 1459 NEWARK, N.J. 07101

PHONES · N. J. 201 778 3000
N. Y. 212 564 7115
TWX NO. 710 989 7098
TELEX NO. 133 321

RECEIVED
JUL 29 1975
R. L. NEWBILL

ACCT. NO.	CODE	INVOICE DATE	INVOICE NO
115	1	07/11/75	45852

SOLD TO
TUBESALES
2211 TUBEWAY
LOS ANGELES, CALIF. 90040

SHIPPED TO
GENERAL ELECTRIC CO.
SAN JOSE, CALIF.

1
2
3

SHIPPED VIA	COMPLETE	PARTIAL	[illegible]	[illegible]	[illegible]	MILL NO.	CUST. ORDER NUMBER
CONSOLIDATED	☒	☐	☒	☐	☐	M-5601-5	5-12250-SD

QTY. ORDERED	BACK ORDERED	DESCRIPTION	QTY. SHIPPED
2 590#	0	SWEPCO FF PIPE T 304 TO ASME SA 312 A & P 2PCS 4" SCH 80 HT F50343 ~~F50309~~ FRT ALLOWANCE 590#01.82 CWT ⟨ROLLED & WELDED PIPE⟩	39.645

Supplier certifies that he is abiding by all equal employment opportunity regulations.

V ZEROS INDICATE NO TESTS HAVE BEEN MADE FOR PRESENCE OF THESE ELEMENTS V

HEAT NUMBER	CHEMICAL ANALYSIS									Yield Point Lbs. Per Sq. Inch	Tensile Strength Lbs. Per Sq. Inch	% Elong. in 2 Inches	Brinell or Rockwell
	C.	Mn.	P.	S.	Si.	Ni.	Cr.	Mo.	Co.				
→ F50343	.041	1.28 CU.12	.021	.017	.42	8.46	18.38	.370	.28	47100	89500	56	145
→ ~~F50309~~	~~.046~~	~~1.22~~ ~~CU.09~~	~~.025~~	~~.013~~	~~.53~~	~~8.22~~	~~18.36~~	~~.230~~	~~.26~~	~~49200~~	~~91500~~	~~54~~	~~160~~

TRANSVERSE TENSION TEST SATISFACTORY. FLATTENING TESTS SATISFACTORY.
HYDROSTATIC TESTED AT 2247 PSI MINIMUM, SATISFACTORY.

NOTARY PUBLIC OF NEW JERSEY
My Commission Expires May 14, 1980

Sworn to and subscribed to before me Victor E. Battistoz

this ______ day of ______ 07/14/75

I hereby certify these tests are correct to the best of my knowledge
SWEPCO TUBE CORPORATION
Anne Kellman

17[illegible] Avenue
San J[illegible] Calif. 95125

ATTN: Purchasing Dept.
1 W/Shipment

Job No.: [illegible]
P.O. No.: 205-[illegible]07
Part No.: 4-3/[illegible] 2 [illegible]1 x 99AC
Spec.: ASTM A296 CF3 ,
Quantity: 2
Contract No.:
Shipping Date: 8/6/75

WISCONSIN CENTRIFUGAL INC.
905 E. St. Paul Ave.
Waukesha, Wisconsin 53186
414-542-5771

8/22/75

CHEMICAL ANALYSIS

Heat No.	No. Pcs.	C	MN	SI	CR	NI	S	P	MO
P520	1	.08	.88	1.00	20.73	9.62	.016	.038	
~~P521~~	~~1~~	~~.07~~	~~.80~~	~~.90~~	~~20.89~~	~~9.00~~	~~.014~~	~~.038~~	

MECHANICAL PROPERTIES

A8

Heat No.	TENSILE	YIELD	ELONG.	R.A.	TEMPERATURE	BHN/ROCKWELL	FERRITE	OTHERS:

NONE ORDERED

WE HEREBY CERTIFY THAT THE HEATS LISTED ABOVE ARE CORRECT TO THE BEST OF OUR KNOWLEDGE.

H. W. McQuillan CHIEF METALLURGIST 8/6/75

Darlene Schmitz NOTARY PUBLIC

June 20, 1976 MY COMMISSION EXPIRES

17[illegible] Avenue
Job No: 9406
P.O. N

[illegible] 95125

ATTN: Purchasing Dept.
1 W/Shipment

P.O. No.: [illegible]
Part No.: 4-3/[illegible] x 99AC
Spec.: ASTM A296 CF8
Quantity: 2
Contract No.:
Shipping Date: 8/6/75

WISCONSIN CENTRIFUGAL INC.
905 E. St. Paul Ave.
Waukesha, Wisconsin 53186
414-542-5771

8/22/75

CHEMICAL ANALYSIS

Heat No.	No. Pcs.	C	MN	SI	CR	NI	S	P	MO
~~P520~~	~~1~~	~~.08~~	~~.88~~	~~1.00~~	~~20.73~~	~~9.62~~	~~.016~~	~~.038~~	
P521	1	.07	.80	.90	20.89	9.00	.014	.038	

A9

MECHANICAL PROPERTIES

Heat No.	TENSILE	YIELD	ELONG.	R.A.	TEMPERATURE	BHN/ROCKWELL	FERRITE	OTHERS:

NONE ORDERED

NEDC-214634

WE HEREBY CERTIFY THAT THE HEATS LISTED ABOVE ARE CORRECT TO THE BEST OF OUR KNOWLEDGE.

CHIEF METALLURGIST 8/6/75

Darlene Schmitz
NOTARY PUBLIC

June 20, 1976
MY COMMISSION EXPIRES

RECEIVED
AUG 11 1975
R. L. NEWBILL

General Electric Co
175 Curtner Ave.
San Jose, Calif. 95125

Date July 11, 1975
No. 429-75

METALLURGICAL LABORATORY REPORT

MECHANICAL PROPERTIES

HEAT NO	YIELD POINT	YIELD STR 0.2 PER CENT OFFSET PSI	ULTIMATE TENSILE STR PSI	ELONG. IN 2 INCHES PER CENT	REDUCTION OF AREA PER CENT	HARDNESS		IMPACT FT LBS
						BRINELL	ROCKWELL	CHARPY

CHEMICAL ANALYSIS

HEAT NO	CARBON	MANGANESE	SILICON	CHROMIUM	NICKEL	MOLYBDENUM	COPPER	SULPHUR	PHOSPHORUS	OTHER ELEMENTS
CF8										
98695	.07	.64	1.31	20.05	9.03			.010	.026	

CORROSION

ACIDIFIED COPPER SULFATE TEST FOR INTERGRANULAR CORROSION (STRAUSS)
NO SPECIMENS TESTED ______ DEGREE OF BEND ______ RESULTS – SATISFACTORY NO CRACKING ______
– UNSATISFACTORY CRACKING ______

BOILING NITRIC ACID TEST (HUEY) – CORROSION LOSS I.P.M. ______ I.P.Y. ______

MAGNETIC PERMEABILITY

PERMEABILITY OF FEEBLY MAGNETIC MATERIALS – USING PERMEAMETER ______ MU.

Remarks: ______

Specification No.: ACI Grade CF8
District Order No.: ______
Customer Order No.: 205-J3R65
Sales Order No.: D-6645379

Items Covered: Spuncast
1 pc 7 15/16 X 2 7/16 X 72"

We certify that the foregoing is a true and correct report of the values obtained and that they comply with the requirements of the specification, except as noted below:

☒ No Exceptions ☐ Exceptions ______

Sworn to and Subscribed Before Me
This ______ day of ______ 19___
______
NOTARY PUBLIC
My Commission Expires ______ 19___

Result As Above Certified
ESCO CORPORATION
Signed Harold Rose
METALLURGICAL DEPT

FORM NO. 12 03151 71

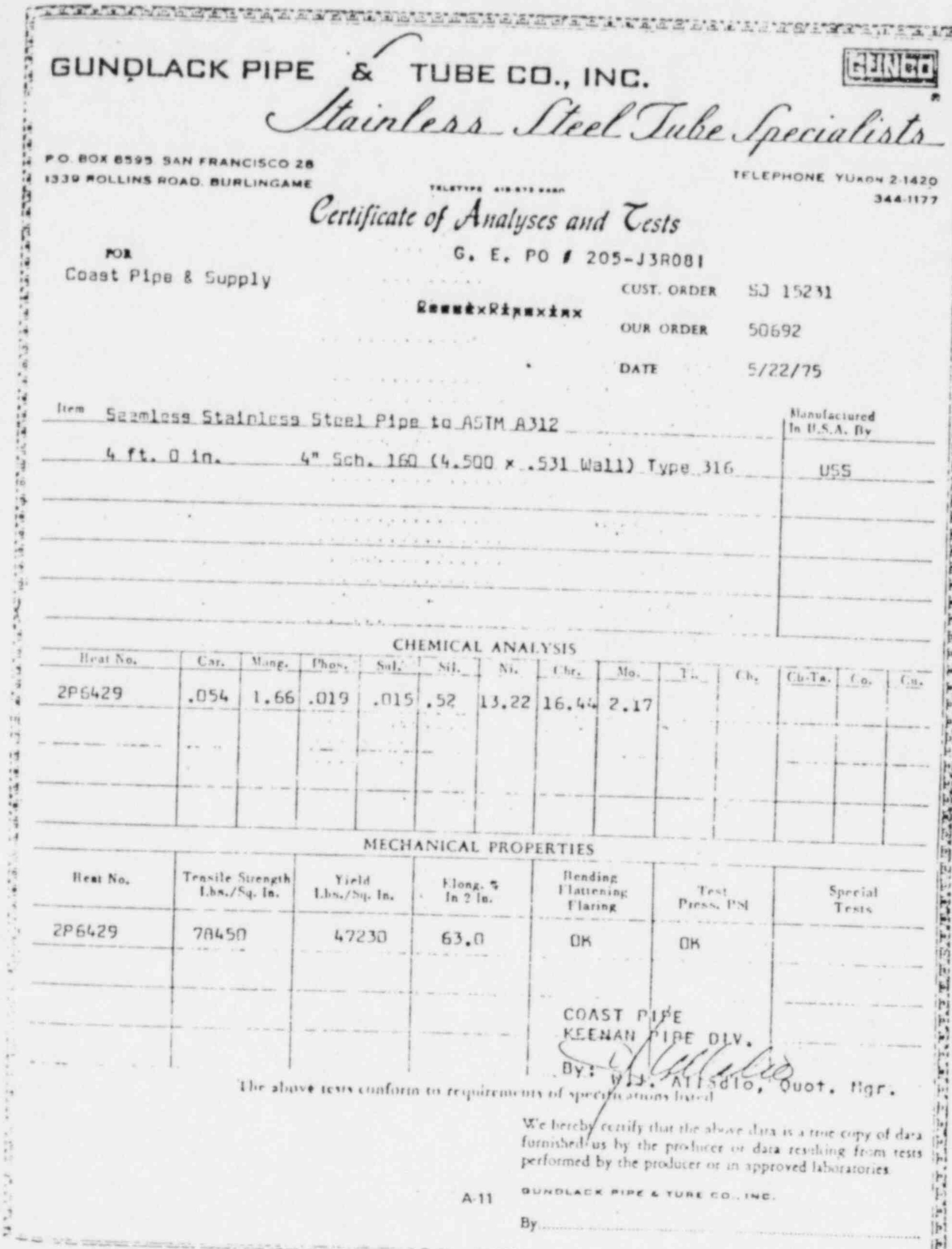

GUNDLACK PIPE & TUBE CO., INC. GUNCO

Stainless Steel Tube Specialists

P.O. BOX 6595 SAN FRANCISCO 28
1339 ROLLINS ROAD, BURLINGAME

TELETYPE [illegible]

TELEPHONE YUkon 2-1420
344-1177

Certificate of Analyses and Tests

FOR
Coast Pipe & Supply

G. E. PO # 205-J3R081

~~[illegible]~~

CUST. ORDER SJ 15231

OUR ORDER 50692

DATE 5/22/75

Item Seamless Stainless Steel Pipe to ASTM A312

4 ft. 0 in. 4" Sch. 160 (4.500 x .531 Wall) Type 316

Manufactured In U.S.A. By USS

CHEMICAL ANALYSIS

Heat No.	Car.	Mang.	Phos.	Sul.	Sil.	Ni.	Chr.	Mo.	Ti.	Cb.	Cb-Ta.	Co.	Cu.
2P6429	.054	1.66	.019	.015	.52	13.22	16.44	2.17					

MECHANICAL PROPERTIES

Heat No.	Tensile Strength Lbs./Sq. In.	Yield Lbs./Sq. In.	Elong. % In 2 In.	Bending Flattening Flaring	Test Press. PSI	Special Tests
2P6429	78450	47230	63.0	OK	OK	

COAST PIPE
KEENAN PIPE DIV.
By: W.J. Allsdio, Quot. Mgr.

The above tests conform to requirements of specifications listed

We hereby certify that the above data is a true copy of data furnished us by the producer or data resulting from tests performed by the producer or in approved laboratories.

GUNDLACK PIPE & TUBE CO., INC.

By ....

NEDC-21463-1

Babcock & Wilcox

Tubular Products Division

ALLIANCE, OHIO-1

BEAVER FALLS, PA.-2

MILWAUKEE, WISCONSIN-3

TEST REPORT

CUSTOMER ORDER NO F-807

DATE | DATE SHIPPED | NUMBER

NUC NUCLEAR
-09

MIDCO PIPE AND TUBE INC
11500 WEST IRVING PARK ROAD
BENSENVILLE, ILLINOIS 60106

STEEL WAS MELTED IN THE USA

SMLS CRO 316 EF CD AW PIPE TO ASTM 312-74 AND ASME SA-312
ASME SECTION III, 1974 ISSUE PLUS SUMMER ADDENDA 1974
CLASS 3 ARTICLE ND 2000.

NO OIL PICKLED

B&W ORDER NO — PARTIAL — COMPLETE

- 020179-201722000350911000

ITEM	OD	WALL	LENGTH	SPECIAL MARKS	PCS	FOOTAGE	HYDRO TEST LBS PER SQ INCH	TESTS MADE
01	4500	337 RL	17/24				2250 5 sec. hold	ETCH BEND FLATTENING ok FLANGE EXPANSION FLARE CORROSION MICRO ULTRASONIC DYE PENETRANT

CORRECTED COPY - CHANGES DEPT. OF
MFG. & FINISH CODE
NOTED-- JBC 5/14/75

... TO YOUR
PURCHASE ORDER
PIECES SHIPPED
FOOTAGE

ITEM	HEAT NO	CARB	MANG	SUL	PHOS	SIL	CHROM	NI	MO	CU	CB	TI
	M6985	.065	1.72	.014	.021	.52	17.07	13.58	2.44			
	check	.065	1.70	.014	.021	.50	17.18	13.30	2.36			

ITEM	HEAT NO	ULTIMATE STRENGTH	YIELD POINT	% ELONG IN 2"	REDUCT IN AREA	HARDNESS
		81900	36500	63		

STRIP ☒ STD NO ☐ FULL SECTION ☐

SWORN TO AND SUBSCRIBED BEFORE ME 7/29/75

Rita J. Pyle

RITA J. PYLE, Notary Public
W. M... B..., Bea. County, Pa.
MY COMMISSION EXPIRES
COMMISSION ...

THIS IS TO CERTIFY THE ABOVE TUBES AND PIPE HAVE BEEN INSPECTED AND TESTED IN ACCORDANCE WITH AND HAVE MET ALL THE REQUIREMENTS OF THE SPECIFICATIONS.

VJ

A-12

THE BABCOCK & WILCOX COMPANY BY

EST REPORT

A. M. CASTLE & CO.

OLD TO:

RAL ELEC CO APED
CURTNER AVENUE
JOSE CALIF 95125

SHIPPED TO:

SAME

UST. ORDER NO.
225 J3R 03

Castle-Pacific
Order No. 89709

SPECIFICATION NO.
ASTM A 312

ITEM NO.		MATERIAL
1	1 LGHT	S/S T 316L WELDED PIPE 4' SCH 80 x 20' RDM

PHYSICALS

	HEAT NO.	YIELD POINT P.S.I.	TENSILE STRENGTH P.S.I.	% ELONG 2"	% RED. AREA	BRINELL	ROCK-WELL	BEND TEST	MACRO	EMBRITT-LEMENT	IZOD IMPACT	
	C0630	47,525	83,250	47.0								

HYDRO TEST: OK FLATTENING TEST: OK

CHEMICALS

	HEAT NO.	% C	% MN	% P	% S	% SI	% NI	% CR	% CU	% AL	% TI	% MG	% MO	% CO
	00630	.018	1.68	.025	.003	.38	11.62	16.22					2.15	

IBED AND SWORN TO BEFORE ME THIS
____ DAY OF ____________ 19___
________________ NOTARY PUBLIC
COMMISSION EXPIRES ____________
AND FOR THE COUNTY OF ____________,
STATE OF ____________

I CERTIFY THAT THESE ARE CORRECT COPIES OF REPORTS NOW ON FILE AT

A. M. CASTLE & CO.

BY

SAN FRANCISCO ☒ LOS ANGELES ☐ SALT LAKE CITY

DISTRIBUTION

Name	M/C
Unit 509 (220)	581
NED Library (5)	328
VNC Library (2)	V01